



Biomechanical Modelling of Knee Loading

Azadeh Nasserì

BSc, MSc

School of Allied Health Sciences
Menzies Health Institute Queensland
Griffith University

Submitted in fulfilment of the requirements of the degree of
Doctor of Philosophy

August 2020

Abstract

The anterior cruciate ligament (ACL) is one of four major intra-articular knee ligaments and plays a key role in knee stability. Rupture of the ACL is one of the most common and debilitating sport-related knee injuries. Most ACL ruptures do not involve direct collisions, but occur during landing, cutting, and pivoting tasks common to sports such as soccer, basketball, and netball. Rates of ACL rupture in young people have increased enormously in Australia over the past two decades. Generally, ACL ruptures are 3.5-4 times more frequent in female compared to male athletes. Among females, those aged 15-19 years are at highest risk of ACL rupture being ~4 times more likely to sustain injury than their pre-pubertal counterparts. Analysis of video footage of ACL injury events, cadaveric experiments, and biomechanical studies has yielded a consensus that external knee loads applied in three planes of motion (i.e., sagittal, frontal, and transverse) contribute to ACL rupture. Laboratory-based biomechanical studies that directly instrumented the ligament have been performed, albeit sparingly for obvious reasons of invasiveness, and show the ACL sustains substantial loading during non-injurious motor tasks. Moreover, studies using external biomechanical measures to examine ACL loading employing computational models have been limited, and have not included, and thus are insensitive to, an individual's knee muscle activation patterns in muscle force estimates

Valid models of the ACL and its loading profile have been challenging to create, and instrumented measures of ACL loading without concurrent modelling of the neuromusculoskeletal dynamics will fail to provide insight into the role of specific muscle and external loads in loading the ACL. Therefore, the mechanisms underlying ACL loading during dynamic motor tasks, through the interaction of muscles, contacting articular bodies, and other soft tissues, remain unclear. This deprives injury prevention

and rehabilitation programs of personalized targets that are mechanistically linked to *in vivo* ACL loading. The purposes of this thesis were to develop and validate a computational model that can accurately estimate ACL force based on outputs of neuromusculoskeletal models in individuals with an intact ACL; determine ACL loading in drop-land-lateral jump task in mature females, therein examining the mechanisms that contribute to ACL loading, and; and determine effects of pubertal maturation on females' ACL loading during a dynamic motor task considered provocative for the ACL.

This thesis involved the development, validation, and application of a computational model to quantify ACL force during dynamic motor tasks. First, an ACL force model was developed using the most relevant, complete, and accessible cadaveric data from the literature. These data comprised measurements of ACL force or strain across various knee flexion angles in response to uni- and multiplanar external knee loads. Using a portion of these data, algebraic equations were fitted to well describe ACL loading in response to both uni- and multiplanar knee loading. The model was then validated using the remaining experimental data not used in model development. The validated ACL force model was then combined with an electromyography (EMG) - informed neuromusculoskeletal model to estimate ACL force developed during a standardised drop-land-lateral jump task performed by healthy females in laboratory conditions.

Ninety-three females, aged 8 to 20 years, volunteered to participate in this study. All participants were recreationally active and had no history of lower limb injury or knee pain. Participants were divided into 3 groups: pre-, early/mid-, or late/post-pubertal based on Tanner's pubertal classification system. Each participant attended a laboratory-based testing session, wherein three repeated trials of a standardized drop-land-lateral jump from a box with box height set to 30% of their lower limb length, while 3D motion

capture, ground reaction forces, and surface EMG were acquired. For purposes of calibrating the EMG-informed neuromusculoskeletal model, three trials of running at a natural self-selected style (speed range from 2.8 to 3.2 m·s⁻¹) were performed.

These laboratory data were then used in a neuromusculoskeletal model to estimate ACL loading. The OpenSim modelling software was used to scale a generic anatomical model to match each participant's gross dimensions, mass, and inertia, followed by morphometric scaling to preserve fibre and tendon operating ranges, and last adjust each muscle's maximum isometric strength based on empirical relationships between mass and height with lower limb muscle volume. Using this scaled model, the external biomechanics (i.e., model motions and joint loading) and muscle tendon unit actuator kinematics (i.e., moment arms, lengths, and lines of action) were determined. The EMG signals were conditioned into normalized linear envelopes, which were combined with the OpenSim external biomechanics and muscle tendon unit actuator kinematics to drive a model in the Calibrated EMG-informed Neuromusculoskeletal Modelling (CEINMS) toolbox. The CEINMS was first calibrated and then run with an EMG-informed neural solution to estimate lower limb muscle and tibiofemoral contact forces. The muscle tendon unit kinematics and forces, along with the joint loads were then incorporated into the validated ACL force model to quantify ACL force. For each participant, the contribution of muscle and intersegmental loads to ACL forces were calculated across the stance phase of the drop-land-lateral jump task. Specific statistical analyses were run to address each of the research questions and encapsulated as a series of research manuscripts in the format of journal articles.

The first study developed and validated a computational model that predicted the force applied to ACL in response to multiplanar knee loading that was estimated by a subject-specific neuromusculoskeletal knee model, as described above. The study

demonstrated these models' utility by applying it to a sample of motion capture data. First, a three-dimensional (3D) computational model was developed and validated using available cadaveric experimental data to estimate ACL force. The ACL force model was valid as it well predicted the cadaveric data, showing strong statistical correlation ($r^2=0.96$ and $P<0.001$), minimal bias, and narrow limits of agreement. Second, by combining a neuromusculoskeletal model with the ACL force model, it was revealed that during a drop-land-lateral jump task the ACL is primarily loaded through the sagittal plane, mainly due to muscular loading. The computational model developed in study one was the first validated accessible tool that could be used to develop and test knee ACL injury prevention programs for people with normal ACL. The method used to develop this model can be extended to study the abnormal ACL upon the availability of relevant experimental data. The paper describing these results was published as Nasser A., Khataee H., Bryant A.L., Lloyd D.G., Saxby D.J. Modelling the loading mechanics of anterior cruciate ligament, *Computer Methods & Programs in Biomedicine*, 184 (2020) 105098. doi: 10.1016/j.cmpb.2019.105098.

Study two determined ACL force and the key muscular and biomechanical contribution to this ACL loading in a standardized drop-land-lateral jump task performed by sexually mature young females. Three-dimensional whole-body kinematics, ground reaction forces, and muscle activation patterns from eight lower limb muscles were collected during dynamic tasks performed by healthy females ($n=24$), all who were recreationally active. Collected data were used to model the external biomechanics, muscle-tendon unit kinematics, and muscle activation patterns using established biomechanical modelling software packages (i.e., OpenSim and MotoNMS). These biomechanical and electromyographic data were then used to calculate the lower limb muscle, joint contact and the ACL forces through an EMG-informed neural solution

combined with a validated ACL force model. Peak ACL force (2.3 ± 0.5 BW) was observed to occur at 14% of the stance phase during the drop-land-lateral jump task. The ACL force was primarily developed through the sagittal plane, and muscles were the dominant source of ACL loading. The main ACL muscular antagonists were the gastrocnemii and quadriceps, while the hamstrings were the main ACL agonists. Our results highlighted the important role of gastrocnemius in ACL loading, which could be considered more prominently in ACL injury prevention and rehabilitation programmes. The paper describing these results is accepted for publication as Nasser A., Lloyd D.G., Bryant A.L., Headrick J., Sayer T.A., Saxby D.J. Mechanism of anterior cruciate ligament loading during dynamic motor tasks. *Medicine and Science in Sports and Exercise*.

Study three determined and compared ACL loading during a drop-land-lateral jump task in females across three pubertal stages of maturation. Further, the relative contributions to ACL force from three planes of motion (sagittal, frontal, and transverse) were compared. In this, sixty-two participants were divided into pre-pubertal (n=19), early/mid-pubertal (n=19) or late/post-pubertal (n=24) groups based on Tanner's pubertal classification system. Each participant completed a biomechanical testing session wherein we collected three-dimensional body motion, ground reaction forces, and EMG during drop-land-lateral jump task. Using these data, the aforementioned ACL force and neuromusculoskeletal knee model was used to assess ACL loading and the key contributions to this loading. To analyse the ACL force in a continuous manner, statistical parametric mapping (SPM) analysis was used. SPM ANOVA and post-hoc t-tests were used to compare total ACL force and contributors to this force over the stance phase of the drop-land-lateral jump task between three groups of females across maturation. Compared to pre- and early/mid-pubertal, females in late/post pubertal group showed significantly higher ACL force during a large percentage of the stance phase, which

encompassed the peak ACL forces. The forces developed through sagittal and transverse planes were significantly higher in late/post-pubertal group compared to the two other groups over large percentages of the stance phase. The contribution of the frontal plane mechanisms to ACL force was not significantly different across sexual maturation, while the pre- and early/mid-pubertal groups were not significantly different for any of the outcome measures. The larger ACL forces observed in late/post-puberty group (14-20 years) may partially explain the higher rate of ACL injury in females aged 15-19 years in the last decades. In addition, it has been shown that ACL growth plateaus at the age of 10, prior to full sexual maturation and cessation of growth in stature. Thus, females in late/post pubertal group are potentially heavier, have similar sized ACL, but with greater ACL forces compared to their less sexually mature counterparts. These reasons together could be the foundation, at least in part, for the higher ACL forces observed in this group. The manuscript describing these results is under review as Nasser A., Lloyd D.G., Minahan C., Sayer T.A., Paterson K., Vertullo C.J., Bryant A.L., Saxby D.J. Effects of pubertal maturation on anterior cruciate ligament forces during a landing task in females. *American Journal of Sports Medicine*.

In conclusion, a computational ACL force model was developed and validated that provided a platform for integration of external biomechanics, muscle and joint contact forces to calculate *in vivo* ACL force. This ACL force model enabled examination of the ACL loading mechanism by exploring the main muscular and biomechanical contributions to ACL loading; and the effects of pubertal maturation on ACL loading in females. The variability in the magnitude and contributions to ACL force across a wide age range of participants suggest estimation of ACL force is necessary to understand the potential ACL injury mechanisms and design ACL injury prevention programs, rather than relying on external biomechanics that are proposed as surrogates of ACL injury.

Acknowledgements

I have received a tremendous amount of support from several people over the last four years, to whom I would like to express my sincere gratitude. First, I would like to thank my two main supervisors. To Professor David Lloyd, you were my first contact at Griffith University, and I am forever grateful that you agreed to take me on into your research team. Thank you for inspiring me with your knowledge, expertise, passion, and dedication to your work. Thank you for showing me what ‘proper science’ is, for frequently providing me with feedback and direction, pushing me to grow as a researcher, and helping me to see my true potential. To Dr David Saxby, thank you for agreeing to be my supervisor, always making the time for my research, teaching me many invaluable skills throughout my academic journey. Thank you for ending every single meeting with encouraging words which helped me build my confidence and overcome the challenges of the research. I cannot thank you enough for your guidance and wisdom to help me to grow professionally and personally.

To my associate supervisors Associate Professor Clare Minahhan, Dr Jonathon Headrick, and Associate Professor Christopher Vertullo, thank you for your support and guidance throughout my PhD. Recognising the different disciplines you represent, your understanding and stream of questions throughout this research has helped me scaffold, shape and reinforce the connection between the multiple disciplines.

To the academics at the School of Allied health Sciences, Griffith University who I have had the pleasure of interacting with and working alongside. You have provided me with many opportunities as a researcher and a teacher that are invaluable. Thank you for your support and guidance. To my PhD student peers, thank you for your friendship over the

last four years; for the coffee and lunch breaks, and many more fun gatherings in between.

You all made my postgraduate studies more enjoyable.

To my family, who are without a doubt my biggest cheerleaders. To my late parents, I am forever thankful for all the sacrifices they made and all the love we share in our family because of them. They left this world too soon but left behind amazing siblings for me who took care of me, loved me unconditionally and never let me feel their absence growing up. To my beloved siblings, thank you for everything you have done for me. Thank you for keeping me grounded and consistently reminding me of my values and my goals. To my husband, Hamid, thank you for your love, always being by my side and putting me first. This journey would not have been possible without your ever-present support, patience and encouragement.

Statement of originality

This work has not previously been submitted for a degree or diploma in any university. To the best of my knowledge and belief, the thesis contains no material previously published or written by another person except where due reference is made in the thesis itself.

Azadeh Nasser

31st August 2020

Publication list

Journal Articles

Nasseri, A., Khataee, H., Bryant, A.L., Lloyd, D.G., Saxby, D.J. (2020) Modelling the loading mechanics of anterior cruciate ligament, *Computer Methods & Programs in Biomedicine*, 184, 105098. <https://doi.org/10.1016/j.cmpb.2019.105098>

Nasseri, A., Lloyd, D.G., Bryant, A.L., Headrick, J., Sayer, T.A., Saxby, D.J. Mechanism of anterior cruciate ligament loading during dynamic motor tasks, *Medicine and Science in Sports and Exercise*. In press.

Nasseri, A., Lloyd, D.G., Minahan, C., Sayer, T.A., Paterson, K., Vertullo, C.J., Bryant, A.L., Saxby, D.J. Effects of maturation on anterior cruciate ligament forces during a landing task in females. *American Journal of Sports Medicine*. Under review.

Conference Papers and Abstracts

Podium presentations

Nasseri, A., Lloyd, D.G., Bryant, A.L., Saxby, D.J. *Anterior cruciate ligament loading and mechanisms of loading during drop-land-cut*, XXVII Congress of the International Society of Biomechanics, Calgary, Canada, 2019.

Nasseri, A., Heiden, T.L., Joss, B.K., Ackland, T.R., Lloyd, D.G., Diamond L.E. *Effects of resistance training on gait and functional outcomes in knee osteoarthritis patients*, 8th World Congress of Biomechanics, Dublin, Ireland, 2018.

Poster presentation

Nasseri, A., Lloyd, D.G., Saxby, D.J. *A computational model of anterior cruciate ligament loading: development and validation*, XXVII Congress of the International Society of Biomechanics, Calgary, Canada, 2019. Nominated for best poster presentations for the David Winter Young Investigator Award.

Commercial/Creative Outputs

International patent

Nasseri, A., Khataee, H., Lloyd, D.G., Saxby, D.J. *Method of calculating in vivo force on anterior cruciate ligament*. Australian patent office application number: PCT/AU2019/051129, Partners: Griffith University and The University of Queensland, October-2019.

Table of contents

| | |
|--|-------|
| Abstract | i |
| Acknowledgements | vii |
| Statement of originality | ix |
| Publication list..... | xi |
| Table of contents | xiii |
| List of figures | xvii |
| List of tables | xxv |
| List of equations | xxvii |
| List of abbreviations..... | xxix |
| CHAPTER 1..... | 1 |
| 1.1 Background | 1 |
| 1.2 Statement of the problem | 4 |
| 1.3 Thesis objective..... | 4 |
| 1.4 Thesis organization | 6 |
| CHAPTER 2..... | 9 |
| 2.1 Anatomy and function of the anterior cruciate ligament..... | 10 |
| 2.2 Anterior cruciate ligament injury | 13 |
| 2.2.1 Prevalence of anterior cruciate ligament injury..... | 14 |
| 2.2.2 Management of anterior cruciate ligament rupture | 15 |
| 2.2.3 Sex-related differences in anterior cruciate ligament injury | 17 |
| 2.2.4 Age-related differences in anterior cruciate ligament injury | 18 |
| 2.3 Mechanisms of anterior cruciate ligament injury: approaches and evidence | 20 |
| 2.3.1 Video analysis of anterior cruciate ligament injury during game play..... | 20 |
| 2.3.2 Study of anterior cruciate ligament mechanics in cadaveric specimens | 22 |
| 2.3.3 Laboratory-based studies of external biomechanics as surrogates for anterior cruciate ligament loading | 26 |
| 2.4 Determining anterior cruciate ligament loading: measurement and models | 43 |
| 2.4.1 <i>In vivo</i> measurements of anterior cruciate ligament loading..... | 43 |
| 2.4.2 Computational models of anterior cruciate ligament | 46 |
| 2.5 Conclusions | 58 |
| CHAPTER 3..... | 61 |
| 3.1 Participants..... | 61 |
| 3.2 Data collection..... | 63 |
| 3.2.1 Hormonal considerations..... | 63 |

| | | |
|----------------|--|-----|
| 3.2.2 | Integrated motion analysis | 64 |
| 3.3 | Data processing | 68 |
| 3.4 | EMG driven neuromusculoskeletal modelling..... | 70 |
| 3.4.1 | Modifying and scaling musculoskeletal model | 70 |
| 3.4.2 | Muscle tendon unit parameter personalization..... | 72 |
| 3.4.3 | Muscle strength personalization | 73 |
| 3.4.4 | Modelling the external biomechanics..... | 73 |
| 3.4.5 | Muscle force estimation using personalised muscle activation..... | 73 |
| 3.5 | Statistical analysis | 77 |
| 3.5.1 | Anterior cruciate ligament model validation..... | 78 |
| 3.5.2 | Comparisons between muscle contributions to anterior cruciate ligament loading | 78 |
| 3.5.3 | Comparisons between female pubertal maturation groups | 79 |
| CHAPTER 4..... | | 81 |
| 4.1 | Abstract | 82 |
| 4.2 | Introduction | 83 |
| 4.3 | Methods..... | 84 |
| 4.3.1 | Cadaveric data preparation..... | 84 |
| 4.3.2 | Model development..... | 86 |
| 4.3.3 | Model validation | 92 |
| 4.3.4 | <i>In vivo</i> experiment..... | 92 |
| 4.3.5 | Signal processing..... | 93 |
| 4.3.6 | Musculoskeletal modelling | 93 |
| 4.4 | Results and Discussion..... | 95 |
| CHAPTER 5..... | | 103 |
| 5.1 | Abstract | 104 |
| 5.2 | Introduction | 104 |
| 5.3 | Methods..... | 107 |
| 5.4 | Results | 115 |
| 5.5 | Discussion | 122 |
| CHAPTER 6..... | | 131 |
| 6.1 | Abstract | 132 |
| 6.2 | Introduction | 133 |
| 6.3 | Methods..... | 135 |
| 6.3.1 | Participants | 135 |
| 6.3.2 | Hormonal considerations..... | 136 |
| 6.3.3 | Dynamic motor task | 137 |
| 6.3.4 | Biomechanical data acquisition..... | 138 |

| | | |
|------------------|---|-----|
| 6.3.5 | Biomechanical modelling..... | 139 |
| 6.3.6 | Statistical analysis | 140 |
| 6.4 | Results | 141 |
| 6.5 | Discussion | 150 |
| CHAPTER 7..... | | 155 |
| 7.1 | Brief thesis summary..... | 155 |
| 7.2 | External biomechanics or ligament loading? | 156 |
| 7.3 | Role of muscles in loading the anterior cruciate ligament across pubertal maturation in females | 161 |
| 7.4 | Limitations | 165 |
| 7.5 | Future research directions | 167 |
| 7.6 | Conclusions | 170 |
| References | | 171 |

List of figures

| | |
|--|----|
| Figure 2.1. Schematic of the anatomy of the knee, showing the many different structures which contribute to knee stability. Highlighted in the red box is the anterior cruciate ligament, the primary ligamentous restraint to anterior-posterior knee stability. Adapted from the Noyes Knee Institute (https://noyeskneeinstitute.com/specialties-and-programs/acl-reconstruction/)..... | 10 |
| Figure 2.2. Combined flexion, valgus, and internal rotation moments at the knee during sidestep cutting. Sidestep cutting is a sporting movement that is often associated with non-contact injury mechanisms of the ACL. This figure is adapted from [54]..... | 12 |
| Figure 2.3. Crucial degrees of freedom of knee motion that affect anterior cruciate ligament loading. | 12 |
| Figure 2.4. Autograft harvesting locations for anterior cruciate ligament. This figure is adapted from Colorado Children’s Hospital (https://www.childrenscolorado.org/conditions-and-advice/sports-articles/sports-injuries/acl-graft-options/)..... | 15 |
| Figure 3.1. Motion analysis marker set, frontal and lateral views..... | 66 |
| Figure 3.2. Single-leg drop-land-lateral jump task. (A) Participant balanced on their dominant leg with hands folded across chest on top of the box, (B) hopped down towards the “X” marked on the ground, and then (C) laterally cut 90° as quickly as possible towards their dominant limb, landing and balancing at a distance of 150% their leg length from the centre of the force plate for 5 seconds. | 68 |
| Figure 3.3. Schematic of muscle contact and ACL force calculation workflow. It is composed of three main parts: experimental acquisition of movement data (yellow), data processing (orange), EMG-driven musculoskeletal modelling and ACL force calculation (blue). The box blocks represent the processing tools and the arrows represent the input/output to/from each tool. ACL: anterior cruciate ligament; EMG: electromyography; GRF: ground reaction forces; MTU: muscle tendon unit..... | 77 |
| Figure 4.1. Knee loading in (A) sagittal, (B) frontal, and (C) transverse planes of motion. | 83 |
| Figure 4.2. Uniplanar ACL forces. (A) ACL force in sagittal plane F_{ACL}^{sag} vs knee flexion angle θ , at different knee anterior drawer forces F_{AD} . Symbols at $F_{AD} = 0$ and 100 N are experimental data from [41, 42]. Other symbols are experimental data from [62]. | |

Continuous curves are our fits derived from Equation(4.4). (B, C) ACL force in frontal plane F_{ACL}^{front} vs knee varus and valgus moments (M_{var} and M_{valg}) at different knee flexion angles θ . Symbols are experimental data from [42]. Curves are our fits derived from Equation (4.4). (D, E) ACL force in transverse plane F_{ACL}^{trans} as vs knee internal and external rotation moments (M_{IR} and M_{ER}) at different θ . Symbols are experimental data from [42]. Curves are our fits derived from Equation (4.5). 88

Figure 4.3. Total ACL force F_{ACL} vs knee flexion angle θ . (A) F_{ACL} in response to combined anterior drawer force F_{AD} and varus moment M_{var} . Symbols are experimental data from [41]. Continuous curve is our fit derived from Equations (4.6), (4.7). (B) F_{ACL} in response to combined F_{AD} and valgus moment M_{valg} . Open circles are experimental data [41]. Other symbols are experimental data from [62]. Continuous curves are our fits derived from Equations (4.6), (4.7). (C) F_{ACL} in response to combined F_{AD} and knee internal rotation moment M_{IR} . Left-pointing triangles are experimental data from [41]. Other symbols are experimental data from [62]. Continuous curves are our fits derived from Equations (4.6), (4.8). (D) F_{ACL} in response to combined F_{AD} . and knee external rotation moment M_{ER} . Diamonds are experimental data from [41]. Other symbols are experimental data from [62]. Continuous curves are our fits derived from Equations (4.6), (4.8) 91

Figure 4.4. ACL force model validation. (A) Comparison of cadaveric experimental ACL force (Expt. force)[62] and simulated ACL force (Sim. force) derived from Equation (4.6). Solid line is regression line ($r^2 = 0.96$; root-mean-squared error $RMSE = 55.04$ N; $P < 0.001$), which is not significantly different from line of identity (dotted line). Dashed lines are 95% confidence intervals. (B) Bland-Altman plot for experimental and predicted ACL forces. Solid line represents mean difference (bias 44 N; $P = 0.01$), and dashed lines are 95% limits of agreement (mean difference ± 1.96 standard deviation, $n=14$ data points). 96

Figure 4.5. Uniplanar ACL forces across the stance phase of the drop-landing task. Silhouettes above (A, C) represent one participant during the stance phase of the task. First and last silhouettes represent the positions before and after the stance phase, respectively, shown for the clarity. (A) Knee flexion angle θ . (B) Sagittal plane knee loading and ACL force. Left axis: muscle and intersegmental forces (F_{muscle} and $F_{intersegmental}$) obtained from neuromusculoskeletal model, and net anterior drawer force F_{AD} ; see Equation (4.1). Right axis: ACL force F_{ACL}^{sag} obtained from Equation(4.3).

(C, D) Frontal and transverse planes knee loadings and ACL forces. Left axis: muscle and intersegmental moments (M_{muscle} and $M_{intersegmental}$), and net varus or valgus moment $M_{var/valg}$, and internal or external rotation moment $M_{IR/ER}$; see Equation (4.2). Right axis: ACL forces F_{ACL}^{front} and F_{ACL}^{trans} obtained from Equations (4.4) and (4.5). The shaded regions are standard deviation of the forces and moments. Direction of sagittal plane knee load: anterior draw (+) and posterior draw (-); frontal plane knee moment: varus (+) and valgus (-); transverse plane knee moment: internal rotation (+) and external rotation (-).
..... 97

Figure 4.6. ACL force across stance phase of drop-landing. ACL forces through sagittal, F_{ACL}^{sag} , frontal, F_{ACL}^{front} , and transverse, F_{ACL}^{trans} , planes contribute to total ACL force F_{ACL} ; see Equation (4.6). Shaded regions show standard deviation of forces. Silhouettes represent one participant during stance phase of the task. First and last silhouettes are the postures before and after the stance phase, respectively, shown for the clarity..... 99

Figure 5.1. Schematic of ACL force calculation workflow composed of three main parts: experimental acquisition of movement data (yellow), data processing (orange), EMG-driven musculoskeletal modelling and ACL force calculation (blue). The box blocks represent the processing tools and the arrows represent the input/output to/from each tool. ACL: anterior cruciate ligament; EMG: electromyography; GRF: ground reaction forces; MTU: muscle tendon unit. F_{muscle} : muscle forces due to their direct line of action; $F_{contact}$: tibiofemoral contact force; F_{ACL} : force in the ACL. 111

Figure 5.2. Knee flexion angle (A) and ACL force (B) across stance phase of drop-land-lateral jump. The tension in the ACL due to forces acting in the anterior-posterior direction (F_{ACL}^{sag}), the force in the ACL due to moments in frontal plane (F_{ACL}^{front}), and the force in the ACL due to moments in transverse plane (F_{ACL}^{trans}) contribute to ACL force (F_{ACL}). Shaded regions show standard error of the mean. Silhouettes represent one participant during stance phase of the task. First and last silhouettes represent posture before and after stance, respectively, and are added to clarify the stages of the task. ACL: anterior cruciate ligament. 116

Figure 5.3. Sagittal plane knee loading (left axis) and ACL force (right axis) during stance. Left axis: muscle forces due to their direct line of action (F_{muscle}^{AP}), tibiofemoral compressive contact force ($F_{contact}^{AP}$), and intersegmental forces ($F_{intersegmental}^{AP}$). F_{net}^{AP} is the net knee joint forces acting in the anterior-posterior direction calculated as $F_{net}^{AP} =$

$F_{muscle}^{AP} + F_{contact}^{AP} + F_{intersegmental}^{AP}$. Right axis: the tension in the ACL due to forces acting in the anterior-posterior direction (F_{ACL}^{sag}). Shaded regions show standard error of the mean. Direction of sagittal plane knee load: anteriorly (+) and posteriorly (-) directed. Silhouettes represent one participant during stance phase of the task. First and last silhouettes are before and after stance, respectively, shown to clarify the stages of the task. ACL: anterior cruciate ligament..... 118

Figure 5.4. Uniplanar ACL forces across the stance phase of the drop-land-lateral jump task. (A) Frontal plane knee loading (left axis) and ACL force (right axis) during stance.

Left axis: varus/valgus muscle moments ($M_{muscle}^{Var/Val}$) and intersegmental knee varus/valgus moments ($M_{intersegmental}^{Var/Val}$), $M_{netvar/val}$ is the net frontal plane (varus/valgus) moment ($M_{net}^{Var/Val}$) calculated as $M_{net}^{Var/Val} = M_{muscle}^{Var/Val} + M_{intersegmental}^{Var/Val}$. Right axis: F_{ACL}^{front} , the

ACL force due to the net frontal plane (varus/valgus) moments ($M_{net}^{Var/Val}$). (B) Transverse

plane knee loading (left axis) and ACL force (right axis) during stance. Left axis:

internal/external rotation muscle moments ($M_{muscle}^{IR/ER}$) and intersegmental knee

internal/external rotation moments ($M_{intersegmental}^{IR/ER}$), $M_{net}^{IR/ER}$ is the net transverse plane

(internal/external rotation) moment calculated as $M_{net}^{IR/ER} = M_{muscle}^{IR/ER} + M_{intersegmental}^{IR/ER}$.

Right axis: F_{ACL}^{trans} , the ACL force due to the net transverse plane (internal/external rotation) moments ($M_{net}^{IR/ER}$). The shaded regions represent the standard error of the mean.

Direction of frontal plane knee moment: varus (+) and valgus (-) and transverse plane knee moment: internal rotation (+) and external rotation (-). Silhouettes represent one participant during the stance phase of the task. ACL: anterior cruciate ligament..... 119

Figure 5.5. Grouped (A) and individual (B) muscle loads applied to the tibia in the sagittal

plane at the first peak in ACL force. Direction of muscle forces: anteriorly (+) and posteriorly (-) directed. Left axes display the absolute muscle forces (N) and right axes

display relative contributions (%) to net anterior-posterior force from all muscles (F_{muscle}). The symbols atop the bars represent significant differences. In (A), symbol

* indicates significant difference from other muscle groups. In (B), the muscles that load the ACL via an anteriorly directed force are compared to each other, wherein † indicates significant difference from gaslat and vasint, # indicates significant difference from gasmed and vaslat, \$ indicates significant difference from recfem. In (B), muscles that support load the ACL via an posteriorly directed force are compared to each other,

wherein ** indicates significant difference from sart, grac, bfsh, and tfl, ¥ indicates significant difference from semiten, ‡ indicates significant difference from bfsh and tfl, € indicates significant difference from tfl. Error bars represent standard error of the mean. ACL: anterior cruciate ligament; gasmed: gastrocnemius medial head; vaslat: vastus lateralis; gaslat: gastrocnemius lateral head; vasint: vastus intermedius; recfem: rectus femoris; vasmed: vastus medialis; bfsh: biceps femoris short head; tfl: tensor fasciae latae; grac: gracilis; sart: sartorius; semiten: semitendinosus; bflh: biceps femoris long head; semimem: semimembranosus..... 121

Figure 6.1. CONSORT flow diagram that illustrates the grouping and flow of the participants. ACL – anterior cruciate ligament; EMG – electromyography. 136

Figure 6.2. Comparisons of the ACL force generated during the stance phase of the drop-land-lateral jump between pre-, early/mid-, and late/post-pubertal females performed with statistical parametric mapping (SPM). **(A)** The SPM ANOVA across 100% of the stance phase. The bold black line is the computed F-curve, the dashed (red) line indicates the critical threshold calculated at $\alpha=0.05$, and the thick black bars correspond to the regions of statistical significance. **(B)** The ACL force for each pubertal group is plotted (pre in even dash green, early/mid in solid red, and late/post in alternating dash blue) with standard error of the mean shown as translucent areas. Shaded grey columns in each plot indicate regions of significant difference in the ACL force between pubertal groups. In the bottom row, the respective post-hoc paired t-tests are plotted, with grey shaded regions corresponding to regions of significant difference. The associated p statistic is listed. ACL – anterior cruciate ligament; SPM – statistical parametric mapping..... 143

Figure 6.3. Comparisons of the ACL force developed through the sagittal plane during the stance phase of the drop-land-lateral jump between pre-, early/mid-, and late/post-pubertal females performed using statistical parametric mapping (SPM). **(A)** The SPM ANOVA across 100% of the stance phase. The bold black line is the computed F-curve, the dashed (red) line indicates the critical threshold calculated at $\alpha=0.05$, and the thick black bars correspond to the regions of statistical significance. **(B)** The ACL force developed through the sagittal plane for each pubertal group is plotted (pre in even dash green, early/mid in solid red, and late/post in alternating dash blue) with standard error of the mean shown as translucent areas. Shaded grey columns indicate regions of significant difference between the pubertal groups. In the bottom row, the respective post-hoc paired t-tests are plotted, with grey shaded regions corresponding to regions of significant

difference. The associated p statistic is listed. ACL – anterior cruciate ligament; SPM – statistical parametric mapping. 145

Figure 6.4. Comparisons of the ACL force developed through the transverse plane during the stance phase of the drop-land-lateral jump between pre-, early/mid-, and late/post-pubertal females performed using statistical parametric mapping (SPM). **(A)** The SPM ANOVA across 100% of the stance phase. The bold black line is the computed F-curve, the dashed (red) line indicates the critical threshold calculated at $\alpha=0.05$, and the thick black bars correspond to the regions of significant difference. **(B)** The ACL force developed through the transverse plane in each pubertal group is plotted (pre in even dash green, early/mid in solid red, and late/post in alternating dash blue) with standard error of the mean shown as translucent areas. Shaded grey columns indicate regions of significant difference between the pubertal groups. In the bottom row, the respective post-hoc paired t-tests are plotted, with grey shaded regions corresponding to regions of significant difference. The associated p statistic is listed. ACL – anterior cruciate ligament; SPM – statistical parametric mapping. 146

Figure 6.5. Comparisons of ACL force developed through the frontal plane during the stance phase of the drop-land-lateral jump between pre-, early-/mid-, and late-/post-pubertal females performed using statistical parametric mapping (SPM). **(A)** The SPM ANOVA across 100% of the stance phase. The bold black line is the computed F-curve, the dashed (red) line indicates the critical threshold calculated at $\alpha=0.05$, and the thick black bars correspond to the regions of statistical significance. **(B)** The ACL force developed in frontal plane in each pubertal group is plotted (pre in even dash green, early/mid in solid red, and late/post in alternating dash blue) with standard error of the mean shown as translucent areas. Shaded grey columns indicate regions of significant difference between the pubertal groups. In the bottom row, the respective post-hoc paired t-tests are plotted, with grey shaded regions corresponding to regions of significant difference. The associated p statistic is listed. ACL – anterior cruciate ligament; SPM – statistical parametric mapping. 147

Figure 6.6. Uniplanar contributions to ACL force at the time of peak ACL force. Left axes display the absolute uniplanar contributions (N) and right axes display relative contributions (%). **(A)** sagittal plane absolute contribution was greater in late/post pubertal group compared to pre and early/mid maturation groups ($P < .001$, $r = -0.75$; $P < .001$, $r = -0.55$; respectively) whereas it's relative contribution was smaller compared to pre maturation group ($P = .003$, effect size (r) = -0.49), **(B)** in frontal plane there were no

between group differences in absolute or relative contributions, and (C) transverse plane absolute contribution was greater in late/post pubertal group compared to pre and early/mid maturation groups ($P < .001$, $r = -0.77$; $P < .001$, $r = -0.64$; respectively), and the relative contribution was greater compared to early/mid pubertal group ($P = .008$, $r = -0.47$). *Significantly different to pre-pubertal group ($P < 0.05$). **Significantly different to early/mid-pubertal group ($P < 0.05$). Error bars, 1 SEM. 149

List of tables

| | |
|--|-----|
| Table 3.1. List of lower limb muscles from which experimental surface EMG data were collected and corresponding acronym. | 65 |
| Table 3.2. Anthropometric measurement description and technique. | 66 |
| Table 3.3. List of forty motion capture markers affixed over participants' body for scaling purposes and biomechanical simulations. | 67 |
| Table 3.4. The marker pairs used in linear scaling of the generic template model. | 72 |
| Table 4.1. Loading parameters at peaks in ACL force during a drop-landing for $n = 13$ participants (mean \pm SD). | 100 |
| Table 5.1. Loading parameters at the two local peaks in the ACL force during the drop-land-lateral jump performed by twenty-four participants reported as mean \pm standard deviation. | 117 |
| Table 6.1. Characteristics of the different pubertal groups. | 142 |

List of equations

| | |
|-------------|-----|
| (3.1) | 74 |
| (3.2) | 75 |
| (3.3) | 76 |
| (4.1) | 86 |
| (4.2) | 86 |
| (4.3) | 87 |
| (4.4) | 87 |
| (4.5) | 88 |
| (4.6) | 89 |
| (4.7) | 89 |
| (4.8) | 90 |
| (5.1) | 112 |
| (5.2) | 113 |
| (5.3) | 113 |
| (5.4) | 114 |
| (5.5) | 114 |

List of abbreviations

3D – Three-dimensional

ACL – Anterior cruciate ligament

ACLR – Anterior cruciate ligament reconstruction

AD – Anterior draw

ANOVA – Analysis of variance

BMI – Body mass index

BW – Bodyweight

CEINMS – Calibrated EMG-Informed Neuromusculoskeletal Modelling Software

CSA – Cross sectional area

CT – Cross term

DOF – Degree of freedom

EMG – Electromyography

FT – Frontal-transverse

GRF – Ground reaction force

JCF – Joint contact force

MOCAP – Motion capture

MRI – Magnetic resonance imaging

MTL – Muscle-tendon length

MTU – Musculotendon unit

NMSK – Neuromusculoskeletal

OFL – Optimal fibre length

RMSE – Root mean square error

SENIAM – Surface Electromyography for the Non-Invasive Assessment of Muscles

SF – Sagittal-frontal

SPM – Statistical parametrical mapping

SPSS – Statistical Package for Social Science

ST – Sagittal-transverse

TSL – Tendon slack length

CHAPTER 1

Introduction

1.1 Background

The anterior cruciate ligament (ACL) is one of the major intra-articular knee ligaments and plays a key role in knee stability [1]. Rupture of the ACL is a common and debilitating knee injury. In Australia, ACL ruptures result in an annual ACL reconstruction rate of 77.4 per 100,000 individuals, which is among the highest in the world, and has been increasing in adolescents and young adults over the past two decades [2]. The majority of ACL injuries occur through sports participation [3], and mainly from non-contact events, meaning they do not involve physical contact between athletes [4]. Rather, ACL injury typically occurs during landing, abrupt change of direction over a planted foot, and pivoting, which are tasks common to sports such as soccer, basketball, rugby, Australian Football, handball, and netball [5]. The ruptured ACL is often treated through orthopaedic reconstruction (ACLR), the aim of which is to restore mechanical stability of the knee. In Australia, approximately 17,000 primary ACLR are performed annually [2]. In addition to direct health care costs (i.e., surgery, and physical therapy), ACL rupture and subsequent ACLR impose substantial burden on the patient due to reduced economic productivity and elevated risk of long-term health consequences, such as early onset knee osteoarthritis [6, 7].

Age- and sex-specific differences in rates of ACL rupture are well documented[2]. Female athletes have been reported to sustain two-to-four times more ACL ruptures

compared to their male counterparts [8, 9], while late- and post-pubertal young women are at approximately four times greater risk of sustaining ACL rupture compared to pre-pubertal girls [10]. Literature [11-14] indicates neuromuscular control deteriorates as females progress through puberty, suggesting changes in contributions to ACL loading from body and inertia, muscle, and articular contact forces. Indeed, compared to earlier stages of pubertal maturation, as females reach later stages of pubertal maturation, they land with straighter knees [15], generate larger ground reaction forces [16], and experience greater external knee moments [17-20]. Collectively, these neuromuscular and biomechanical changes across pubertal maturation may place the ACL under greater load. Further to this, anatomical changes occurring across mid-to-late stages of pubertal maturation, such as rapid lower limb growth [21], may conspire to increase ACL loading in young women. Indeed, a plethora of studies speculate about the role of puberty-related changes to anatomy [22], external joint biomechanics [20], force generation and strength expressed relative to body mass [15, 23], and neuromuscular control [24, 25] in ACL loading. However, conclusive causal mechanism(s) of ACL loading in live humans has not been identified.

Within the research field of biomechanics, there is consensus that some combination of external knee loads, applied through three planes of motion (i.e., sagittal, frontal, and transverse), are present to varying degrees during non-contact ACL injury events [26]. However, the mechanisms by which external knee loads are transmitted to the ACL remain contentious, as this transfer is controlled by the complex interaction of muscles, contacting articular bodies, and other soft tissues [27, 28]. Biomechanical studies of many types (e.g., videography of in-field injury events, experiments on cadaveric specimens, and various laboratory-based computational analyses) have attempted to elucidate the mechanisms of ACL loading and unloading during dynamic

tasks. However, these studies have rarely examined ACL loading directly or used the individual's unique muscle activation patterns in muscle force estimates.

Earlier studies [29-40] modelled ACL force, *in silico*, reporting the important role of muscles in ligament loading. However, these past efforts were limited by the use of simplistic loading conditions, bespoke models developed for specific individuals or specimens, computationally prohibitive methods, analysis confined to the sagittal plane, or lack of model validation. Indeed, the issues surrounding model validation are of concern. Previous models [36, 37] assumed ACL loading in response to multiplanar externally applied knee loads is equal to the sum of ACL forces exerted by equivalent multiple, but independently applied, uniplanar loads. However, experiments [41, 42] clearly show ACL force can be different from the pure summation of multiple uniplanar loading equivalents. Rather, ACL loading is influenced by the knee flexion angle and specific multiplanar loading conditions experienced.

Due to these modelling limitations, an improved and validated model that can estimate ACL loading and its contributors through a computationally inexpensive approach would be valuable to the scientific community. Given the magnitude of ACL loading may be affected by the activation of muscles surrounding the knee, the computational models used to predict ACL forces must employ validated methods for estimating muscle forces. As there are different approaches to estimate muscle force, uncertainty remains regarding the roles of certain muscles, such as gastrocnemii, in loading the ACL during dynamic tasks [43, 44]. Therefore, the precise mechanisms underlying ACL loading during dynamic activities remain unclear, impeding further development of injury prevention and rehabilitation programs with population based (e.g., adolescent females) targets mechanistically linked to *in vivo* ACL loading.

1.2 Statement of the problem

An abundance of biomechanical research has focused on identifying and characterizing the modifiable risk factors of non-contact ACL injury, typically examining external biomechanics (i.e., segment and joint kinematics, ground reaction forces (GRF), and joint moments). Sex- and maturation-related differences in these external biomechanics have been identified, suggesting female pubertal development may result in abnormal external knee biomechanics. In turn, based on the correlations between external biomechanics and ACL injury rates, it is suggested that abnormal external knee biomechanics partly explain the disproportionately higher rates of female ACL injury. However, external biomechanics (i.e., kinematics, GRF, and net joint moments) do not represent the internal mechanics (e.g., ligament or joint compression forces) [45]. Focussing on external biomechanics as a proxy measure of ACL injury risk diverts research efforts away from mechanistically-focused approaches that directly address the complex and multifactorial issue of “too much force through the ACL breaks it” [46]. Therefore, computational models are required to determine ACL loading and elucidate muscle contributions to that loading which could be used to develop targets for prevention or post-injury rehabilitation programs. However, a validated causal model of ACL forces which can be applied to cohort analysis of live humans does not currently exist.

1.3 Thesis objective

The purposes of this thesis were to develop and validate a computational model suitable for estimating ACL force in healthy knees subject to complex applied loads and muscle forces. Second, to use this ACL force model, in combination with neuromusculoskeletal models, to explore the mechanism of ACL loading, and the contributions to this loading, during a provocative dynamic task. Finally, to use this model to explore the effects of

sexual maturation on ACL loading in females performing a dynamic motor task considered provocative of ACL loading. To this end, this thesis was divided into three studies, each addressing a specific aim. The specific aims of this thesis were to:

1. Develop and validate a computational model of ACL force based on the empirical relationship between ACL force and knee loading observed in cadaveric experiments. Once validated, illustrate the model's functionality in predicting ACL force in live humans by combining this model with a validated neuromusculoskeletal model to predict ACL force during a drop-land-lateral jump task performed by late/post pubertal young females.
2. Using the neuromusculoskeletal and ACL force models, determine the mechanism of ACL loading as well as contributions of knee-spanning muscles to ACL force during drop-land lateral jump in late/post pubertal young females.
3. Determine the effects of pubertal maturation in females on their ACL loading by comparing the ACL force and its contributors during drop-land lateral jump performed by females at different stages of pubertal maturation.

The broad hypotheses associated with each specific aim were:

1. An empirical computational model could be developed and would accurately predict ACL force, with minimal computational demand, and can be readily combined with neuromusculoskeletal models.
2. During a dynamic drop-land-lateral jump task, the ACL will receive most of its loading via the sagittal plane mechanism, and second, the quadriceps will be the primary ACL antagonists while the hamstrings would be the main ACL agonists.
3. As females progress through pubertal maturation, the ACL force generated during a dynamic drop-land-lateral jump task would increase and the contributions to ACL force from the sagittal, frontal, and transverse planes would change.

1.4 Thesis organization

The specific aims and the corresponding hypotheses listed above are addressed in three studies within this thesis. Each of these three studies are presented in the format of journal articles. Overall, this thesis comprises seven chapters:

Chapter 1 provides a general introduction and describes the objectives, aims, and broad hypotheses of this thesis.

Chapter 2 is a literature review that provides information on the aetiology of ACL injury and describes current knowledge of the ACL loading mechanism. Herein, the limitations of commonly employed models and the current gaps in literature are highlighted.

Chapter 3 presents the general methods and procedures (i.e., those common to the experimental chapters) employed for data collection and processing within this thesis. Information on participant recruitment, data acquisition, and data processing methods, and details on the personalisation process of neuromusculoskeletal models are included in this chapter.

Chapter 4 describes the development, validation, and implementation of a computational ACL force model that accurately predicts *in vivo* ACL force based on knee kinematics, externally applied knee loads, and muscle forces determined through EMG-informed neuromusculoskeletal modelling. This chapter addresses the first aim of this thesis and has been published in *Computer Methods and Programs in Biomedicine*.

Chapter 5 describes the implementation and use of the validated computational ACL force model to determine the ACL loading mechanism and the contributions to ACL force during a dynamic motor task in sexually mature young females. This chapter addresses the second aim of this thesis and is accepted for publication in *Medicine and Science in Sports and Exercise*.

Chapter 6 describes the effects of pubertal maturation in females on the magnitude of, and contributions to, ACL force generated during the performance of a dynamic motor task. This chapter addresses the third aim of this thesis and is, at the time of this thesis completion, under review in the *American Journal of Sports Medicine*.

Chapter 7 synthesizes the research findings within the current literature and expands on the implications of this work, addressing feasibility and translational potential of the ACL force model. Limitations and future directions are discussed, and overarching conclusion are made.

At the end of this thesis are listed the publications, documents, and report to which I have referenced throughout the text.

CHAPTER 2

Literature review

This chapter provides an overview of the literature surrounding the neuromuscular and biomechanical contributors of anterior cruciate ligament (ACL) loading, and the potential effects of pubertal maturation in females on their ACL loading. First, a brief review of the anatomy of the ACL is presented, followed by the epidemiology of ACL injury, general management of ACL injury and its imparted socioeconomic burden, differential rates of ACL injury between the sexes, and potential age-related (i.e., pubertal maturation) effects on ACL injury. Then, the literature comprising the current state of knowledge on ACL injury mechanisms is explored by reviewing video analysis of ACL rupture events, cadaveric experiments, and in-vivo laboratory based biomechanical approaches. The effects of sex, maturation, and task complexity on the external biomechanics statistically associated with risk of ACL injury during dynamic tasks are then reviewed.

Finally, an overview of the current approaches used to assess ACL loading, instead of surrogate external biomechanical measures, is provided. These approaches include direct *in vivo* measurement (i.e., invasive instrumentation of the ACL or non-invasive image-based techniques), detailed computational knee models with explicit representation of the ACL (i.e., finite element method and elasto-structural models), and mathematical models that describe the phenomenon of ACL loading as an input to output relationship.

2.1 Anatomy and function of the anterior cruciate ligament

The knee is stabilized through the complex interaction of articulating cartilage surfaces atop the tibia and femur, active and passive muscle forces, and passive soft tissues such as ligaments, menisci, and the joint capsule. The ACL is one of four major ligaments of the knee: the posterior cruciate ligament, medial collateral ligament, and lateral collateral ligament (Figure 2.1). Together, these ligaments act to restrain knee motions to physiological ranges [47].

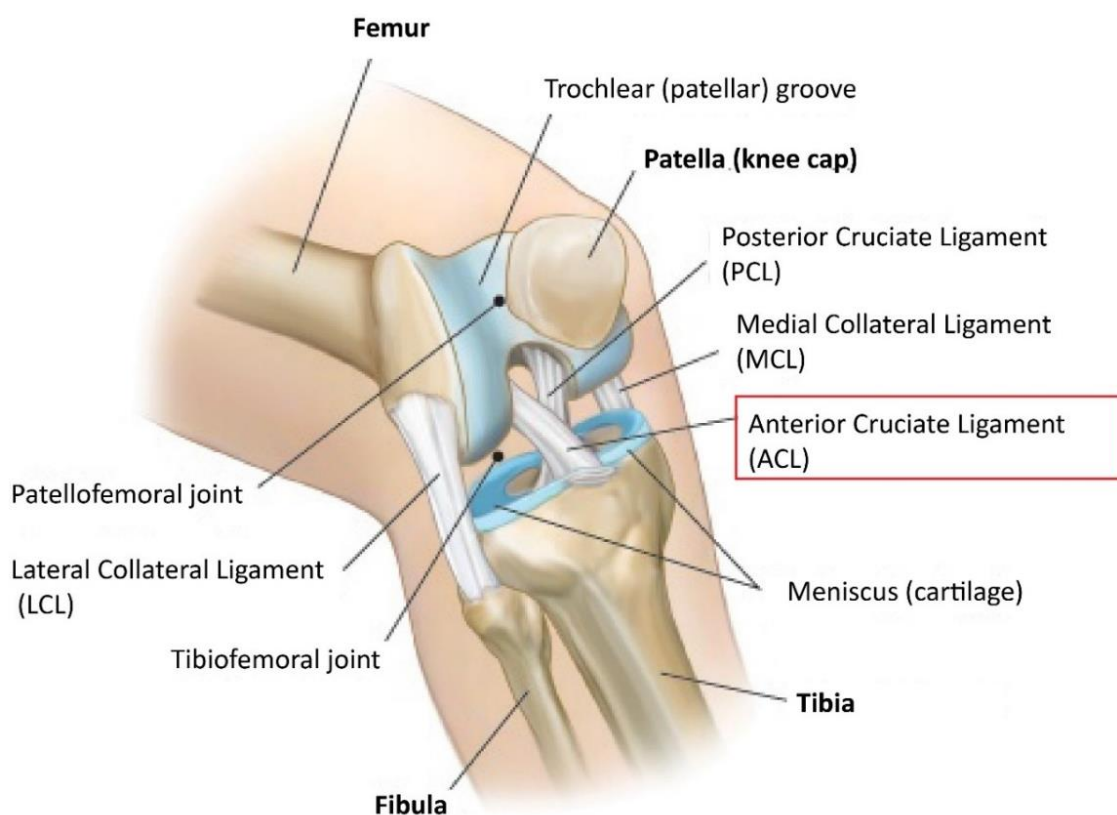


Figure 2.1. Schematic of the anatomy of the knee, showing the many different structures which contribute to knee stability. Highlighted in the red box is the anterior cruciate ligament, the primary ligamentous restraint to anterior-posterior knee stability. Adapted from the Noyes Knee Institute (<https://noyeskneeinstitute.com/specialties-and-programs/acl-reconstruction/>).

The ACL makes its distal insertion slightly medial to the anterior intercondylar area of the tibia plateau, partly blending with the anterior horn of the lateral meniscus. At

its proximal origin, the ACL twists and fans out posteriorly and laterally to attach to the posteromedial aspect of the lateral femoral condyle [48]. The ACL is composed of the anteromedial and posterolateral bundles, each of which is comprised of collagen fibres sheathed by connective tissue. The collagen matrix is mostly of Types I (~90%) and III (10%) [49]. Due to their unique anatomy, the ACL bundles develop strain at different positions of knee flexion [50, 51]. Moreover, the ACL is comprised of fibres of uniform and non-uniform diameters, which contributes to the resiliency of the ACL as the fibres of non-uniform diameter aid in resisting elongation while the uniform fibres resist shear. Overall, the unique fibre geometry of the ACL makes it stronger than most ligaments [52, 53].

The primary role of the ACL is to constrain anterior tibial translation, but also internal rotation and varus or valgus motion [41, 55, 56]. However, due to the number of degrees of freedom that exist within the knee joint, the complex interaction of muscle forces, contact between articulating bodies, and body and inertial loading during motor tasks, several mechanistic scenarios have been shown to load the ACL. These include anterior force applied directly to the tibia generated by muscles due to their lines of action [38, 42, 43, 57, 58], posterior force applied directly to the femur generated by muscles due to their lines of action [43], anterior force applied to the tibia due to compressive joint contact forces acting on a posteriorly sloped tibia [59, 60], varus/valgus moments [41, 60], and internal/external rotation moments [41, 55, 60] (Figure 2.2 and Figure 2.3). Moreover, these many loads can be applied to the knee in isolation or combined, resulting in complex patterns of ACL strain [61, 62].

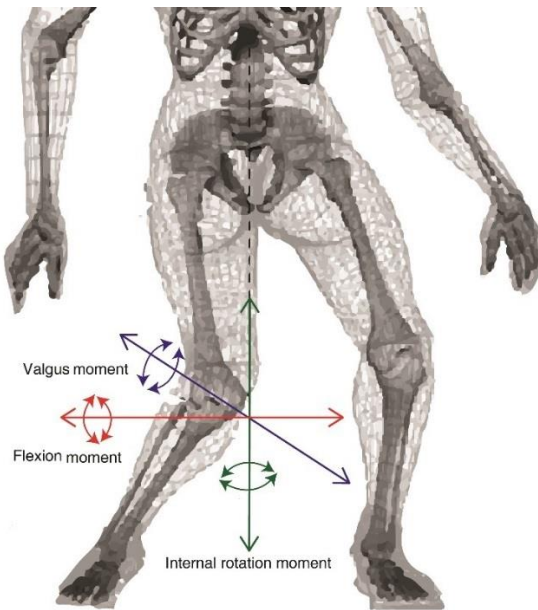


Figure 2.2. Combined flexion, valgus, and internal rotation moments at the knee during sidestep cutting. Sidestep cutting is a sporting movement that is often associated with non-contact injury mechanisms of the ACL. This figure is adapted from [54].

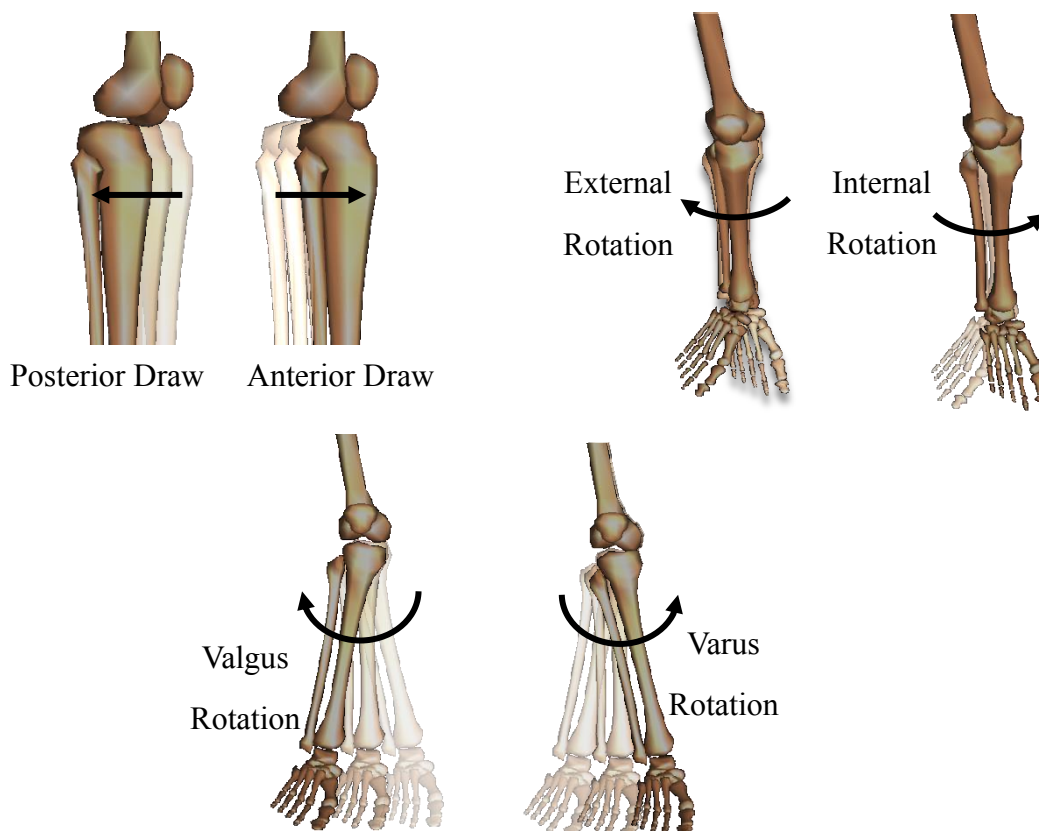


Figure 2.3. Crucial degrees of freedom of knee motion that affect anterior cruciate ligament loading.

2.2 Anterior cruciate ligament injury

Rupture of the ACL is a debilitating intra-articular knee injury. The vast majority of ACL injuries occur due to sports participation [3]. For sport-related ACL injuries, the majority do not involve direct collision between players (although the exact proportions vary somewhat by sport), but involve rapid accelerations and/or changes of direction [63]. From the presence of body large accelerations, we can logically deduce the presence of multiplanar externally applied knee loading generated during these manoeuvres and subsequently the presence of large muscle forces both create the accelerations and to act as joint stabilizers [64, 65]. Across various sports, non-contact injuries have been found to make up 50-80% of ACL injuries [66-68].

Notably, ACL ruptures are 3.5-4 times more frequent in female compared to male athletes [69] and are becoming increasingly common among young athletes [70, 71]. It has been speculated that increased involvement in high intensity and competitive sporting activities combined with extensive practicing of difficult game-specific skills, rather than strength, balance, and stabilisation skills, throughout the primary growth years increases the risk of ACL injury in young athletes, from the recreational to the elite levels [72-74]. However, analyses linking sport preparatory (e.g., practice, training, etc) behaviour with ACL injuries remain statistical in nature, without any causal studies showing, for example, training intensity increases ACL forces.

Following ACL rupture, the ACL deficient knee is often treated with an orthopaedic procedure known as ACL reconstruction (ACLR). An ACLR typically restores anterior-posterior passive knee stability [75], but may not restore normal internal-external tibial rotation [76] or the neurosensory function of the ACL [27, 46]. Following ACL rupture and ACLR, individuals often fail to return to pre-injury activity or sport

levels [77], may struggle with persistent functional deficits about the knee [78], have high risk of future early onset of knee osteoarthritis [79], and are at greater risk of second ACL injury as well as other lower-limb injuries compared to their uninjured counterparts.

2.2.1 Prevalence of anterior cruciate ligament injury

Ruptures of the ACL are among the most common ligamentous knee injuries sustained during physical activity, with most cases being the individuals under the age of 35 years [2, 80]. Due to the lack of explicit tracking of rupture incidence at a national level in Australia, the majority of ACL injury incidence statistics are inferred from national registries of surgical reconstruction of the ACL [3, 81] or orthopaedic governing bodies such as the Australian Orthopaedic Association (AOA) [82, 83]. In Australia, approximately 72% of ACL reconstructions are due to a sport-related injury, with Australian Rules Football, basketball, netball, rugby union, rugby league, soccer, and skiing being the most frequently involved sports [84, 85]. Australia has the highest estimated incidence rate of ACL ruptures globally (52 per 100,000 population) when compared against other Organisation for Economic Cooperation and Development (OECD) nations [85, 86].

Alarming, it appears the high rates of ACL injury is increasing in Australia. Zbrojkiewicz *et al* [2] reported, during a 15-year period from 2000 to 2015, the overall incidence of ACL reconstructions increased by 43%, from 54.0 to 77.4 per 100,000 population. During this same period, the annual incidence of ACL reconstruction in people under the age of 25 years grew by 73.8% in contrast to a 28.4% increase in incidence for those aged 25 years or more [2]. Further, the Zbrojkiewicz and colleagues forecast that into the next decade, assuming that trends over the past 15 years will be maintained, an estimated overall growth in ACL injury incidence for the period 2000 to 2024 to be highest for females and males under 25 years (8.5% & 5.4% growth,

respectively, per year) [2]. The projected increase in ACL injury incidence in Australia is an emerging public health problem warranting continued investigation.

2.2.2 Management of anterior cruciate ligament rupture

Following an ACL injury, surgical reconstruction is usually required, without which the risk for long term degenerative sequelae is drastically increased [74]. Surgical reconstruction is most commonly performed using one of three different graft sources taken from the individual's affected or contralateral leg (i.e., an autograft): hamstring, bone-patellar ligament-bone, or quadricep tendon [87] (Figure 2.4).

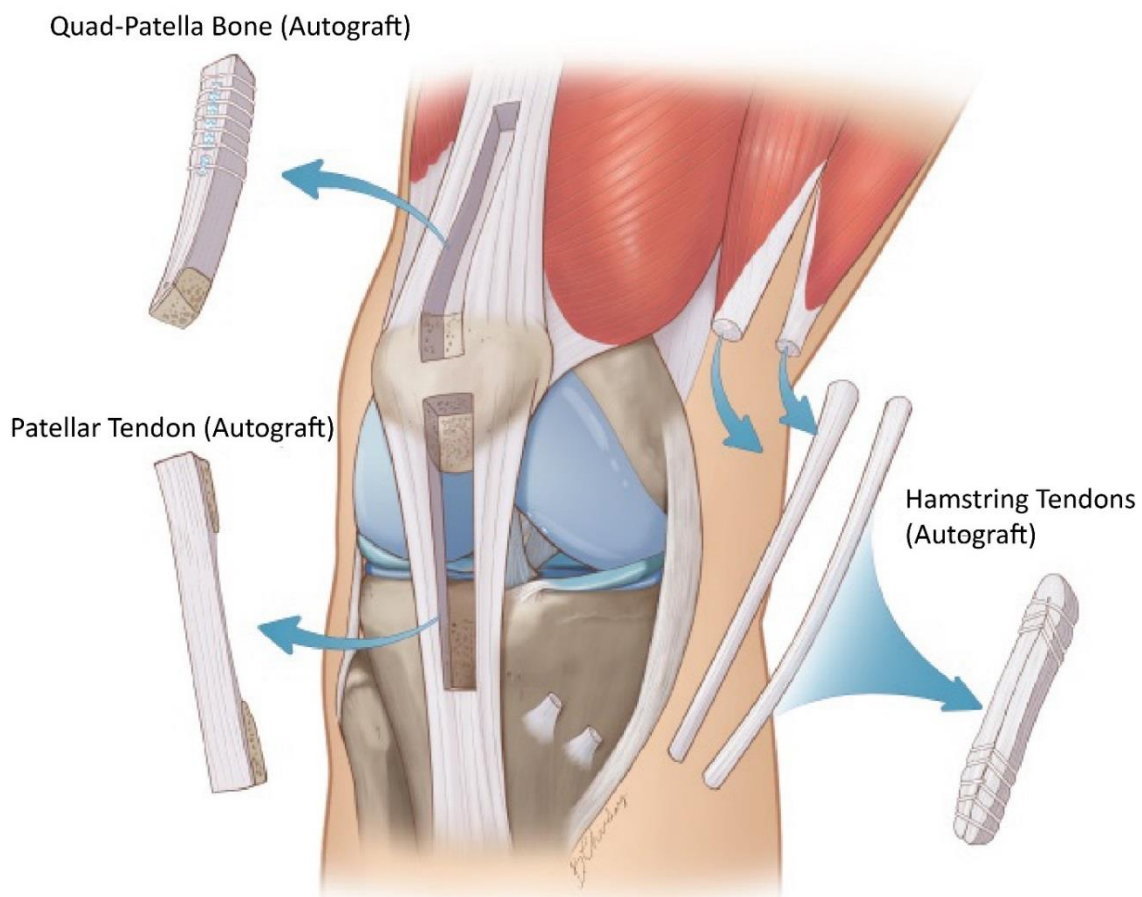


Figure 2.4. Autograft harvesting locations for anterior cruciate ligament. This figure is adapted from Colorado Children's Hospital (<https://www.childrenscolorado.org/conditions-and-advice/sports-articles/sports-injuries/acl-graft-options/>).

Globally, hamstring autografts are the preferred method to reconstruct the ACL. However, in the United States, ~44% of reconstructions used a hamstrings autograft, while 42% of cases used bone-patellar ligament-bone [88]. In contrast, the hamstring autograft is largely favoured to the bone-patellar ligament-bone option in Europe and Oceania. Indeed, 90% of ACL reconstruction performed in Sweden using a hamstrings autograft [89], 78% in New Zealand [90], and 92.4% in Australia [91]. Recently, Grassi *et al.* [92] reported declining popularity for bone-patellar ligament-bone in regard to graft choice, however, the evidence favouring one surgical reconstruction method vs another is inconclusive with advantages and disadvantages associated with each surgical method.

Regardless of the surgical method, the reconstructed ACL is followed by extensive rehabilitation often lasting close to one year [93, 94]. The orthopaedic and post-operative rehabilitation impose substantial financial burden both in terms of direct costs for therapy but also loss of economic productivity during the long period of convalescence. In Australia, the total estimated hospital costs associated with ACL injuries has been estimated over \$75 Million AUD a year [95], while broader costs imposed by high rates of early-onset knee osteoarthritis following ACLR are enormous (estimated in the several Billions AUD annually) [96].

Following ACLR, the individual may sustain profound long-term changes to their graft donor muscles. In the case of a hamstrings ACLR, tendon is harvested during surgery from the semitendinosus in isolation or in combination with the gracilis. Following harvesting, the donor hamstring muscles experience changes to their anatomy, such as failure or poor tendon regeneration [97-100], proximal and/or medial migration of the common medial hamstring insertion within the popliteal fascia onto the tibia [101], muscle atrophy and muscle belly proximal retraction [102-117], and fatty infiltration [101, 115]. Unsurprisingly, knee flexion [118, 119] and internal rotation [77, 120] strength are

chronically reduced following ACLR, being lower than both healthy controls and the unaffected contralateral side in ACLR patients. The impaired muscle function may partly explain the greater risk of secondary ACL injury following ACLR [121] and, if hamstring autografts are used, hamstring strain injury [122]. More alarmingly, ~50% of individuals who sustain ACL injury and undergo subsequent ACLR, develop knee osteoarthritis (OA) within 7-15 years after injury [7, 78], with ominous implications for public health [123].

Clearly, there is an urgent need to prevent ACL injuries, particularly in young females. However, to prevent or lower the risk of an injury, the injury mechanism must be understood in precise terms. Further, the knowledge of the injury mechanism must be translated (e.g., through a technology) so it can aid development of preventive protocols while enabling young people to remain active and engaged in sport.

2.2.3 Sex-related differences in anterior cruciate ligament injury

Abundant data exist demonstrating greater incidence of non-contact ACL injuries among female athletes compared with male athletes in sports involving jumping, planting, and cutting such as basketball, soccer, team handball, netball, and alpine skiing [124-128]. These higher rates of ACL injury in females compared to male athletes has been observed at both high school and collegiate levels for various sports and during both practice and competition [126, 128]. Female athletes may also experience greater severity of knee injuries, indicated by higher odds of surgery per injury event and a greater number of days spent in rehabilitation after the injury [125]. Importantly, through continuous long-term knee injury surveillance of both male and female athletes, it has been shown in specific populations that rates of ACL injury in male athletes have actually decreased over the past decade, while females during the same period show no decrease in rates of ACL injury [125, 126]. This might suggest that protective mechanisms that lower risk of ACL injury in males were absent or not effective in females.

Both sex (biological phenomena) and gender (partly a social construction) may interact to explain the elevated risk of ACL injury in females; however, it is difficult to tease their respective influences apart as they are tightly correlated for most people. Indeed, the markedly high ACL injury incidence in females has been attributed to anatomical (e.g., Q-angle in the lower extremity and trunk/leg/foot alignments), biomechanical (e.g., landing techniques), physiological (e.g., sex hormone fluctuations), and neuromuscular (e.g., inadequate hamstring strength and recruitment) features, which have been shown to be different between the sexes. Likewise, societal behaviours and cultural factors (e.g., levels of sport participation) may also influence differences in ACL injury rates between the sexes [124, 127, 129]. Nevertheless, it is still unclear if the risk factors for ACL injury are themselves different between females and males, or if females are simply more likely to have the underlying risk factors [127]. Therefore, an improved implementation of effective injury prevention programs for at-risk populations could be achieved by a better understanding of the risk factors [124].

2.2.4 Age-related differences in anterior cruciate ligament injury

Sports are some of the most popular extracurricular activities among high school-aged youth, with more than half of all high school students participating in some form of sport [130]. Increased participation in higher level sport at earlier ages has been associated with increased prevalence of ACL injuries in youth [131], with more than fifty percent of ACL injuries occurring in high school- and college-aged athletes [127]. As most of the epidemiological studies have focused on adult athletes, the age of occurrence of ACL injury is not well defined in the literature. Shea *et al.* [71] assessed the incidence of ACL injury in paediatric and adolescent soccer athletes and reported that at ages 11–12 years both males and females had increased frequency of ACL injury with risk appearing to increase up to the age of 18 years. They concluded ACL injury occurs in skeletally

immature soccer players and females appear to have an increased risk of ACL injury compared with males, even in the skeletally immature [71]. Further, it has been reported that younger female athletes are more likely to sustain ACL injury compared with their older counterparts [132], which might be attributed to anatomical and neuromusculoskeletal changes associated with maturation and/or less sport participation experience.

Although engaging in sport at young ages increases physical competency, decreases health risks, decreases body mass index, and promotes social interaction, sustaining sport-related injury can counteract these beneficial effects [70, 72]. Injuries can impose emotional, physical, social, and economic tolls on athletes [130]. It has been reported that the rate of sport injuries in Australian adolescents is approximately 25%, with an 8% annual drop out in recreational sporting activities due to injury. Knee injuries are among the most common serious injuries, accounting for 60% of high school sport-related surgeries [130], and participating in pivoting sports such as football, basketball, and team handball is associated with the highest incidence of ACL injury in adolescents [74]. Grimmer *et al.* classified the high risk sports for adolescents as frequently involving jumping and landing [73]. In youth sport, involving dynamic and rapidly changing environment, high frequency of jumping, sprinting, and pivoting might produce high strains on the muscular-skeletal system, thereby increasing the risk of injury [133]. Regardless of the treatment method, athletes with ACL injury have a higher rate of early retirement from active participation in sports compared to athletes without this injury [134], with commonly cited reasons being residual knee instability, reduced range of motion, and/or stiffness and pain [70]. However, with the many health and social benefits, sports participation should not be disparaged. Therefore, it is essential to better

understand the ACL injury mechanisms, particularly in females, and in relation to pubertal maturation.

2.3 Mechanisms of anterior cruciate ligament injury: approaches and evidence

The precise mechanisms by which an ACL rupture is caused *in vivo* remains contentious. There are four general categories in ACL injury mechanism research. These categories are “in-field” analysis, such as video analysis of gameplay involving injury events, experiments performed on cadaveric specimens, laboratory-based biomechanical studies of live humans, and computational modelling and simulation, the latter used in laboratory-based studies. The key findings, strengths, and limitations are now reviewed.

2.3.1 Video analysis of anterior cruciate ligament injury during game play

Videography is a powerful tool to capture the real-world conditions surrounding an ACL injury event. Even though there are limitations associated with videography estimates of body motion, such as lack of instruments to assess body-ground forces and errors in kinematic measurements caused by two-dimensional assessments of three-dimensional tasks, it is the only current method that actually captures some aspect of *in vivo* ACL ruptures.

Considerable video analysis has been conducted examining the conditions surrounding ACL rupture for various sporting codes such as gridiron football [135], rugby union [136], soccer [137, 138], handball [139], and Australian Football [140]. As different sporting codes have different rules, methods of scoring and defending, size of players, etc., the exact conditions and rates of injuries vary, although, key themes have been identified. First, most injuries do not occur due to direct physical impact between

players, meaning, most injuries are “non-contact”. In these cases, the cause of injury is likely related to the way the athlete performs various tasks.

The second theme that emerges is that ACL injuries typically occur during motor tasks that involve large accelerations of the body. It is generally understood that no one ruptures their ACL standing still or moving in a straight line at near constant speed. The sporting manoeuvres that are considered high risk for ACL injury involve large accelerations and often combined with lateral movements (e.g., pivots or side-step cuts) [135, 136, 139] or landing [138-140]. Further, video-based assessment of lower limb posture has identified heel-first or flat foot contact with the ground [136], external foot rotation [135], near full knee extension [136, 137, 139, 141], substantial hip flexion [137, 141], and lateral trunk flexion [142] to be present during many instances of ACL injury.

Systematic review of video analysis studies [141] reveals ACL injury is likely to happen when players are in close proximity, but not usually in direct contact, there is high foot-to-ground friction, as well as in specific lower limb postures. From these findings, researchers have speculated that several concurrent biomechanical and neuromuscular features are likely present and expose the ACL to large forces: 1) large muscle forces required to change direction (i.e., lateral movement); 2) single-leg tasks (likely because they focus body forces to one side rather than two) causing compression and demanding large quadriceps forces. Although these speculations seem reasonable, two-dimensional videography by itself cannot provide comprehensive biomechanical analysis as body ground forces are not measured nor are muscle activation patterns. However, there are promising new technologies that in the future will enable predicting three-dimensional knee kinematics and net moments using only two-dimensional videography [143]. These technological advances will afford powerful new insights into the net knee loading sustained during ACL injuries in game play. Regardless of future technology capabilities,

a consistent feature of current videography analysis of ACL injury is the timing of the apparent ACL injury. It has been estimated that ACL injury occurs between 30 to 100 milliseconds after initial foot-ground contact during sporting manoeuvres [144, 145]. Given this time window, clinical researchers should focus their attention towards the conditions at the knee during the early temporal phases of athletic tasks.

2.3.2 Study of anterior cruciate ligament mechanics in cadaveric specimens

Experiments conducted on cadaveric specimens have been used to investigate ACL loading mechanisms [41, 42, 62, 146]. These studies often involve controlled experimental conditions, making the generated data precise and accurate. In these types of experiments, the cadaveric specimens (retaining all or portions of the shank and thigh) are prepared by isolating the muscles and/or ligaments across the knee. The specimens are mounted into a rig of varying levels of complexity and the knee's articulations can be instrumented with pressure film to measure contact between articulating bodies. Similarly, the ligament(s) can be instrumented with strain gauge(s) to directly measure their elongation, relative to a reference state, in response to applied loads. The rig is then manipulated, and more recently robotically-controlled, to move the knee to specific postures and/or apply specific forces and moments [41, 42, 62, 146], with the resulting ACL behaviour measured.

The advantages provided by this type of experiments are important. First, robotic control enables application of precise and configurable kinematics and loads to the knee, meaning the researcher can be confident of the applied mechanical conditions down to the precision of the robotic system. This is a level of confidence not achieved through video analysis or biomechanical study of live subjects. Second, the ACL and other articular structures can be instrumented such their mechanical response to applied knee kinematics and loading can be directly measured. Again, this level of insight could not be

achieved through videography and is rarely performed in laboratory-based biomechanical analysis, with notable exception of limited studies using invasive *in vivo* measurement [147]. Finally, through study of cadaveric specimens, the researcher can perform destructive experiments by incrementally increasing loading conditions, which cannot be done retrospectively and is not ethical for live human studies.

Many cadaveric experiments have been conducted to gain insight into the ACL injury mechanics. These studies can be categorized into uniplanar and multiplanar knee loading experiments. Uniplanar knee loading means applying a unique load to the knee through one specific plane of motion, e.g., anteriorly directed force applied to the tibia to simulate anterior drawer. Several uniplanar knee loading conditions have been examined for their effects on ACL loading, including anterior tibial force, compression, varus/valgus, and internal/external tibial rotation [56, 148, 149]. Compressive joint contact forces, generated by body and inertial forces as well and muscle forces, may cause further tibial anterior draw force due to the posterior slope of the tibial plateau [150]. Each of these uniplanar loading conditions have the ability to load the ACL, but their combined effects have been shown to place more load on the ACL than each scenario in isolation [62].

Markolf and colleagues provided the biomechanical community with the first rigorous cadaveric experiments examining relationships between applied knee loads and ACL forces. They applied uniplanar [42, 57, 61, 151] and multiplanar [41, 152] loads to the knee and measured the ACL force directly by instrumenting the ligament with a load cell. They demonstrated even though the anterior tibial force is arguably the most direct mechanism for loading the ACL [41, 149], internal tibial rotation torque is also an important mechanism for generating ACL force at near full knee extension [149]. Moreover, the combination of tibial anterior force and internal rotation could generate the

highest forces with the knee extended [41]. Markolf and colleagues [41] also revealed that, compared with each load applied in isolation, varus and valgus moments applied in combination with anterior tibia force increased the ACL force. However, the ACL force was moderated in flexed knee postures when an internal tibial rotation moment was additionally applied to anterior tibia force, demonstrating the complex and often counterintuitive relationships between external knee loading and ACL forces.

Markolf and colleagues [41, 149] also found external tibial rotation moments did not generate particularly large ACL forces, and acted to moderate ACL loading effects of anterior tibial forces. Markolf *et.al* [152] also explored the role of compression on ACL force in the presence of complex multiplanar knee loading. They found increasing levels of tibiofemoral compression significantly increased anterior tibial translation and hence ACL force without significantly altering knee internal and valgus rotations [152]. Thus, combined loading conditions in the sagittal plane alone can induce high ACL loading via anterior tibial translation, independent of internal or valgus rotations of the tibia [152]. Collectively, these experiments revealed combined loading can generate higher ACL forces than uniplanar loading alone, and the knee posture and specific multiplanar loads applied to the knee need to be considered [41, 42, 61, 152].

Although the experiments performed on cadaveric specimens provided valuable information regarding the fundamentals of the ACL loading mechanism, they may not represent the *in vivo* loading conditions of dynamic tasks. During the experiments by Markolf *et.al* [41, 42, 61, 152], the ACL force was directly measured under multiplanar knee loading conditions over a wide range of knee postures (flexion angles), however, the magnitude of the applied joint compression, anterior tibia drawer, internal tibia rotation moments, and valgus moments were small in comparison to what occur in the live human knee during gait [38, 39, 58] and sporting activities [153]. These small loads

were used because of the technological limitations in the experimental cadaveric setup at the time, such as the possibility of ACL bone cap failure [41, 42, 61, 152]. Therefore, from the studies of Markolf and colleagues, it is not possible to gain insight into the relationships between knee and ACL loading during physiologically relevant conditions.

More recently, experiments conducted on cadaveric specimens have simulated loading across a wide range of high-risk injurious scenarios (i.e., landing) [62, 152]. In these studies, ACL strains were measured in response to impulsive axial compression, simulated muscle forces, anterior tibial shear, valgus moments, and internal tibial rotation moments in both uniplanar and multiplanar configurations. However, the ACL response was measured at single knee flexion angle and the effect of different knee flexion angles was not reported [62]. In simulated landing, multiplanar loading resulted in significantly greater peak ACL strain compared to the strain in response to equivalent uniplanar loading. Furthermore, the additive nature of combined multiplanar loading was disproportional and nonlinear, meaning ACL strain in response to multiplanar loading was different to the simple summation of ACL strain in response to each uniplanar load in isolation.

Interestingly, the contribution of externally applied knee valgus and internal tibial rotation moments to peak ACL strain were similar and only became substantial when these moments were above 50 Nm and 40 Nm, respectively. These findings suggest valgus and internal rotation moments make important contributions to ACL loading only when they are of large magnitude, applied in isolation, or combined with relatively small anterior shear force. Moreover, these contributions may be less important in the presence of higher anterior force applied on the tibia, similar to *in vivo* ACL loading conditions [152]. Further, the highest peak ACL strain levels were observed at elevated knee valgus and internal tibial rotations, with knee valgus rotation having a significantly greater impact

on peak ACL strain compared to internal tibial rotation [62]. However, it is important to note that the reported knee valgus and internal rotations (e.g., 27° of valgus and 38° internal rotation) are well beyond physiological *in vivo* knee motion ranges. Thus, the suggested loading patterns responsible for injury [62], could be correct for cadavers with high ranges of permitted knee rotation, but might not reflect the *in vivo* ACL injury mechanism in a live human.

Most experiments performed on cadaveric specimens were conducted under quasi-static conditions with no active knee musculature. Where simulated muscle forces were present, they were limited to a small number of knee-spanning muscles with relatively low force magnitudes compared to the levels expected during *in vivo* activities [62, 152]. This is important because muscle forces can influence the ACL forces and knee kinematics in complex ways, such as increasing the anterior component of the force in the patellar tendon acting on the tibia or stabilizing the knee by resisting applied tibial torque. Thus, the specific effects of muscle action on the ACL depends upon the relative magnitudes of knee spanning muscle forces, knee posture, external knee loads, and their interactions [152]. Overall, experiments performed on cadaveric specimens have emphasized the important multiplanar nature of ACL loading [41, 62, 152] and provide our fundamental understanding of the ACL loading mechanism. However, *in vivo* laboratory biomechanical studies are essential to understand how human motor control and biomechanics can influence ACL loading.

2.3.3 Laboratory-based studies of external biomechanics as surrogates for anterior cruciate ligament loading

As reviewed in the above sections on video analysis of ACL injury and cadaveric experiments, there is strong evidence that multiplanar loading of the knee places

particularly high loads on the ACL. To understand the mechanism of ACL injury, biomechanical studies have replicated the tasks associated with ACL injury such as landing, cutting, and pivoting, common to sports such as soccer, basketball, and netball in laboratory conditions. Generally, these studies have deployed three levels of increasingly relevant analysis: (1) external biomechanics, which is concerned with body and joint motions (i.e., kinematics), body and joint loads (e.g., ground reaction forces and generalized joint loads from inverse dynamics analysis), and electromyography (EMG) (i.e., indirect measures of muscle activation); (2) direct and indirect measurement of ACL mechanics *in vivo* (e.g., strain gauges or load cells implanted into the ACL), and (3) computational modelling of the ACL and other tissues. Collectively, these biomechanical studies have aimed to identify movement paradigms that may put the ACL at elevated risk of injury, predict ACL injury rates from biomechanical measures, and identify differences between the sexes and ages that may explain the particularly high risk of injury in young females.

Over the past several decades, numerous variations of jumping and landing [154, 155], side-step cutting [156], and other sporting tasks [157, 158] have been the focus of hundreds of laboratory-based studies examining various biomechanical parameters. Most of these studies examined the external biomechanics of the individual's performing particular motor tasks considered relevant from an ACL injury perspective. External biomechanics have been the focus because they can be calculated non-invasively, are easily determined with modern biomechanics software, do not require high-levels of technical computing skill, do not require sophisticated computational modelling, and (some) can be extracted from videography of real-world ACL injury.

In these studies, the external biomechanical variables of interest range from the posture of body segments, joint motions, foot-ground contact forces, and externally

applied joint loading. Many of these biomechanical variables have been assumed as surrogates for ACL loading. The justifications for use of these surrogates has been inspection of ACL injury events captured through videography and inferences made about the loads present, and/or the relationships between external multiplanar loading and ACL forces established through experiments performed on cadaveric specimens. In the following sections the review will focus on the specific experimental paradigms including external biomechanical measures taken during dynamics tasks, that have been examined for both males and females, young and old, and simple and complex tasks, with some studies mixing these conditions for complex analyses.

2.3.3.1 Sex-related comparison of external biomechanics

It has been suggested that abnormal multiplanar knee kinematics place individuals at higher risk of ACL injury compared to both normal kinematics and abnormal kinematics confined to a single plane of motion [26, 159]. Abnormal kinematics refer to joint motions that are significantly different to those performed by healthy, non-injured individuals, and those that are longitudinally not susceptible to injury. Documented abnormal kinematics include reduced hip and knee flexion in the sagittal plane, increased knee valgus and hip adduction in the frontal plane, increased knee and hip internal rotation in the transverse plane. These abnormal kinematics occur at or around the instant of initial foot-ground contact or at their respective peak values during performance of sporting tasks considered high-risk for ACL injury [159]. The underlying assumption is if the kinematics of someone who has had an ACL injury (retrospective analysis) or goes on to sustain one (prospective) are substantially different to those displayed by healthy, normal, otherwise un-injured individuals, then those differences may explain past injuries or risk of future injury. However, the validity of this underlying assumption is not rigorously established, nor are causal mechanisms clearly identified.

To explain the higher rates of ACL injury in females, researchers have focused on examining sex differences in neuromuscular control, specifically, altered movement patterns of the lower limb during demanding athletic tasks such as side step cutting and landing [160-163]. Different posture and movement patterns can affect task performance and the loads transmitted through the lower body, potentially increasing risk of ACL injury [161]. Longitudinal study of the sex differences in pubertal and post-pubertal young adults performing a drop vertical jump found no differences in knee valgus between pubertal males and females, but found the knee valgus was greater in post-pubertal females compared to their male counterparts [161]. An increase in knee valgus when performing demanding athletic tasks has been identified in females during their rapid adolescent growth, and may be a maturation-related factor behind increased risk of ACL injury in young females [161, 163]. Notably, this increase in knee valgus was not observed for male participants across their maturation [161, 163], however, as will be noted later in this review knee valgus measures during dynamic motor tasks should be interpreted cautiously.

Despite the reported sex differences in knee flexion angles, systematic reviews of lower limb kinematics during landing tasks have reported knee valgus as the only kinematic variable for which there is consistent support of sex differences, with females displaying increased valgus (or apparent valgus) [160, 164]. Likewise, a more recent systematic review and meta-analysis reported healthy women show greater knee valgus rotation than their male counterparts for a range of weight bearing tasks such as walking, running, jump-landing and cutting movements [165].

These reported sex-related differences in non-sagittal knee kinematics (i.e., knee valgus) should be interpreted cautiously due to potential measurement errors. First, the traditional approach in measuring segmental and joint kinematics during human motion

is a process called direct kinematics. In direct kinematics a motion capture system tracks the position of skin mounted markers, which are then used to create anatomical reference frames for each segment of interest (e.g., thigh). Then, the spatial transformation between adjacent segments (e.g., thigh and shank) can be expressed in an anatomically meaningful set of ordered rotations (e.g., knee flexion/extension, varus/valgus, and internal/external rotation).

The direct kinematics approach to solve three-dimensional human kinematics has been used extensively since the late 1980's with the advent of commercially-available motion capture systems and has formed the basis of thousands of biomechanical studies. However, the knee motions computed through direct kinematics may contain errors from multiple sources and these errors are both substantial in magnitude and difficult to minimize. Non-sagittal knee angles determined using direct kinematics from skin markers acquired in a three-dimensional motion capture laboratory are substantially different to the motion of the skeleton due to the presence of soft tissue motion between the skin surface markers and the underlying skeleton [166, 167]. Unfortunately, it appears this soft tissue motion is within the frequency range of the skeletal motion, meaning it cannot be suppressed with a targeted filter using the conventional signal processing methods. Commonly, this issue of soft tissue impairing the accuracy of lower limb kinematics is referred to as soft tissue artefact.

In addition to inaccurate knee varus/valgus rotations calculated from skin surface markers during walking and side step cutting, it has been shown conclusively these measures could even trend in the opposite direction to the skeletal motion [166, 167]. Benoit and colleagues [166, 167] designed an experiment whereby skin surface markers and cortical bone pins were used concurrently to track lower limb motion during walking and side-step cutting. They reported during walking the knee varus/valgus rotations,

along with the knee translations, calculated from skin surface markers were inaccurate compared to the gold standard bone pin-derived kinematics. The errors between kinematics determined from skin-surface and bone-pin markers increased in magnitude when examining the side-step cutting. Critically, the knee varus/valgus motion calculated from skin surface markers had the opposite trend compared to the corresponding motion determined from the bone pin markers, meaning when the knee was experiencing varus (determined by bone motion), the skin surface markers computed a valgus rotation (see Figure 4 in [166]). Thus, the results of studies using direct kinematics methods to examine non-sagittal rotational knee motions and translations during dynamic activities should be interpreted cautiously.

It is important to note that knee kinematics outside of what is considered normal ranges may simply represent natural variability in human motion and should not necessarily be considered an indicator of ACL injury risk. Persistent differences in the way males and females move their bodies and joints when performing the same tasks have been identified; however, the tools used to measure kinematics not only contain error, but this error may not be equally applicable to males and females. For example, a major source of error in measurement of non-sagittal knee rotations and knee translations is soft tissue between the skeleton and skin-surface. Females typically have more body fat than males, particularly in the thighs and hips; areas of the body on which motion capture markers are placed. Indeed, Stagni *et al.* [168] demonstrated conclusively the region-specific nature of soft tissue error and highlighted the issues in measuring the non-sagittal knee kinematics in females. Apart from measurement considerations, the literature shows a large variability in the lower limb kinematics of healthy individuals. This might reflect the different experimental protocols and tasks performed [159], but also may be due to natural variability in the way individuals perform motor tasks.

Furthermore, it is not clear why different kinematics in females and males would predispose females to ACL injury, as this may well be a case of correlation but not causation.

In addition to kinematic measurement errors caused by soft tissue artefact, measurement of non-sagittal knee rotation is highly sensitive to the definitions of the coordinate systems used for different body segments. This is particularly important when decomposing the transformation between segments using the International Society of Biomechanics' recommended joint coordinate systems. Indeed, if markers are placed incorrectly on the body, the result can be dramatic instances of "kinematic crosstalk". That is, small errors in marker placement (often due to difficulty of locating bony anatomy through palpation) can result in misaligned coordinate axes leading to motion about one axis to be mistakenly computed as motion about another axis [169]. Indeed, if the knee's primary axis (i.e., the flexion extension axis) is poorly defined (i.e., human error in approximating the intercondylar line at the skin surface), the result will be crosstalk between flexion/extension motion and the second and third ordered rotations, i.e., spuriously smaller flexion combined with larger varus/valgus and internal/external rotations. This error can be considerable and along with soft tissue artefact, measures of varus/valgus and internal/external rotation motions have only moderate repeatability within and between testing sessions [170].

Overall, caution is warranted when interpreting the results of studies suggesting increases in knee valgus in specific populations (e.g., females). This caution is due to the abovementioned issues surrounding measurement of knee varus/valgus with skin surface markers combined with the computational method of direct kinematics, and the potential for misalignment of the knee's joint axes that could introduce crosstalk into the joint coordinate system. Despite these issues, the weight of evidence suggests females likely

have different movement strategies during dynamic tasks such as landing and change of direction, although the exact differences are contentious and kinematics analysis offers limited insight into why these differences exist or what relevance they may offer to ACL loading. Therefore, conclusions about ACL injury mechanics should not be derived from external measurement of kinematics alone.

Examining the forces and moments externally applied to the body and joints may provide insight into the higher risk of ACL injury in females during athletic tasks. A considerable amount of research has focused on the net loads generated at the knee (and other joints) during tasks associated with ACL injury. As previously discussed, cadaveric experiments demonstrated the loads applied to the knee through sagittal, frontal, and transverse planes can increase ACL force and strain [41, 42, 62, 152], and these loading conditions have been explored in laboratory-based biomechanical studies. Furthermore, external forces and moments have high repeatability within and between testing sessions [170] so may be better variables to assess the biomechanical mechanisms of ACL loading than segment and joint kinematics.

Compared to males, females show stiffer single-leg landing which may be due to less hip and knee flexion displacements, greater peak ground reaction forces (GFR), and absorbing less total energy with more relative energy absorption at the ankle [171]. A stiffer landing could potentially load the ACL as it is an important non-contractile knee component. Additionally, in a study of sex-differences in double-leg landing with external body born load under various landing techniques, females exhibited larger peak GRF, greater knee valgus moments, and hip adduction range of motion compared to males [172]. However, many of these differences disappeared when the landing strategy was considered, suggesting skill or technique may underpin some of the reported differences in landing mechanics between the sexes, rather than an innate biological mechanism.

Indeed, direct comparisons of single- and double-leg landing in both sexes [173] revealed no sex-specific differences in GRF, knee kinematics, and external knee loading. Rather, differences were associated with the skill level and landing strategy used by the individuals [173].

Comparison between males and females across stages of maturation has shown greater external knee valgus (reported as internal knee varus) moment generated by females during a bilateral drop-land-jump task [174]. On the other hand, when landing biomechanics of males and females were compared during a countermovement jump landing versus landing from a vertical jump with no additional subsequent movement, the differences between sexes were dependent on the type of jump landing [175]. Interestingly, males generated greater hip extension moments and GRF compared to females during the landing from a jump with no subsequent movement suggesting stiffer landing style in men [175]. Together, these findings suggest the sex- differences in landing biomechanics identified from analysing a single type of landing task may be limited and not representative of differences (if they exist) between males and females in terms of net joint loading during dynamic activities.

Overall, it remains unclear if there are true sex-related differences in external knee loads evidenced during drop landing and jumping tasks. Moreover, knee motion and generalized knee loads may not have direct links to ACL loading nor explain differences in ACL injury risk between the sexes. Indeed, the forces experienced by the musculoskeletal system appear to be the most important factors in understanding the mechanism of non-contact ACL injury, where body experiences large muscle-driven accelerations. Consequently, researchers have also attempted to understand the role of muscles during provocative tasks and examine potential differences between the sexes.

When the knee is exposed to large moments and forces during physical activity, muscles are the active elements capable of maintaining joint stability [65]. Therefore, coordinated muscle contractions (i.e., appropriate activation timing and/or magnitude) are essential to generate joint loads to accelerate the body as well as to resist and distribute joint loads to prevent exposure of internal structures to harmful and injurious loads. Sex-related differences in neuromuscular action are suggested to be important explanatory factors for the higher rate of ACL injury in females. Compared to males, females use different knee joint stabilisation strategies (i.e., different muscle activation patterns), such as greater activation of the rectus femoris, gastrocnemius, and tensor facia latae during isometric weight bearing activities [176]. It is known the rectus femoris and gastrocnemii can contribute to ACL loading [44], thus, their elevated activation in females, as indicated by EMG, is an indirect and, possibly, weak (more on this later) indication of increased muscle force production, partly explaining the elevated ACL injury risk in females.

During drop-landing, women may demonstrate deficits in rapid hip extension moment generation, which consequently causes earlier knee extensor (i.e., quadriceps) activation [177]. This is in agreement with the higher hip extensor recruitment in males and greater use of quadriceps in females during a landing task when the two sexes were compared [173]. Thus, hip extensor weakness in females might lead to dependence on knee extensor muscles, which have the capacity to generate anteriorly directed force on the tibia and, potentially, increase ACL loading. Further, it has been suggested that adolescent female athletes exhibit muscle activation patterns that might not provide sufficient knee stability during demanding tasks such as unanticipated side step cutting manoeuvres [178]. These activation patterns in females involve higher quadriceps (i.e., rectus femoris) and gastrocnemius activation, and reduced hamstring activation at early contact phase of the task. Interestingly, the hamstring peak activation observed at the pre-

contact phase suggesting an attempt to prepare the knee for impact. However, this earlier activation of the hamstring might reduce their stabilization capacity when it is required sometime after foot-ground contact [178]. This is because the hamstring muscle group maximally contract before foot-ground contact, while this maximum capacity is most useful for ACL stabilization after the initial foot contact where the ruptures typically occur. Further, the higher gastrocnemii activity may be required by the females to enhance joint stability as it helps in knee flexion [179] but at the same time could place the ACL under greater strain [180] by contributing to posteriorly directed force on the femur relative to the tibia [44], potentially increasing the risk of ACL injury in the female population. Again, there needs to be caution in relying on the magnitude of muscle activations measured by EMG to infer the action of muscle in loading or unloading the ACL [27, 46].

In conclusion, despite the reported sex-related differences in knee kinematics such as greater knee valgus in females compared to males, the accuracy of non-sagittal knee kinematic measures is not established [159, 166, 167, 170] and thus it is unclear if greater knee valgus is an ACL injury risk factor in females. Similarly, there is no general consensus regarding sex-related differences in joint moments or their role as ACL injury risk factors. Some studies found females may experience greater externally applied valgus knee moment during landing tasks, or they may land with a stiffer technique, resulting in absorbing less total body energy. However, when the landing strategies were considered, no sex differences were found, suggesting differences are due to landing/jumping skill rather than being sex-related [174, 175]. Finally, the literature examining neuromuscular activation between males and females have reported females generally use muscle activation strategies that might not be optimal for the knee stabilization during demanding tasks such as landing and cutting [178].

2.3.3.2 Age-related comparison of external biomechanics

It has been reported that the risk of ACL injury increases with maturation [181]. Structural and inertial changes to the body such as increase in height, mass, and segment lengths throughout maturation could lead to higher external forces applied to the body [25, 182], which might influence the development of movement strategies and ultimately ACL forces. In particular, post-pubertal adolescent female athletes are at the greatest risk for ACL injury [24, 25]. This may be due to their decreased neuromuscular control and aberrant knee biomechanics [24, 54] during demanding dynamic motor tasks, which may impair their ability to modulate external forces, compared to adolescent males. It has been suggested these sex differences develop as a result of maturation and may not exist before puberty [24, 183]. Differences between sexes could increase throughout sexual maturation due to distinct hormonal changes between the males and females [184]. Indeed, a result of sexual maturation is often pronounced disparity in strength and performance between the sexes.

Males exhibit marked changes in biomechanical parameters related to landing across the course of sexual development. Generally, as males mature they demonstrate greater absolute and relative force production [185] and reduced motion of the knee in the frontal plane such as less dynamic knee valgus [186, 187]. In contrast, as females mature, they exhibit no decrease, or may in fact increase, in knee valgus rotations and moments during dynamic tasks [154, 182, 187]. A longitudinal study of females found larger valgus moments during landing [20] coincides with increases in ACL injuries incidence. Interestingly, females who were highly specialized in one sport, demonstrated larger maturation-related changes in knee valgus rotation and moment compared to females who played a range of sports and were less specialized [188]. In addition, other studies have reported as females mature, they demonstrate increasing hip adduction

angles and land with potentially stiffer lower limbs [15, 174, 187, 189]. These biomechanical changes in females as they sexually mature may be indicative of compromised neuromuscular control. Therefore, it is crucial to understand the role of muscles in relation to knee stabilization, so that ACL injury prevention training programs can be developed.

Neuromuscular deficits are commonly defined as deficits in power, strength, or coordinated muscle activation [190]. It has been suggested these deficits reflect compromised neuromuscular capacity to resist and distribute external joint loads experienced during physical activity. Consequently, these loads will be transferred to passive tissues (i.e., articulating bodies, menisci, and ligaments) thereby increasing injury risk [190]. However, few studies have examined changes in muscle activation patterns as a function of age. This might be due to the challenges related to measuring muscle activation patterns (via EMG) in paediatric populations and lack of standardization in the measures used to quantify knee control or muscle activation patterns. In a review of literature [191] that included only six studies, the challenges of generalizing the findings regarding the effects of age and maturation on muscle activation patterns were acknowledged and no strong conclusion was presented. One study that has examined differences in EMG patterns between boys and men during repetitive hopping tasks, found as task demands increased, mature males generated more effective leg stiffness likely through feedforward and reflexive pathways [192]. Yet, the literature to date provides no insight into this process in females or its effects (if any) on ACL loading.

In conclusion, consideration of maturation might be an important factor in assessing ACL injury risk profile in females. Across pubertal maturation in females, structural and inertial changes to the body, without matching strength and neuromuscular adaptations, may underlie the observed increase in knee loads and hence the increased

risk of ACL injury. However, these speculations have yet to be examined at the level of joint and ligament forces.

2.3.3.3 The effect of task planning, complexity, and cognitive demands

Non-contact ACL injuries typically occur during dynamic manoeuvres like sidestepping and single-leg landing, where an athlete must accelerate through multiple planes of motion. These tasks require concurrent movements in the frontal and transverse planes, which is believed to increase stress on, and the possibility of injury to, the ACL compared with tasks confined to the sagittal plane [41, 62]. However, the mechanisms and critical loads during dynamic, multiplanar movements are poorly understood [18]. Therefore, to understand the ACL loading mechanism during dynamic tasks, laboratory biomechanical studies have attempted to closely replicate real-world injurious sporting events by increasing temporal and visuospatial task demands.

Biomechanical and neuromuscular characteristics of unplanned tasks have been examined in laboratory studies that aim to replicate game situations when athletes demonstrate a sudden reaction to an external stimulus (e.g., movement of a ball or an opponent) or act quickly to gain better position within the playing area [193]. A systematic review of the literature on the effects of task expectancy in knee biomechanics [194] revealed that compared to planned side-step cutting, individuals demonstrated decreased knee flexion, increased knee valgus rotation, increased internal tibial rotation, and increased knee moments in all three planes of motion during the weight acceptance phase of the unplanned cutting task. The studies included in this systematic review used different approach velocities (ranging from 3.0 to 5.5 m s⁻¹), which might have impacted the kinematic and kinetic variables examined, meaning the differences could potentially be due to speed of approach rather than task planning. However, in some studies where the approach speed was controlled, large effects of task planning were still observed in

the external biomechanics and muscle activation patterns [195-197], suggesting task expectancy is an important factor to consider.

When side-step cutting was unplanned, a generalised co-contraction strategy of the muscles surrounding the knee was used compared to more selective activation of the medial knee muscles and co-contraction of the medial flexor and extensor muscle groups when the same task was planned [195]. This suggests when an individual makes quick decisions involving rapid change of direction, the generalised activation strategy of their muscles may not provide enough support for the increased frontal and transverse plane moments generated by unplanned tasks and may place the ACL at high risk of injury. This indicates that during planned cutting, tasks muscles of the knee adequately support external varus and valgus moments [153, 198], whereas in unplanned condition individuals are not using muscle activation patterns that could stabilize the knee joint. All the above mentioned individual joint biomechanics are typically assessed in isolation. However, the complex interaction between the segments/joints can be assessed through a dynamical systems approach by providing greater insight into the state of the system (e.g., high or low risk). For instance, coordination variability is reported to increase as a function of task complexity and reduced task planning time [199]. Overall, understanding the effect of anticipation on postural adjustments and incorporating perceptual components in training could aid optimising postural adjustments and muscle activation patterns to reduce external knee joint loading and better stabilize the knee joint, respectively.

Another approach in mimicking real world non-contact ACL injury scenarios is adding secondary cognitive tasks to increase task complexity. The effects of increasing numbers of virtual defender(s) (i.e., 1, 2, and 3) and a simple visual stimuli (i.e., an arrow) to signify cut direction were examined during side stepping tasks [200]. Compared to

arrow condition, sidestepping in response to the virtual defender(s) resulted in different postures and knee moments such as smaller hip external rotation at initial foot contact and larger peak knee valgus moments. More recently, the effect of allocation of attention imposed by a secondary cognitive task (i.e., counting with different complexities) on landing mechanics has been examined [201]. Individuals demonstrated decreased knee flexion angles at initial contact, increased peak posterior and vertical ground reaction forces during the first 100 ms of landing, as the complexity of the secondary cognitive task was increased. This suggests imposing additional cognitive challenge could lead to landing mechanics associated with increased ACL loading [201]. These results [201] are in agreement with the findings from a study on females where effects of simultaneous cognitive demands (i.e., grabbing an overhead ball and/or decision making) were examined during execution of a drop vertical jump [202]. The imposition of this cognitive demand resulted in lower peak knee flexion and greater peak knee valgus angles, and peak vertical GRF in comparison to standard task performance condition. Thus, task complexity and cognitive state interact to modify lower limb biomechanics, which may partially explain high rates of ACL injury during complex game play scenarios where athletes are attempting to evade defenders.

To develop ACL injury risk screening and prevention programs targeting relevant and modifiable neuromusculoskeletal risk factors, it is essential to use laboratory tasks that more closely mimic the real-world events of non-contact ACL injury. Researchers have tried to increase the performance requirements of the laboratory tasks to create more demanding and provocative testing environment. This has been approached by changing the anticipation status of the task (pre-planned vs. unplanned) [193, 203], incorporating additional cognitive demands to the tasks such as having virtual defensive player [200-202], all of which influence the lower limb biomechanics and neuromuscular profiles.

Collectively, these findings highlight the effects of stimuli complexity on the task performance, which might have implications for ACL injury screening and prevention protocols.

In conclusion, despite the enormous effort to understand the ACL injury mechanism [30, 32, 43, 204], the majority of the research in past decades has focused on external biomechanics of the lower limb such as joint kinematics, external joint moments, and muscle activation patterns (i.e., EMG), which are considered surrogate measures of ACL load and/or ACL injury risk [193, 195, 200, 203, 205]. These surrogate measures may provide useful information in identifying the conditions or circumstances that might promote the ACL injury risk. However, these external surrogate biomechanical measures do not represent the internal mechanics (e.g., ligament or joint compression forces) [45] and have limitations if used to assess loading of the internal structures. For example, external loading applied in cadaveric studies will induce different loading to the ACL dependent on the simulated muscle forces [206]. Furthermore, assessing muscle action based on EMG signals alone might carry errors, since muscle activation by itself does not afford direct information about muscle force and action [27, 207]. Muscle force production depends on many factors such as cross-sectional area, length and velocity of muscle [207], and the final action of muscles forces depend on their lines of action [46]. Indeed, the loading in the ACL during dynamic movement is a result of complex interaction between many factors including the forces and moments that are applied to the knee joint, the position and orientation of the lower limbs, and the muscle forces and lines of action. Therefore, only if the ACL force can be determined, concurrent with the external biomechanical measures, can the true ACL loading mechanisms be understood.

2.4 Determining anterior cruciate ligament loading: measurement and models

Studying the ACL load during dynamic motor tasks can be achieved by direct or indirect measurements and computational modelling. Measurement, in comparison to computational modelling, has the advantage of accuracy, precision, and lower uncertainty. However, direct measurement as a routine approach in ACL research is not feasible because the measurement of loads developed inside the body can be very challenging, requiring expensive equipment, and surgically invasive techniques. Therefore, computational models which can provide estimates of joint, muscle, and ligament forces using non-invasive measurements of movement, external loading, and muscle activations have been developed.

2.4.1 *In vivo* measurements of anterior cruciate ligament loading

Direct *in vivo* measurement of internal body mechanics is often necessary to develop and validate computational models, evaluate the assumptions about loading mechanism, and gain insight into which movements and conditions generate higher internal loading. In addition to ACL load, direct *in vivo* measurement has been deployed for joint contact (e.g., knee [208, 209] and hip [210, 211]) and tendon [212, 213] force measurements. In particular, the tibiofemoral contact force measurements from instrumented prosthetic implants have proved extremely useful in evaluating the robustness of different computational modelling approaches [209], in an international competition to demonstrate which laboratory and, moreover, methods could best predict *in vivo* contact forces using only gait laboratory external biomechanical measures and medical imaging.

In vivo measurements of ACL strain have also been conducted for a range of motor tasks (e.g., isometric contractions of the lower limb muscles, squat, lunge, sit-to-

stand, stationary cycling and stair climbing, rapid deceleration task, etc) and under different conditions (e.g., weight bearing and non-weight bearing) [147, 214-223]. These measurements were made using implantable sensors whereby a transducer was arthroscopically embedded into the anteromedial bundle of the healthy ACL. Overall, these direct measurements show isometric contractions of the quadriceps can generate high ACL strains when the knee is at low flexion (15-30°) [215], and the corresponding strain produced is lower when the knee is more flexed [214, 215, 223].

Direct measurement has also revealed weightbearing, compared to non-weightbearing, can cause higher ACL strain for the same motor task [221]. The ACL strain in response to open- and closed-chain exercises, is an area of clinical interest, yet is a topic of debate in musculoskeletal rehabilitation practice. Direct measurement found during open-kinetic chain exercise, increased muscle activity, generated by applying external weight or resistance, leads to higher strain in the ACL [215, 220], whereas this effect on ACL strain was not observed during closed kinetic chain exercises [219, 222]. This might mean closed kinetic chain exercises could be used when high levels of muscle activation are desired (e.g., rehabilitation exercise aimed at recruiting the quadriceps), but large ACL strains are to be avoided (e.g., during early rehabilitation following ACLR). Direct measurement of ACL strain during dynamic task (e.g., single-leg hopping and stop-landing tasks) have also been performed, and peak ACL strain was observed at the time of peak ground reaction force shortly after landing. Notably, the peak ACL strains reported from direct measurement of dynamic motor tasks were much higher compared to those recorded during a Lachman test for the same participant [147].

More recently, advanced non-invasive imaging techniques have been used to indirectly measure ACL strain during dynamic tasks. Magnetic resonance imaging (MRI) and high-speed biplanar radiography have been used in combination to indirectly measure

in vivo ACL strain during single-leg jump and treadmill gait [204, 224]. In this method, MRI of the lower limb is acquired in a static posture and used to derive three-dimensional models of the femur, tibia, and associated ACL attachment sites. These three-dimensional models of the bones and ligaments attachment regions are then registered to biplanar radiographs. This registration enables estimation of the three-dimensional bone and ligament positions via radiography while the individual performs a dynamic motor task [225]. For single-leg jumping, the ACL strain was reported to be inversely associated with knee flexion angle when a simple correlation between these two biomechanical measures was performed [204]. This inverse correlation was in agreement with previous direct and imaging-based measurements from other tasks [147, 226]. Peak ACL strain was observed ~50 milliseconds before landing [204], and decreased during landing. However, these patterns are not consistent with the existing literature, as videography analysis [144] of injury events and previous destructive testing of human cadavers [62, 227] indicate the time of peak ACL loading to occur shortly after initial foot-ground contact.

Currently, comprehensive biomechanical data, comparable to that which was generated and made public as part of The Grand Challenge to Predict *in vivo* Knee Loads [209], has not been reported in the study of ACL biomechanics, which limits interpretation of the results of the existing studies. If acquired concurrently, comprehensive biomechanical data (e.g., motion, external loading, muscle activations, and medical imaging) and direct measurement of *in vivo* ACL strain would enable development, verification, and validation of ACL load models and loading mechanisms [204]. This would clarify the strengths of different modelling approaches, but also provide great insight as to how therapeutic exercises may aid in modulating ACL loading and inform rehabilitation protocols (e.g., retraining, surgical intervention, assistive device).

In conclusion, measurement of ligament force/strain can be very challenging, requiring expensive and surgically invasive techniques. Further, imaging based methods used for ACL strain measurements face known issues surrounding measuring the “unloaded” ACL to establish a reference length [228] and thus reported ACL strains may carry error. Moreover, direct measurement decoupled from physics-based computational models is only useful for establishing normative or physiological data during standard activities, as the measurement alone does not explain its causes. Consequently, there is a clear need to use simulations via musculoskeletal and computational models to investigate the mechanical loading, its causes, behaviour of soft tissues (e.g., muscle and ligament) during movement, and the resulting effects on other structures within the musculoskeletal system [229, 230]. There are various approaches to computational modelling of the knee and neuromusculoskeletal system, and in the following sections examples of the most common approaches are reviewed.

2.4.2 Computational models of anterior cruciate ligament

There are various computational approaches (i.e., finite element, elasto-structural and mathematical models) used for studying ACL mechanics. All these modelling methods require motion data (e.g., joint kinetics and kinematics and muscle forces) as boundary conditions, of which estimation of *in vivo* muscle forces may be the most challenging. It is essential to determine a set of muscle forces that satisfy the physics of the rigid multi-body system. Indeed, determining the *in vivo* muscle forces is an indeterminate issue since the forces and moments necessary to create joint motions are produced by the joint reaction forces as well as the many active and passive soft tissue forces [231]. This means many combinations of muscle activations and forces generate a certain joint moment and thus the mechanical problem has many solutions. This issue is profound since different muscle force solutions for a given posture and external loading can have divergent effects

on the internal loading of the articular tissues, such as cartilages, ligament, and menisci, etc. For example, different estimates for knee joint compression forces have been observed when different approaches were used to estimate muscle forces [209] despite identical input data (i.e., external biomechanics).

2.4.2.1 Estimation of *in vivo* muscle forces using neuromusculoskeletal models

The function of muscles can be investigated, and muscle forces can be quantified using neuromusculoskeletal (NMSK) models. An NMSK model is a mathematical and computational representation of the human body and its internal structures such as bones and muscles interconnected by joints. Biomechanical simulations commonly use experimental data (e.g., 3D trajectories of the markers associated with each body segment, ground reaction forces) to move NMSK models in space and compute joint angles and moments [232-234]. Muscle tendon unit (MTU) kinematics (i.e., muscle tendon lengths and muscle moment arms) can also be readily estimated, once the joint angles are determined. Collectively, NMSK modelling can be undertaken using several musculoskeletal modelling software, with OpenSim [230] being particularly popular as it is free and open-source.

Different algorithms are employed for the neural solutions within NMSK models to resolve the muscle redundancy problem and thereby compute muscle activations, and subsequently, muscle forces. These algorithms determine a unique set of muscle activation patterns to produce specific experimental joint moments by satisfying a criteria for their activation. For example, static optimization, the most widely employed method to estimate muscle activation, uses *a priori* criteria expressed in an objective function to predict the muscle activations that satisfy the measured joint moments [235]. With little experimental evidence for their validity, the static optimization objective function aims to minimise the sum of squared muscle activations. The assumption being that humans

organise their muscles to minimise muscle activation. Other criteria have been used, such as minimisation of muscle forces or energy expenditure [236], however, these are logical derivatives of minimized muscle activation. Apart from the lack of evidence to support use of pure optimization when predicting muscle activations, many implementations of the static optimisation formulation neglect certain aspects of muscle-dynamics by assuming the tendon is rigid. Consequently, muscle excitations and activations generated via static optimisation do not correctly represent the timing or amplitude of experimental EMG data [237, 238] and unconstrained static optimisation is unable to reproduce atypical muscle co-contraction and neuromuscular strategies used to stabilise joints [239, 240].

On the other hand, experimental EMG can be used to help solve for the muscle redundancy problem and possibly generate more physiologically plausible estimates of internal biomechanics. These so called EMG-informed approaches [240-242], which employ experimental EMG in the computation of muscle activations, are proven to be efficient and overcome many limitations of (unconstrained) static optimisation methods [209]. In EMG-informed approaches, muscles are commonly represented as the parallel of a contractile element and an elastic element, in series with an elastic component representative of the tendon [243]. Thus, muscle activation and force estimation strongly depend on the defined MTU parameters (i.e., tendon slack length, optimal fibre length, pennation angle, and muscle maximal isometric force). To ensure dynamically consistent estimation of muscle forces, it is essential to calibrate the internal MTU parameters, while restraining them to be within physiological ranges, using other measured data such as experimental joint moments and EMG [237, 241, 242, 244-247].

The EMG-informed methods might be limited by issues surrounding the use of EMG data to drive neural solutions. These issues include limitations in the number

muscles from which experimental EMG can be collected, and noise and cross talk in EMG signals. In the Calibrated EMG-informed Neuromusculoskeletal Modelling Software (CEINMS) [241, 242], these issues are addressed by calibration and by using EMG-informed hybrid methods to account for muscles without EMG and expand the number of modelled MTU while accounting for EMG errors. The CEINMS is an OpenSim toolbox, and employs experimental EMG signals, joint angles, joint moments, and MTU kinematics from OpenSim to calibrate MTU parameters and constrain them within physiological ranges. Once calibrated, CEINMS predicts muscle activations and forces [241, 242, 248]. The Hybrid EMG-assisted neural solutions implemented in CEINMS synthesise the MTU excitations without corresponding experimental data and minimally adjust the experimental excitations to ensure dynamically consistent muscle force solutions. Therefore, the resulting NMSK models are able to better track experimental joint moments along with EMG data [237, 238, 241, 245, 249], and reproduce more physiologically plausible internal biomechanics [241, 245].

To ensure the validity of estimated muscle forces, they should be possible physically (i.e., satisfies the physics of the rigid multi-body system), plausible physiologically (i.e., respect known behaviour of skeletal muscle), and respect the empirically-observed muscle excitation patterns, known to vary between individuals, [250] control tasks [251, 252] and in response to pathology [253] or training [254, 255]. Recent studies have shown muscle modelling methods that incorporate both subject- and task-specific biomechanics (i.e., motions and external loading) and muscle activation patterns (i.e., conditioned EMG) can generate muscle forces that well satisfy the physics of the rigid multi-body system [240, 242], yield physiologically plausible muscle fibre mechanics [256], respect many empirically observed features of muscle coordination

such as co-contraction [237], and well estimate knee joint compression forces measured using instrumented prosthetic implants [257].

Importantly, this approach to neuromusculoskeletal modelling which is “informed” by EMG data has been widely applied to different joints (knee, hip, and shoulder), healthy populations performing many different motor tasks [153, 198, 240, 258-260], and in clinical populations of people who have suffered a stroke [247], undergone ACLR [261-263], or have osteoarthritis [237, 264]. Importantly, EMG-informed neuromusculoskeletal modelling of lower limb incorporating the knee joint satisfies the available criteria (e.g., patient specific scaling of the model, simulations that match external biomechanics and respect the experimental EMG) that are used for validation of the models [265]. These validated musculoskeletal models have been previously performed for a wide range of tasks such as walking, running, and side-step cutting [195, 198, 237].

2.4.2.2 Finite element and elasto-structural models of ACL

The mechanics of the ACL are important to consider when investigating the injury mechanism. Traditional biomechanics using multibody musculoskeletal models do not provide quality estimates of loading of largely deformed tissues. This is because they do not well account for the mechanics of internal tissues (e.g., ligaments) due to the complexities in modelling internal tissue mechanics, and thus resort to simplified kinematic joint. Finite element and elasto-structural models are approaches to study the mechanics of deformable joints [266, 267] and articular tissues such as ligaments [268, 269], cartilage [270, 271], menisci [272, 273], and muscle [274]

Despite numerous variations in formulation and details, these models are constructed based on three-dimensional geometrical data of bones and attachment sites

of the passive and active structures, with the mechanical properties of the reconstructed structures determined from experimental data, literature, or optimization. Once constructed, the measured or estimated joint motion, muscle and external loads, are applied to the model as boundary conditions. These deformable joint models can then determine secondary joint kinematics, the deformation and internal loading of the ligaments and other soft tissues, contact pressures/stresses, etc.

The finite element method is a numerical tool to solve mechanical problems. In biomechanics it is used to study the complex interaction of motion, morphology, and loading within the joint and inside constituent tissues. The finite element method uses numerical solution techniques to analyse non-linear, continuous, and complex deformation of tissues by discretising the tissues into many small elements and formulating their constitutive behaviour [275]. Several finite element knee models have been developed and validated for analysis of ACL mechanics [40, 275-277]. For example, in a complex knee loading scenario, Navacchia *et.al* used finite elements models of male and female individuals and estimated ACL force during impact of a landing task, and demonstrated significant contribution of tibiofemoral contact force to ACL force, which was exacerbated when combined with externally applied valgus and internal rotation moments [40].

Although finite element analysis is a powerful method for quantifying the mechanics of soft tissues such as ligaments [278], it is computationally demanding to incorporate finite element joint model into neuromusculoskeletal model of human dynamics [279]. Therefore, most analysis using the finite element method is conducted at one time point within dynamic cycle of movement. Furthermore, finite element models require extensive and explicit knowledge of the material properties and precise geometry of the included tissues, which makes the widespread use of this method in cohort or

longitudinal studies impractical. Thus, due to computational demands, and inherent complexity, finite element models are not widely used to study the relationships between the joint biomechanics, muscle force, and whole-body dynamics.

Elasto-structural models are used as a less computationally demanding alternative to the finite element method. In this approach, many components within the joint are simplified. For example, bone is assumed rigid [280] and ligaments as linear one-dimensional elements [32-34, 38, 39, 58, 281-284], while the menisci are neglected or modelled as multi-body systems [285], and cartilage mechanics are simplified or modelled analytically to determine contact mechanics [286]. These models can be embedded within whole-body simulations of movement to establish dynamic consistency between the full body movement and joint-level mechanics [229]. Although elasto-structural models are simplified compared to finite element models, they still require an explicit description of the geometry of the system (i.e., articulating bodies, tissues, etc) and the mechanics of the actuators and other elements. These must be measured through resource-intensive medical imaging, estimated from statistical shape models of these tissues [265, 284], or resolved through exhaustive optimization methods. Moreover, due to the stiff elements within the knee and its over-constrained nature, small errors in the geometry of the system may cause non-physiological events (i.e., interpenetration or subluxation) or numerical problems (i.e., optimizers failing to converge or taking days to solve). Even after extensive optimization, non-physiological behaviour, such as discontinuities in the joint kinematics, can still be observed [287].

Despite the abovementioned limitations, elasto-structural models have been the primary modelling class used to study the behaviour of the ACL under different loading and kinematic conditions [32-34, 38, 39, 58, 281-283]. Pandy and colleagues were the first to implement a modern elasto-structural model of the knee. Their model included

detailed bone geometries, numerous ligaments, and knee-spanning muscles [33, 281, 282], and was used to study dynamic tasks of walking and rising [34, 38, 39, 58, 288], which revealed the importance of knee spanning muscles in generating contact and ligament loading within the knee. Since then, similar models have been applied to study drop landing [32] which proved challenging for the model to match experimentally measured data, likely identifying a lower-bound for the ACL force developed during this task.

Elasto-structural models have been combined with data from experiments on cadaveric specimen to provide insight into the complex relationships between muscle, joint contact, and ground reaction forces on ligament loading [35]. In those experiments, artificial muscle forces and loads were applied to a cadaveric knee specimen mounted in a custom robotic rig [35]. The ACL was instrumented with a strain gauge and the measured strain was used in validation of the subsequent elasto-structural model, which was built to match the geometry of the cadaveric specimen, while using literature data for the mechanical properties of the muscle-tendon and ligaments. The model performed well against the ACL strain measurements and confirmed prior speculation that posteriorly directed externally applied forces during rapid deceleration may have a protective effect on the ACL by applying considerable posterior force to the tibia. However, this study did not apply complex loading to the knee, which we know is present during the tasks commonly associated with ACL injury (i.e., side-step cutting and single-leg landing) [153, 198, 261]. Nonetheless, this demonstrates that elasto-structural models can be accurate predictors of the ACL strain when the geometry and mechanical properties of the knee's internal tissues are explicitly known. This requirement for explicit knowledge of the system geometry and mechanical properties could potentially limit the practicality

of these models to small cohorts where availability of highly detailed geometrical and mechanical is possible.

Overall, finite element and elasto-structural knee models have highlighted the critical role of muscles in ligament and articular contact loading during dynamic tasks. This means that external biomechanics (i.e., joint postures and net moments) do not directly provide insight into the causal factors behind ligament loading. Rather, computational models are required to understand the complex, dynamical, and non-linear relationships between external loads, muscle activation, joint contact, and ligament forces. However, the computational cost imposed by finite element and elasto-structural models is a barrier to their widespread use, particularly in clinical or in-field studies. In future, improved computational hardware and algorithms might facilitate the use of these computational models for real-time applications. However, even if computational model renders finite element and elasto-structural models fast enough to be incorporated with neuromusculoskeletal models of muscle dynamics [279], the additional requirements of accurate system geometry and explicit knowledge of the mechanical properties of the tissues involved will make these models difficult to deploy regularly [278]. Nonetheless, new developments in artificial intelligence [265] may provide powerful new techniques to reduce the time and computational burden of finite element and elasto-structural models which will enable use of physics-based approach in human biomechanics.

2.4.2.3 Phenomenological mathematical models of anterior cruciate ligament loading

Phenomenological mathematical models of the ACL function are a non-invasive and computationally inexpensive approach to quantify ACL loading. These mathematical models use joint angles, joint moments, muscle and tibiofemoral contact forces as input to predict the force or strain developed within the ACL. For the study of live humans,

these models are necessarily coupled with a method to estimate muscle forces, typically though neuromusculoskeletal modelling or mechanical optimization [31, 36, 37].

The premise of these mathematical models is that ACL loading is a phenomenon that can be described with mathematical formula without the need for explicit representation of the ACL in the model [31, 36, 37, 41, 42, 62, 152]. To this end, the ACL load is a function of known inputs, with the emphasis on the validity and generalizability of the function. Practically, in these mathematical ACL models, simple equations represent the relationships between the joint external (i.e., intersegmental loads) and internal (generated/resisted by muscle, contact, and ligaments) loads for one or multiple planes of motion. In each equation, the “ligament load” is an unknown but can be solved for, provided the joint kinematics and external loads, muscle forces and/or joint compression force are known. The ligament load represents the net load sustained by all knee ligaments and other passive soft tissues about the knee and is not equivalent to the load developed in the ACL. The load in the ACL is then determined by set of algebraic equations, developed to describe empirically observed behaviour of the ACL, under different magnitudes and combinations of externally applied knee loads, acquired from experiments performed on cadavers.

Kernozek *et al.* developed the modern phenomenological mathematical model of ACL force and demonstrated its application in human landing biomechanics. This model was a uniplanar model confined to the sagittal plane [31], and based on experiments performed on cadavers wherein ACL force was measured in response to small magnitude externally applied loads over a wide range of knee flexion angles [41, 42]. These experiments used only 0 N and 100 N of external load applied anteriorly to the tibia, thus Kernozek *et al.* developed a simple equation for the resulting ACL force based on net anterior tibia force and knee angle. In their equation, it was assumed the ACL force was

proportional to the applied external load [31]. Their results indicated that during a bilateral landing task, peak ACL force occurred early in landing, between forefoot touch down and heel impact. They also found patellar tendon and compressive forces contributed most to ACL force, especially at small knee flexion angles, while hamstrings and the posterior component of the ground reaction forces decreased ACL force. Overall, this study introduced a simple and readily deployable mathematical model of ACL force for biomechanical studies. However, this model was restricted to the sagittal plane and was not validated. Moreover, their model may underestimate the ACL force if used to model more provocative movements such as those associated with ACL injury risk where multiplanar knee loading is present [41, 62, 152] as it is unclear whether the established relationships between modest magnitudes of applied joint loading and ACL force can be extrapolated to larger magnitudes or complex loading combinations.

Weinhandl and colleagues [36, 37] extended the model developed by Kernozek and colleagues [31] to include loading contributions from frontal and transverse planes. This was done by developing exponential functions to estimate the contributions to ACL force from loading applied to the knee through frontal and transverse planes from the same cadaveric experiments [41, 42] used in the original model by Kernozek and colleagues [31]. In this extended model by Weinhandl and colleagues [36], the ACL force was calculated as the sum of the forces estimated through each isolated plane of motion. Using their model, Weinhandl *et al.* estimated ACL loading during anticipated and unanticipated side-step cutting in females [36], reporting higher ACL load during unanticipated compared to anticipated side-step cutting. They also reported the ACL was primarily loaded through a sagittal plane mechanism, however, acknowledged ACL loading resulted from an interaction of sagittal, frontal, and transverse plane knee loads [36]. Overall, this model was purported to account for the multiplanar mechanism of the

ACL loading by summation of the uniplanar ACL loads. However, cadaveric studies clearly indicate the effects of multiplanar loading on ACL force is not the linear sum of the ACL forces developed from equivalent uniplanar knee loads [41, 62], upon which their ACL loading model was based [36, 37]. Rather, combined knee loading produces disproportionate (i.e., weighted) and non-linear (i.e., powered) effects on ACL forces. Inspection of the results from uni- and multiplanar loading of cadaveric specimens [41, 62] reveals that linear summation of equivalent uniplanar loading can over- or underestimate the ACL force measured during multiplanar knee loading depending on knee angle and magnitude of combined external loads. However, Weinhandl *et al.* did not present validation of their formulations and in their mathematical expressions, nor did they account for the non-linear summation feature. In addition, their mathematical formulations [36] do not correctly reproduce the ACL force values even when supplying the same cadaveric data used to derive the formulations as inputs to their model.

Overall, validated computational models are essential to study ACL forces during dynamics tasks. Amongst the many models developed, the ones that have been validated (e.g., elasto-structural and finite element models), require explicit knowledge of the system geometry and mechanics in order to estimate accurate ACL force values. This requirement of explicit knowledge may limit the feasibility of such models to be used in large cohort studies, or for clinical and in-field applications. Thus, mathematical modelling is an alternative approach for computationally inexpensive ACL force estimation. However, it is essential for these models to be validated and account for the multiplanar nature of ACL loading, yet these features appear to be missing in the existing models.

2.5 Conclusions

Age- and sex-related differences in rates of ACL rupture are well documented. Female athletes have been reported to be at higher risk of ACL injury compared to their male counterparts, and females at later stages of pubertal maturation are at approximately four times greater risk of sustaining ACL rupture compared to pre-pubertal girls. To understand the ACL injury mechanism and explain the age- and sex-related differences in injury rates, the vast majority of literature has focused on external biomechanics (i.e., joint kinematics, generalized joint forces and moments, GRF, and muscle activation patterns) as surrogate measures of ACL loading and potentially modifiable risk factors for ACL injury. Indeed, a plethora of studies have speculated about the role of puberty-related changes to anatomy, external joint biomechanics, strength, and neuromuscular control on ACL loading. However, external biomechanics do not represent the loading of the internal structures, such as the ACL.

In all cases, ACL injury is due to excessive force (i.e., tension) applied to the tissue, whereby excessive being any value greater than what it can resist without breaking. The logical questions are then how we can move our bodies, load our joints, and coordinate our muscles to increase or decrease the ACL force and whether this can be brought under voluntary control. Regarding movement tasks, prior studies have quantified the *in vivo* ACL force using surgically implanted strain gauge or indirect measurements (i.e., biplanar radiography). However, due to the limitations associated with these approaches (e.g., invasiveness, time and resource demands, small field of view), they are not feasible approaches for cohort analysis. Moreover, the set of muscle coordination patterns that can produce a given movement and external loading are infinite [289]. Thus, when decoupled from neuromusculoskeletal models, direct/indirect measurement of ACL loading *in vivo* provides an ACL loading profile for the specific

individual using their body in a specific way; however, does not quantify the causal contributors to the ACL loading. At best, this provides examples of physiological loading profiles.

Alternatively, computational models (e.g., finite element and elasto-structural model) have been developed to determine ACL force during dynamic tasks and to gain insight into the causal contributors. The computational cost and requirement for explicit formulation of the systems (i.e., geometry, mechanical properties, etc) makes finite element and elasto-structural models impractical for cohort analysis. Notably, the combination of validated neuromusculoskeletal and phenomenological models of ACL loading has not been attempted in the literature let alone used to explore the effect of maturation in females on ACL loading. Despite a vast literature surrounding the topics of ACL injury and its peculiarities to young females, the mechanisms of ACL loading in live humans during dynamic activities remains elusive.

CHAPTER 3

General methods

This chapter describes the gait laboratory data collection, data processing, and neuromusculoskeletal modelling used in this thesis. The experimental gait laboratory data consist of three-dimensional motion capture (MOCAP), ground reaction forces (GRF), and surface electromyography (EMG) concurrently and synchronously acquired, while human participants completed various motor tasks. These data were collected from ninety-three participants at the Centre for Health, Exercise & Sports Medicine, University of Melbourne, Australia. The experimental data were processed and used in a neuromusculoskeletal modelling framework to determine intersegmental loads (i.e., net joint forces and moments) and estimate muscle and joint contact forces. Finally, an ACL loading model was developed and validated using publicly available measurements from experiments conducted on cadavers (presented in detail in Chapter 4). This ACL loading model was subsequently applied to the live human laboratory data to investigate ACL force generation, its contributors, and the effect of maturation on both ACL loading and its contributors, presented in Chapters 4-6. Finally, this General methods chapter concludes with an overview of the statistical analyses that were performed to investigate the ACL model's validity, ACL force generation, and its contributors in Chapters 4-6.

3.1 Participants

Ninety-three healthy physically active females were recruited from the University of Melbourne campus, surrounding schools, and local sporting clubs in Melbourne,

Australia. After the required permissions were gained from these organizations, advertisement via newsletters, posters and/or brochures were released that targeted females aged between 7 and 25 years. All interested participants and parents/guardians were screened for eligibility via an online process.

Inclusion criteria were: aged between 7 and 25 years, regular physical activity participation (i.e., performed at least 30 minutes of moderate or vigorous physical activity daily with no restrictions on type of activities), and of healthy weight (i.e., body mass index (BMI) $<30 \text{ kg/m}^2$) to avoid excessive soft tissue artefact causing motion analysis issues [166]. Candidate participants were excluded if they had a history of lower limb injury, medical condition affecting walking, running and jumping, knee pain, any previous ACL, meniscal or patellofemoral joint injury. Further, candidate participants were excluded if they were using bi- or tri-phasic oral contraceptive pill, or orthotics (medically prescribed or over the counter).

Participants of or older than 18 years of age or parents/guardians of those under 18 years of age completed an online questionnaire, providing a yes or no response for each of the inclusion/exclusion criteria. If eligible, participants (and parents/guardians of those under 18 years of age) provided their written informed consent via email or pre-paid postage. Participants were categorised into one of three pubertal maturation groups based on self-rated Tanner staging for breast development, growth spurt (i.e., 7.5-9.0 cm growth in the past 6-months), and menarche (i.e., first occurrence of menstruation [290, 291]). The pubertal maturation groups were pre-pubertal (Tanner stage 1), early/mid-pubertal (Tanner stages 2 and 3 and either growth spurt or menarche), or late/post-pubertal (Tanner stages 4 and 5, both growth spurt and menarche). Participants provided their pubertal maturation assessment by completing an online, de-identified questionnaire containing pictures and modified diagrams [290, 291]. The questionnaire also included

the question “*The adolescent has grown 3-3.5 inches (7.5-9cm) in the past 6 months or is past this growth spurt*” that indicated if the adolescent growth spurt had occurred. The question “*The adolescent has begun menarche (period)*” was taken from the modified pubertal maturation observational scale [183, 292] to indicate whether menarche had commenced. Participants aged more than 12 years completed the questionnaire themselves to improve reliability and validity [293, 294], whereas for those under 12 years of age, all pubertal assessment information was provided by a parent/guardian.

3.2 Data collection

3.2.1 Hormonal considerations

Due to the potential for the high levels of estrogen during and after puberty to influence lower limb biomechanics [22, 295], the following approaches were taken to ensure all participants underwent biomechanical testing with low levels of estrogen. Eumenorrheic participants not using a monophasic oral contraceptive pill were tested within their early follicular phase (i.e., first 7 days of menstrual cycle). For those using a monophasic oral contraceptive pill or had not yet experienced menarche, testing was performed at their convenience any time during their menstrual cycle. In addition, salivary concentrations of endogenous estrogen (5 mL, Nutripath Integrative Pathology, Melbourne, Australia) were measured at the time of testing from each participant to confirm that they were tested with low estradiol levels (including the pre-pubertal group). Saliva samples were stored at -20° C and subsequently analysed via enzyme immunoassay according to the manufacturer's instructions. Low levels were defined as estradiol concentrations <18 pmol/L, based on reference ranges for the follicular phase.

3.2.2 Integrated motion analysis

3.2.2.1 Laboratory setup

A 12-camera motion analysis system (Vicon Motion Systems Ltd, Oxford, UK) was used to acquire the position of skin-mounted retroreflective markers in a three-dimensional (3-D) capture volume. Prior to motion data collection in each testing session, the laboratory was inspected for any reflective material that could be inadvertently captured by the cameras. Following this, any remaining objects, other than markers, appearing in the camera image space were masked. Subsequently, a dynamic calibration was performed using an MX calibration wand with five reflective markers. The calibration process consisted of waving the wand in a figure of eight pattern, while walking throughout the capture volume. The 12 cameras simultaneously recorded the 2-dimensional (2-D) marker positions from which Vicon Nexus software (version 1.8.5) calculated the 3-D position within the laboratory space. After each attempted calibration, quality was assessed, and calibration was accepted only if the image error for all the cameras was ≤ 1 mm. In the event image error was > 1 mm, the calibration was repeated until the ≤ 1 mm threshold was met [296].

Three ground-embedded force platforms (OR6-6-2000, Advanced Mechanical Technology Inc, AMTI, Watertown, MA, USA) were used to record GRF during motor tasks. Prior to data collection in each testing session, an L-shaped frame was placed at the edge of the force plate to establish the three planes of reference also known as the XYZ global co-ordinate system. All cameras captured the three markers on the L-shaped frame which allowed the system to correctly detect their location in space. All marker trajectories and GRF were captured at 120 Hz and 2400 Hz, respectively.

For each participant, their skin surface was prepared by shaving, abrading, and cleaning specific areas with an alcohol swap. Eight surface EMG sensors were placed on selected muscles of the lower limb (Table 3.1) consistent with the surface EMG for non-invasive assessment of muscles (SENIAM) guidelines [297]. The EMG data were sampled at 2400 Hz using Noraxon DTS 2400 wireless telemetry sensor system (Noraxon, Arizona, USA). Hypoallergenic sports tape was wrapped around thigh and shank segments to hold all surface EMG sensors in place during motion, thus reducing movement artefact.

Table 3.1. *List of lower limb muscles from which experimental surface EMG data were collected and corresponding acronym.*

| Muscle name | Acronym |
|-----------------------|----------------|
| Vastus medialis | VM |
| Vastus lateralis | VL |
| Biceps femoris | BF |
| Semitendinosus | ST |
| Tibialis anterior | TA |
| Medial gastrocnemius | MG |
| Lateral gastrocnemius | LG |

3.2.2.2 Participant preparation

Each participant was asked to wear a pair of athletic shorts and a t-shirt with holes for designated trunk markers. At the beginning of each testing session, following a saliva sample collection, each participant's anthropometric data, including height, mass, and leg length, were measured (see Table 3.2 for full description of measurement methods). Then, the footedness subscale of the Lateral Preference Inventory [298] was used to select the dominant lower limb for subsequent analysis.

A total of 40 reflective markers (radius = 13 mm) were attached to the participant's body (Figure 3.1 and

Table 3.3) using double sided tape in accordance with Schache and Baker configuration [299]. Six markers were removed after static calibration and 34 markers were captured during the dynamic trials. Non-reflective tape was used to prevent any part of the t-shirt or shorts from obscuring the cameras view of markers.

Table 3.2. *Anthropometric measurement description and technique.*

| Measure | Description | Technique |
|------------|---|--|
| Body mass | Participant mass | Via a weighing scale (Model 209, Salter Ltd, Kent, UK) recording in kilograms (kg) to the nearest 500 grams. Participant remove shoes for measurement. |
| Height | Participant height | Via a stadiometer in metres (m) to the nearest millimetre (mm). Participant removes shoes for measurement |
| Leg length | Distance between greater trochanter and floor | Via a standard measuring tape is used while participant is standing. |

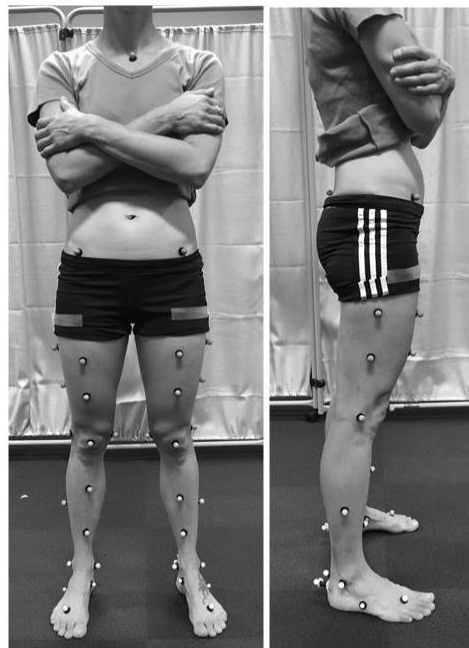


Figure 3.1. *Motion analysis marker set, frontal and lateral views.*

Table 3.3. List of forty motion capture markers affixed over participants' body for scaling purposes and biomechanical simulations.

| Body segment | Marker name | Anatomical landmark |
|--------------|----------------|--|
| Trunk | MAN | Jugular notch |
| | T2 | 2 nd thoracic vertebrae |
| | T10 | 10 th thoracic vertebrae |
| Pelvis | LASIS/RASIS | Right/left anterior superior iliac spine |
| | SACR | Midpoint of both Posterior superior iliac spine |
| Thigh | LTHAP/RTHAP | Right/left proximal anterior thigh |
| | LTHAD/RTHAD | Right/left distal anterior thigh |
| | LTHLP/RTHLP | Right/left proximal lateral thigh |
| | LTHLD/RTHLD | Right/left distal lateral thigh |
| | LLEPI/RLEPI | Right/left lateral epicondyle of knee |
| | LMEPI/RMEPI* | Right/left medial epicondyle of knee |
| | RPAT/LPAT | Right/left patella |
| Tibia | LTiAP/RTiAP | Right/left proximal anterior tibia |
| | LTiAD/RTiAD | Right/left distal anterior tibia |
| | LTiLAT/RTiLAT | Right/left lateral tibia |
| | LLMAL/RLMAL | Right/left lateral malleolus |
| | LMMAL/RMMAL* | Right/left medial malleolus |
| Foot | LHEEL/RHEEL | Right/left distal calcaneus |
| | LHEEL2/RHEEL2* | Right/left proximal calcaneus |
| | LMFS/RMFS | Right/left mid foot superior |
| | LMFL/RMFL | Right/left mid foot lateral |
| | RTOE/LTOE | Right/left junction between of 2 nd and 3 rd metatarsal phalangeal |

*indicates the six markers were removed after static calibration.

3.2.2.3 Data acquisition

After participant preparation, participants completed a standing calibration trial used eventually to scale and pose a musculoskeletal model. Participants were instructed to stand still, feet approximately shoulder width apart and arms folded across chest in the centre of one of the embedded force plates for three seconds. After acquisition of a trial of quiet upright stance, participants performed a series of running and drop-land-lateral jump motor tasks. Running was performed at each participant's natural running speed (between 2.8 and 3.2 m·s⁻¹). For the drop-land-lateral jump, participants began by standing on their dominant leg at the centre of the box, which was positioned 10 cm from the force

plate, with their hands folded across their chest. Box height was normalized to 30% of each participant's leg length to impose a similar task demand across individuals of different stature. Participants were instructed to drop down and land on their dominant leg on the marked target at the centre of the force plate, and immediately perform a 90° lateral jump landing on their contralateral leg on the marked target set at a distance of 150% their lower limb length from the centre of the force plate (Figure 3.2). Participants were asked to perform the drop-land-lateral jump task as quickly as possible. Immediately after each trial, GRFs were inspected to ensure clean dominant foot force platform strikes. Participants completed running and drop-land-lateral jumps until at least three clean trials of each task were obtained.

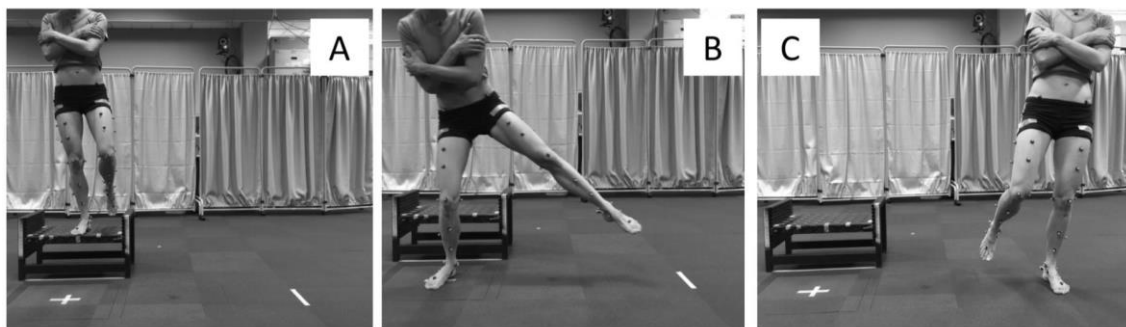


Figure 3.2. Single-leg drop-land-lateral jump task. (A) Participant balanced on their dominant leg with hands folded across chest on top of the box, (B) hopped down towards the “X” marked on the ground, and then (C) laterally cut 90° as quickly as possible towards their dominant limb, landing and balancing at a distance of 150% their leg length from the centre of the force plate for 5 seconds.

3.3 Data processing

In this thesis, we used musculoskeletal modelling in OpenSim open-source software [230] to determine the external biomechanics of the running and drop-land-lateral jump tasks. To do so, the data from the motion capture experiments were first prepared, the biomechanics were then modelled in OpenSim, and the outputs from OpenSim modelling were used for subsequent neuromusculoskeletal and ACL load modelling.

First, raw marker of all trials recorded during the laboratory session were reconstructed, labelled, and cleaned (e.g., mislabelling corrected, small gaps in trajectories filled through interpolation) in Vicon Nexus software (version 1.8.5). Then, marker, GRF, and EMG data were elaborated in MATLAB (R2018a, The MathsWorks, USA) using the MOtoNMS toolbox [300]. The MOtoNMS software prepares the data for OpenSim [230] by facilitating the conversion of data acquired in the motion capture laboratory (stored in 3cd file format) to formats supported by OpenSim (.trc and .mot). Marker trajectory and GRF data were filtered using a second-order 6 Hz low-pass Butterworth zero-lag filter [301]. The stance phase of the two tasks was defined from heel strike to toe-off events, which were automatically identified using the vertical component of GRF from the force platform in contact with the foot. The detection threshold was set at 40 N.

The EMG signals were band-pass filtered (zero-lag double-pass fourth order Butterworth, 30-300 Hz), full-wave rectified, and then low-pass filtered with a cut-off frequency of 6 Hz to produce linear envelopes. Each linear envelope was subsequently amplitude normalized to each muscle's maximal excitation value obtained from all available running and drop-land-lateral jump trials. The hip, knee, and ankle joint centres were computed from the static pose trial for subsequent musculoskeletal scaling. The hip joint centres were determined using the Harrington equations [302], while knee and ankle joint centres were determined based on midpoint between medial and lateral epicondyle markers and medial and lateral malleoli markers, respectively.

3.4 EMG driven neuromusculoskeletal modelling

3.4.1 Modifying and scaling musculoskeletal model

For modelling the external biomechanics, a full-body generic musculoskeletal model (i.e., Rajagopal model) was used. This model consisted of 37 degrees-of-freedom (DOF) and 80 muscle tendon unit (MTU) actuators [303], and was deployed in the OpenSim (version 3.3) [230] modelling environment. However, the generic model is configured such that it does not contain generalized coordinates for non-sagittal planes at the knee, nor components to compute medial and lateral tibiofemoral mechanics. Therefore, it required modification to ensure we can resolve the generalized loads in 6 DOF at the knee and eventually to resolve tibiofemoral contact forces for each compartment.

To do this, the generic model was modified in two steps. First, dummy tibias of negligible mass and associated universal joints were added to the knee mechanism without changing the original knee mobilities of flexion/extension with other coupled motions. Specifically, abduction/adduction rotation, internal/external rotation, superior-inferior translation, and anterior/posterior translation were prescribed as functions of knee flexion. Second, the generic model's ankle and hip joints were expanded to 6 DOF to enable calculation of generalized loads, however, the newly expanded DOFs had zero mobility space. At the ankle, in addition to plantar/dorsi flexion mobility that is present in the generic Rajagopal model, two rotational mobilities (internal/external and adduction/abduction rotations) and three translational mobilities (superior/inferior, anterior/posterior, and medial/lateral) were defined, however, these additional mobilities also have zero mobility space. The original hip has flexion/extension, adduction/abduction, and internal/external rotational mobilities with physiological boundaries, and superior/inferior, anterior/posterior, and medial/lateral translational

mobilities were added, but again with zero space meaning they do not contribute to the kinematics, but generalized loads are solved for them during inverse dynamics [304].

This modified generic musculoskeletal anatomical model was then linearly scaled to match each participant's gross dimensions, mass, and inertia. For the purpose of linear scaling, individual scaling factors for each bone (the ratio of Euclidean distances between pairs of MOCAP markers and corresponding virtual landmarks on the OpenSim generic model) were calculated. Prominent bony landmarks and hip, knee, and ankle joint centres were used for scaling. The marker pairs selected to compute scale factors to adjust width, height, and depth of model bodies are outlined in Table 3.4. In any dimension, where multiple marker pairs are listed, the corresponding scale factor was an average of scale factors calculated from each marker pair [305]. The muscle tendon unit pathways, defined by muscle origin, insertion and via points, were scaled along with the underlying bones.

Table 3.4. *The marker pairs used in linear scaling of the generic template model.*

| Bodies | Scaling dimension | | |
|---------------|--------------------------|--|--------------------------|
| | Width | Height | Depth |
| Trunk | NA | LASIS-MAN RASIS-MAN RASIS-T10 LASIS-T10 | MAN-T10 MAN-T2 |
| Pelvis | LASIS-RASIS | SACR-LHJC SACR-RHJC RASIS-RHJC LASIS-LHJC | RASIS-SACR LASIS-SACR |
| Femur | MEPI -LEPI | RHJC-MEPI RHJC-LEPI | NA |
| Shank | MMAL-LMAL | MEPI-MMAL LEPI-LMAL | NA |
| Foot | MT1-MT5 | NA | HEEL-MT5 HEEL-MT1 |

NA: scale factor of value 1 was used; LASIS: left anterior superior iliac spine; RASIS: right anterior superior iliac spine; MAN: jugular notch; T2: 2nd thoracic vertebrae; T10: 10th thoracic vertebrae; SACR: midpoint of right and left posterior superior iliac spine; LHJC: left hip joint centre; RHJC: right hip joint centre; MEPI: medial epicondyle of knee; LEPI: lateral epicondyle of knee; MMAL: medial malleolus; LMAL: lateral malleolus; MT1: 1st metatarsal phalangeal joint; MT5: 5th metatarsal phalangeal joint; HEEL: distal calcaneus.

3.4.2 Muscle tendon unit parameter personalization

Following linear scaling, muscle and tendon dimensionless operating ranges are not necessarily preserved, as the relationships between internal MTU parameters (i.e., optimal fibre length (OFL) and tendon slack length (TSL)) and overall MTU length after scaling are not maintained [258]. Therefore, to ensure the dimensionless fibre and tendon operating ranges of healthy muscle are preserved, each MTU actuator's TSL and OFL were optimised via morphometric scaling [306]. This morphometric scaling is appropriate for healthy paediatric population, since the ratio of TSL and MTU lengths have been reported to be preserved during growth [307].

3.4.3 Muscle strength personalization

In young healthy people, total lower limb muscle volume is correlated with body mass and height, and the distribution of individual muscle volumes in the lower limb is similar between subjects [308]. Therefore, in this thesis, each muscle's maximum isometric strength was scaled based on each participant's mass and height using the relationships of lower limb muscle volume with mass and height reported by Handsfield [308], similar to the implementation of Rajagopal *et al.* [303].

3.4.4 Modelling the external biomechanics

After all of the previously described personalization steps were performed on the generic musculoskeletal model, the final model was used in OpenSim v3.3 [230] to determine the external biomechanics. OpenSim inverse kinematics, inverse dynamics, and muscle analysis tools were used to determine model kinematics, net joint forces and moments, and MTU kinematics, respectively [230]. To reduce processing time and human error, and to ensure consistency between trials and participants, modelling of the external biomechanics was batch-processed using Batch OpenSim Processing Scripts (BOPS) [309]. Once batch-processed, each trial's output was scrutinized for consistency and physiological behaviour. Any trials showing irregular biomechanics were visualized to determine the source of the irregular biomechanics. If a processing error occurred, this was corrected and re-modelled.

3.4.5 Muscle force estimation using personalised muscle activation

In this thesis, the Calibrated EMG-Informed NeuroMusculoSkeletal (CEINMS) modelling software [241, 242] was used to estimate muscle forces. The CEINMS uses a modified Hill-type muscle model in which its function depends on the internal parameters

of the MTU actuator and its activation [258, 310]. The CEINMS solves the following equation for muscle force estimation:

$$F^m = cF^{max}[f_a(\tilde{l}_m) \cdot f_v(\tilde{v}_m) \cdot a + f_p(\tilde{l}_m) + d_m \cdot \tilde{v}_m] \cdot \cos \varphi \quad (3.1)$$

where F^m is the muscle force, F^{max} is the maximal isometric force, c is the strength coefficient used to constrain the ability of muscles to generate force, which is specific to each muscle or muscle group, a is the activation, \tilde{l}_m is the normalised fibre length, \tilde{v}_m is the normalised muscle velocity, d_m is the muscle damping element introduced to avoid singularities when $F^m = 0$ or $F^{max} = 0$, and φ is the pennation angle. Thus, it is important to have appropriate definition of MTU parameters to have correct estimation of muscle function.

Even though morphometric scaling of the MTU parameters has been applied to each model (explained in section 3.4.2), the OFL and TSL values may not be optimal for the individual being studied, which could affect the estimated muscle dynamics and their consistency with the external biomechanics. Thus, to produce more physiologically plausible internal biomechanics, a calibration step was performed in CEINMS to enhance the personalisation of the MTU parameters and provide better dynamic consistency. This calibration enabled the model to better track both externally applied joint moments and EMG [241] by making small adjustments to the internal MTU parameters. The CEINMS calibration process minimizes joint moment tracking errors by adjusting the previously scaled MTU parameters (explained in sections 3.4.1 and 3.4.2) within bounded range (i.e., 95%-105% of initial values) [241, 245, 248]. In addition to MTU parameters, strength coefficient values which control gain on muscle force production and have initial value of 1, were permitted to vary between 0.5 and 1.5 during calibration.

After calibration, CEINMS was used in EMG-assisted mode [241, 248] which employs computational neural solutions whereby experimental EMG data are used in combination with mechanical optimization to synthesize muscle activations for all the MTU of the lower limb. The EMG-assisted approach is appropriate because it is not feasible, nor within the current data set, to acquire EMG from all the muscles of the lower limb, therefore, an optimization procedure is needed to estimate the excitation for the remaining muscles. Further, it is acknowledged that measured EMG contains some electrotechnical noise (despite being conditioned through signal processing), therefore, a compromise between tracking experimentally measured EMG and tracking external biomechanics (e.g., joint moments) was used. In this EMG-assisted approach, the experimental EMG data are minimally adjusted and MTU excitations for the muscles without experimental EMG data were synthesised, using static optimisation (i.e., minimization of summed squared excitation), to best match the external sagittal plane joint moments of the lower limb (i.e., hip, knee, and ankle). The adjusted and synthesized excitations were achieved by minimising the terms of the following objective function:

$$E = \alpha E_{MOM} + \beta E_{EXC} + \gamma E_{EMG} \quad (3.2)$$

where, E_{MOM} is the sum of the squared differences between predicted and experimental joint moments, E_{EXC} represents the sum of squared excitations for all MTUs, and E_{EMG} is the sum of the differences between adjusted EMG excitations and recorded EMG excitations. Factors α , β , and γ are positive weighting coefficients [248]. The value of α and β were set to 1, and weighting of γ was optimised in order to minimise the tracking errors of adjusted muscle excitations and predicted joint moments.

From the OpenSim modelling, whole body motion and joint angles, net joint forces and moments, and lower limb MTU kinematics were determined (explained in

section 3.4.4). These biomechanical data were incorporated, along with the conditioned EMG signals, into CEINMS to first: calibrate the MTU parameters as explained earlier in the current section; and second: to estimate muscle activations and subsequently muscle forces. Muscle forces estimated in CEINMS were then multiplied by their respective line of action in the tibia's anterior posterior direction, and by their moment arms in the knee's frontal and transverse planes (computed in OpenSim) to calculate the muscle torques in three planes of motion. Then, medial and lateral compartment knee contact forces (JCF^{MC} and JCF^{LC} , respectively) were calculated by solving the following static equilibrium equation:

$$(JCF^{MC/LC} \cdot d_{IC}) + M_{MTU}^{MC/LC} + M_{ext}^{MC/LC} = 0 \quad (3.3)$$

where, $M_{MTU}^{MC/LC}$ is the overall muscle torque acting on the medial/lateral knee compartment, $M_{ext}^{MC/LC}$ is the external moment around the medial/lateral contact point, and d_{IC} is the distance between the contact points (i.e., intercondylar distance). The overall processing flow involved in using laboratory human motion data to determine muscle, contact and ACL forces is displayed in a block diagram (Figure 3.3). The ACL model displayed in this diagram, has been developed and validated as part of this thesis which is explained in Chapter 4.

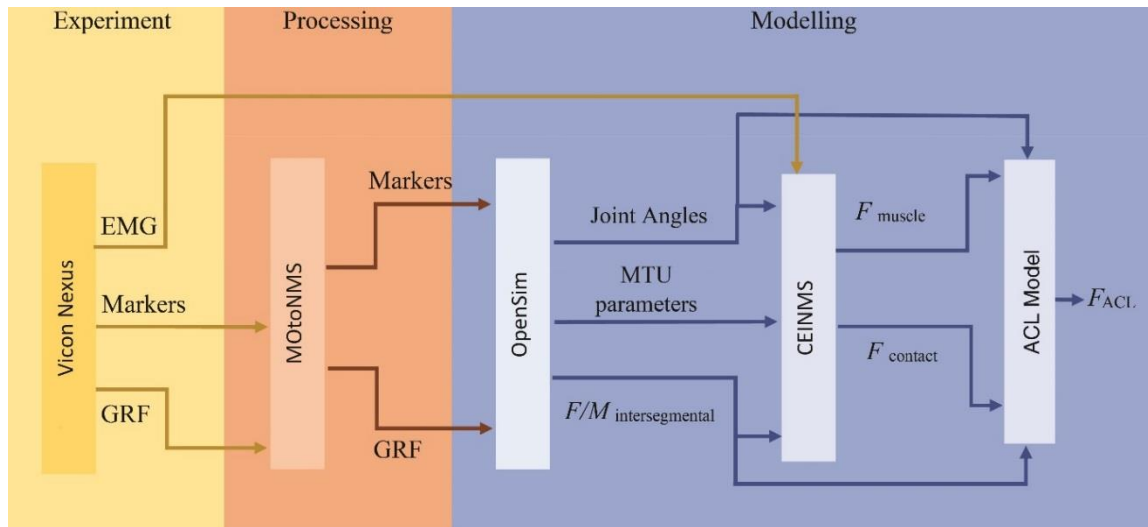


Figure 3.3. Schematic of muscle contact and ACL force calculation workflow. It is composed of three main parts: experimental acquisition of movement data (yellow), data processing (orange), EMG-driven musculoskeletal modelling and ACL force calculation (blue). The box blocks represent the processing tools and the arrows represent the input/output to/from each tool. ACL: anterior cruciate ligament; EMG: electromyography; GRF: ground reaction forces; MTU: muscle tendon unit.

3.5 Statistical analysis

In thesis Chapters 4 and 5, the focus is on the development, validation, and application of an ACL loading model. The data from the late/post pubertal group were used in these studies wherein a sample of convenience (i.e., $n=13$) was used for Chapter 4 and the entire sample ($n=24$) was used for Chapter 5. Statistical tests were conducted to investigate the validity of the ACL loading model by comparing the model-estimated ACL force with ACL force/strains directly measured from cadaveric specimens with instruments surgically implanted into the ACL. Following ACL model development and validation, the contribution of individual knee muscles and muscle groups (organized by commonly assumed function about the knee) to ACL loading was explored by examining the contributions at discreet points in the drop-land-lateral jump task.

In thesis Chapter 6, the focus was on the effects of sexual maturation on ACL loading. Therein, the ACL loading and its contributors were examined both in a time continuous manner, using statistical parametric mapping, and in discrete points within the task using traditional statistical tests. These data were compared between the experimental groups across the stages of pubertal maturation. All statistical analyses were performed in MATLAB (R2018a, MathWorks, Inc., MA) for thesis Chapter 4, in IBM SPSS v25 (IBM, Armonk, NY) for thesis Chapter 5, and a combination of IBM SPSS v25 and SPM1d software (v0.4, www.spm1d.org), implemented in MATLAB, for thesis Chapter 6.

3.5.1 Anterior cruciate ligament model validation

The accuracy of the ACL force model was assessed by the root-mean-square error (RMSE), squared Pearson's correlation coefficient (r^2) and Bland-Altman analysis to quantify the level of agreement between the model-estimated ACL force and corresponding cadaveric measurements of ACL loading.

3.5.2 Comparisons between muscle contributions to anterior cruciate ligament loading

The contributions to ACL loading at the instance of peak ACL force, from the individual muscles and muscle groups (based on their commonly assumed function about the knee) were examined. At the instance of peak ACL force, individual muscles were either an ACL loader or supporter if they acted to increase or decrease the ACL load, respectively. The non-parametric equivalent of one-way ANOVA (i.e., Kruskal-Wallis) and *post-hoc* t-tests were used to determine the specific differences between the contributions of individual muscles and muscle groups to ACL force. Statistical significance was set at $p < 0.05$ for the non-parametric ANOVA and then adjusted based on Bonferroni correction

for *post-hoc* t-tests (with the alpha of 0.0125, 0.0083 and 0.0071 for grouped muscles, individual loaders, and individual supporters; respectively).

3.5.3 Comparisons between female pubertal maturation groups

Between-group differences in demography and anthropometry were tested using one-way ANOVA and *post-hoc* t-tests. To analyse ACL force in a time-continuous manner, statistical parametric mapping (SPM) was used with the open-source SPM1d software (v0.4, www.spm1d.org) and implemented in MATLAB. The SPM ANOVA were used to compare ACL force during stance phase of the drop-land lateral jump, and its contributors, generated by the different pubertal groups. Results for these comparisons were reported as SPM [50] curves. Where a statistically significant SPM ANOVA result was found, *post-hoc* comparisons between groups were undertaken using SPM t-tests with Bonferroni correction. Thus, an alpha of 0.0170 was used to determine statistical significance.

CHAPTER 4

Modelling the loading mechanics of anterior cruciate ligament

Acknowledgement of co-authorship

This chapter includes a co-authored paper that has been re-formatted for this thesis. The bibliographic details/status of the co-authored paper, including all authors, are:

Nasseri, A., Khataee, H., Bryant, A.L., Lloyd, D.G., Saxby, D.J. Modelling the loading mechanics of anterior cruciate ligament, *Computer Methods & Programs in Biomedicine*. 2020. <https://doi.org/10.1016/j.cmpb.2019.105098>.

I made a substantial contribution in the conception and design of this study, analysis and interpretation of data, drafting and revising of the final manuscript.

Student/ Corresponding author: Azadeh Nasseri

Principal supervisor: David G Lloyd

4.1 Abstract

Background and Objectives: The anterior cruciate ligament (ACL) plays a crucial role in knee stability and is the most commonly injured knee ligament. Although ACL loading patterns have been investigated previously, the interactions between knee loadings transmitted to ACL remain elusive. Understanding the loading mechanism of ACL during dynamic tasks is essential to prevent ACL injuries. Therefore, we propose a computational model that predicts the force applied to ACL in response to knee loading in three planes of motion.

Methods: First, a three-dimensional (3D) computational model was developed and validated using available cadaveric experimental data to predict ACL force. This 3D model was then combined with a neuromusculoskeletal model of lower limb and used to estimate *in vivo* ACL forces during a standardised drop-landing task. The neuromusculoskeletal model utilised movement data collected from female participants during a dynamic task and calculated lower limb joint kinematics and kinetics, as well as muscle forces.

Results: The total ACL force predicted by the 3D computational ACL force model was in good agreement with cadaveric data, as strong correlation ($r^2 = 0.96$ and $P < 0.001$), minimal bias, and narrow limits of agreement were observed. The combined model further illustrated that the ACL is primarily loaded through the sagittal plane, mainly due to muscle loading.

Conclusions: The proposed computational model is the first validated model that can provide an accessible tool to develop and test knee ACL injury prevention programs for people with normal ACL. This method can be extended to study the abnormal ACL upon the availability of relevant experimental data.

4.2 Introduction

We are interested in quantifying force applied to the anterior cruciate ligament (ACL) during athletic tasks. The ACL is one of the major intra-articular knee ligaments and plays a key role in knee stability [1]. Non-contact ACL ruptures are common and debilitating sport injuries, usually occurring without physical contact between athletes [4], and often lead to serious long-term health consequences, such as early onset knee osteoarthritis [6]. Video analysis of non-contact ACL injuries [139] and medical imaging of intra-articular injury patterns [311, 312] suggest that landing, change of direction, and pivoting motor tasks are associated with non-contact ACL injury. The consensus is that external knee loads applied in three planes of motion (i.e., sagittal, frontal, and transverse) contribute to ACL rupture; reviewed in [26] (see Figure 4.1). However, the mechanisms by which external knee loads are transmitted to the ACL (through the interaction of muscles, contacting articular bodies, and other soft tissues) during dynamic motor tasks remain contentious [27, 28].

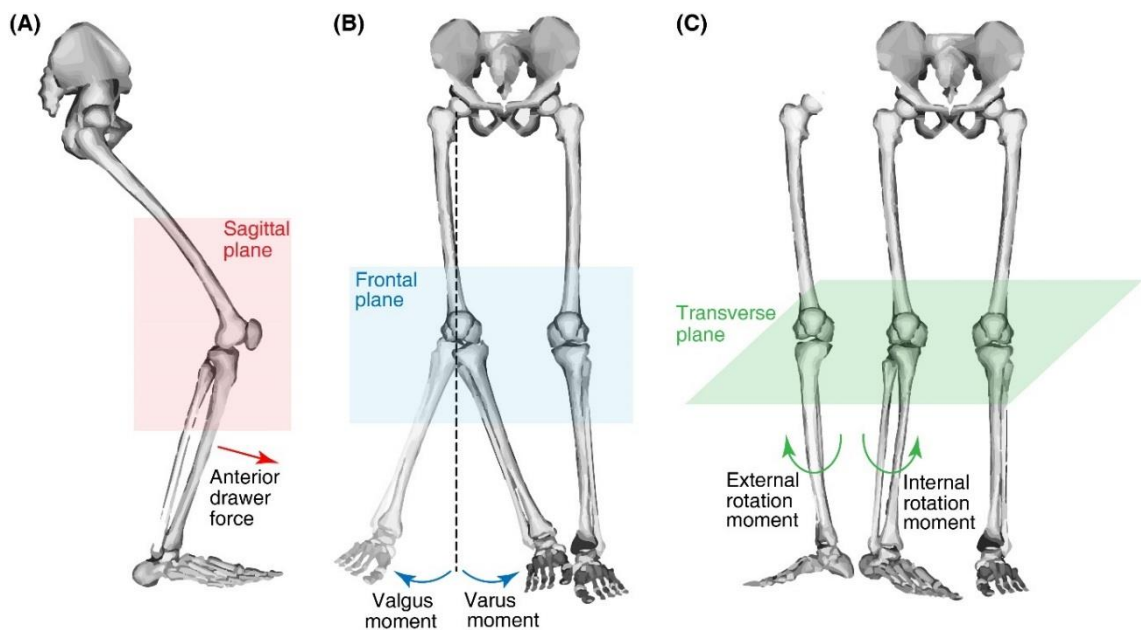


Figure 4.1. Knee loading in (A) sagittal, (B) frontal, and (C) transverse planes of motion.

Earlier studies [29-37] have modelled ACL force (i.e., the force applied to the ACL), but were limited by simplistic loading conditions, have not been able to predict the experimentally observed ACL forces, or were developed based on limited sample data. For example, previous models [36, 37] assume that ACL force in response to multiplanar external knee loads is equal to the sum of forces exerted by multiple independent uniplanar loads. However, experiments [41, 42] have provided evidence that ACL force can be different than such pure summation and is influenced by knee flexion angles. Others modelled the lower bounds to ACL force with rapid fluctuations in simulated ACL force during dynamic tasks [32]. which seem non-physiological. Therefore, an improved and validated model is needed to quantify ACL force.

Here, we have developed a three-dimensional (3D) computational model that provides a novel representation of the ACL loading mechanism. The model predicts ACL force in response to multiple external loads applied to the knee across a range of knee postures. The model was developed based on experimental cadaveric data [41, 42, 62], and then validated using a subset of data [62] not employed in model development. The model, when applied to *in vivo* human movement data from our laboratory, suggests that the primary force applied to the ACL is through the sagittal plane and mainly due to muscle loading.

4.3 Methods

4.3.1 Cadaveric data preparation

To develop and validate our model of ACL force, we use two sets of experimental data [41, 42, 62] in which uniplanar and multiplanar external loads were applied to the cadaveric knees via robotic rigs. Markolf and colleagues' data [41, 42] presents ACL force without muscle support over knee flexion angles θ , 0° to 90° . Kiapour *et al.* data

[62] presents ACL strain (i.e., elongation relative to resting length) at a single knee flexion angle $\theta = 25^\circ$, in response to a larger loading range and more load combinations than Markolf *et al.* [41, 42] experiments. Kiapour *et al.* data [62] also artificially applied muscle loading, which influenced transmission of external knee loads to the ACL and other articular tissues. Therefore, to calculate contribution of muscles to knee loading, we mimicked Kiapour *et al.* cadaveric experiment [62] by implementing a musculoskeletal model [303] in the OpenSim modelling environment [230]. To simulate the artificially-supplied quadriceps and hamstrings muscle forces (i.e., 1200 N and 800 N, respectively [62]), we assumed that these forces were equally distributed among individual muscles from each group (i.e., 300 N for each quadricep and 200 N for semitendinosus, semimembranosus, biceps femoris short head, and biceps femoris long head). The musculoskeletal model was then set to the reported knee posture [62] by flexing knee and tilting the pelvis-ground joints both by 25° . Since the cadaveric specimen was mounted upside down and truncated mid- femur (without specifications) [62], the modelled pelvis was adjusted to be of minimal mass (0.1 kg), and the sign for the gravitational acceleration constant was changed from negative to positive [62]. To incorporate effects of robotic loads applied to the knee [62], compression and anterior drawer forces and varus/valgus and internal/external tibia rotation moments were applied to the musculoskeletal model. Cadaveric experimental muscle force contributions were also modelled by first calculating muscle moment arms and lines of action. Muscle contributions to anterior drawer force, compression force, varus or valgus moment, and internal or external rotation moment were estimated by: muscle force (artificially supplied [62]) \times muscle lines of action (or moment arms), depending on the plane of motion, defined relative to the tibia using spatial transformations available through the OpenSim

application programming interface. Using these muscle contributions, we calculate net loading in each plane of motion. In the sagittal plane, net anterior drawer force F_{AD} was:

$$F_{AD} = F_{muscle} + F_{intersegmental} + F_{contact} \quad (4.1)$$

where F_{muscle} is muscle force, $F_{intersegmental}$ is intersegmental force representing robotically applied force [62], and $F_{contact}$ is knee joint contact force, which was the product of muscle compression onto a posteriorly sloped tibia [313]. In frontal and transverse planes, respectively, net varus or valgus moment $M_{Var/Val}$ and net internal or external rotation moment $M_{IR/ER}$ were:

$$M_j = M_{muscle} + M_{intersegmental} \quad (4.2)$$

where M_{muscle} and $M_{intersegmental}$ are muscle and intersegmental moments for $j = Var/Val$ or IR/ER . Finally, to unify measurement of ACL response across cadaveric data [41, 42, 62], we converted measured ACL strain [62] to ACL force as: Force = $(CSA \times E \times Strain)$, where for a typical ACL with linear elasticity [314], average ACL cross-sectional area (CSA) $\sim 65 \text{ mm}^2$ and Young's modulus $E \sim 113 \text{ MPa}$ [315]. Together, these unified data [62] were used in the model development.

4.3.2 Model development

This study involves development, validation, and application of a computational model to quantify ACL force. First, we developed an ACL force model using the most relevant, complete, and accessible cadaveric data [41, 42, 62], and validated it using a subset of data from [62]. The ACL force model was then applied to estimate *in vivo* ACL force during a dynamic task, in order to help us understand ACL loading mechanisms during sporting tasks that are considered high-risk for ACL injury.

To quantify total ACL force, first we modelled the resultant ACL forces from externally applied knee loading in each plane of motion. We fitted a set of simple algebraic equations to experimental data[41, 42, 62], which measured resultant ACL force across knee flexion angles 0-45° in the presence of specific external knee loads. In sagittal plane, ACL force F_{ACL}^{sag} was modelled as a function of knee anterior drawer force F_{AD} and knee flexion angle θ by fitting Equation ((4.3) to data [41, 42, 62]:

$$F_{ACL}^{sag} = a_1 F_{AD} \theta^2 + a_2 F_{AD} \theta + a_3 F_{AD} + a_4 e^{(a_5 F_{AD} + a_6 \theta)} \quad (4.3)$$

where fit parameters are $a_1 = 1.8 \times 10^{-4} \pm 5.6 \times 10^{-7}$, $a_2 = -0.02 \pm 0.1 \times 10^{-4}$, $a_3 = 1.16 \pm 0.005$, $a_4 = 32.15 \pm 0.02$, $a_5 = 3.9 \times 10^{-5} \pm 1.8 \times 10^{-4}$, and $a_6 = -0.022 \pm 2.3 \times 10^{-5}$ (Figures Figure 4.1 A and Figure 4.2 A). Parameter values correspond to mean \pm standard error. To model ACL force in frontal plane F_{ACL}^{front} as a function of knee varus or valgus moment (M_{var} or M_{valg}) and flexion angle θ , Equation (4.4) was fitted to data [42]:

$$F_{ACL}^{front} = \begin{cases} b_1 M_{var} \theta^2 + b_2 M_{var} \theta + b_3 M_{var} + b_4 e^{(b_5 \theta)} & , if \text{ varus} \\ c_1 M_{valg} \theta^2 + c_2 M_{valg} \theta + c_3 M_{valg} + c_4 \theta e^{(c_5 \theta)} + c_6 e^{(c_7 M_{valg})} & , if \text{ valgus} \end{cases} \quad (4.4)$$

where $b_1 = -0.0014 \pm 0.1 \times 10^{-3}$, $b_2 = 0.18 \pm 0.01$, $b_3 = -6.8 \pm 0.21$, $b_4 = 23.85 \pm 2.03$, $b_5 = -0.14 \pm 0.03$ for varus moment; and $c_1 = -0.001 \pm 3.6 \times 10^{-8}$, $c_2 = 0.08 \pm 3.2 \times 10^{-6}$, $c_3 = 2.5 \pm 5.2 \times 10^{-5}$, $c_4 = -3.3 \pm 0.6 \times 10^{-5}$, $c_5 = -0.04 \pm 6.7 \times 10^{-7}$, $c_6 = 29.3 \pm 0.3 \times 10^{-4}$, and $c_7 = 0.02 \pm 3 \times 10^{-7}$ for valgus moment (Figures Figure 4.1 B and Figure 4.2 B, C). Likewise, in transverse plane, ACL force F_{ACL}^{trans} was modeled as a function of knee internal or external rotation moment (M_{IR} or M_{ER}) and flexion angle θ by fitting Equation (4.5) to data [42]:

$$F_{ACL}^{trans} = \begin{cases} m_1 M_{IR} \theta^2 + m_2 M_{IR} \theta + m_3 M_{IR} + m_4 e^{(m_5 \theta)} & , \text{if internal rotation} \\ n_1 M_{ER} \theta^2 + n_2 M_{ER} \theta + n_3 M_{ER} + n_4 e^{(n_5 \theta)} & , \text{if external rotation} \end{cases} \quad (4.5)$$

where $m_1 = -0.005 \pm 2.4 \times 10^{-7}$, $m_2 = 0.63 \pm 0.2 \times 10^{-4}$, $m_3 = -20.03 \pm 3.8 \times 10^{-3}$, $m_4 = 36.6 \pm 3.4 \times 10^{-2}$, $m_5 = -0.04 \pm 7.1 \times 10^{-6}$ for internal rotation moment; and $n_1 = 0.001 \pm 2 \times 10^{-3}$, $n_2 = -0.16 \pm 0.02$, $n_3 = 7.8 \pm 0.4$, $n_4 = 23.3 \pm 2.5$, $n_5 = -0.06 \pm 0.01$ for external rotation moment (Figures Figure 4.1C and Figure 4.2D, E).

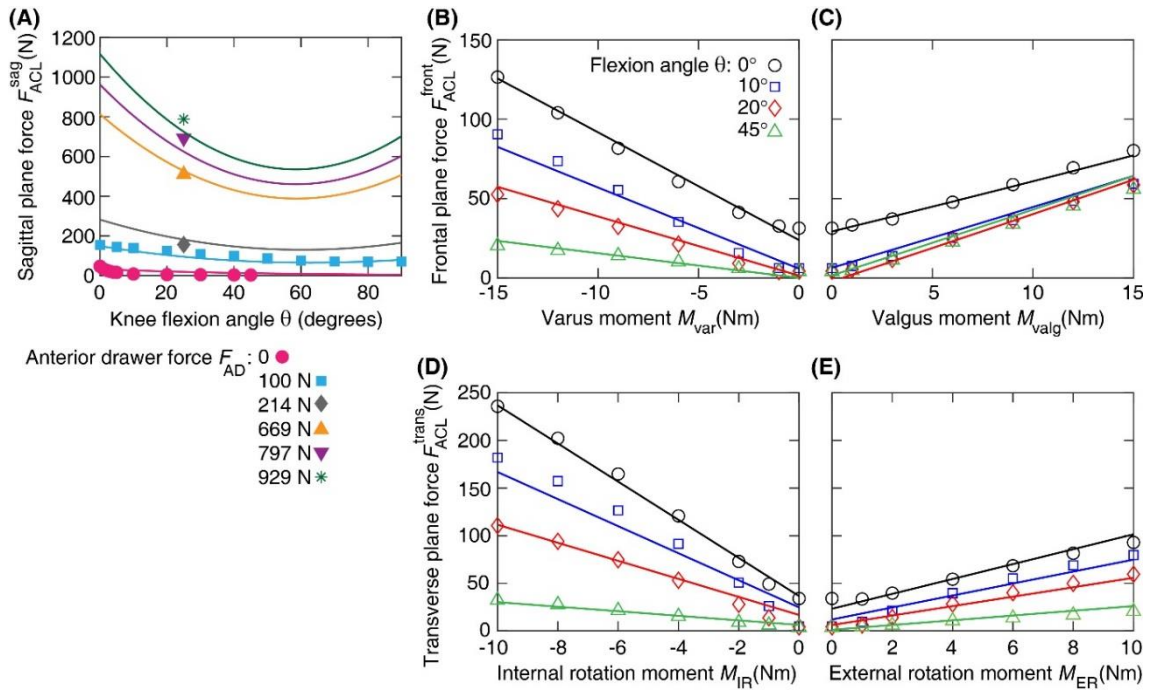


Figure 4.2. Uniplanar ACL forces. (A) ACL force in sagittal plane F_{ACL}^{sag} vs knee flexion angle θ , at different knee anterior drawer forces F_{AD} . Symbols at $F_{AD} = 0$ and 100 N are experimental data from [41, 42]. Other symbols are experimental data from [62]. Continuous curves are our fits derived from Equation(4.4). (B, C) ACL force in frontal plane F_{ACL}^{front} vs knee varus and valgus moments (M_{var} and M_{valg}) at different knee flexion angles θ . Symbols are experimental data from [42]. Curves are our fits derived from Equation (4.4). (D, E) ACL force in transverse plane F_{ACL}^{trans} as vs knee internal and external rotation moments (M_{IR} and M_{ER}) at different θ . Symbols are experimental data from [42]. Curves are our fits derived from Equation (4.5).

We now determine total ACL force F_{ACL} . Summation of Equations (4.4)-(4.5), when compared to experimentally measured multiplanar ACL force [41], indicates that total ACL force is not equal to sum of uniplanar ACL forces, i.e., $F_{ACL} \neq F_{ACL}^{sag} + F_{ACL}^{front} + F_{ACL}^{trans}$. Pure summation results in over- and under-estimation of F_{ACL} , depending on knee flexion angle θ and external loading (F_{AD} , M_{var} , M_{valg} , M_{IR} , and M_{ER}) magnitudes. This implies that interactions between multiple uniplanar ACL forces influence the total force transmitted to ACL. To account for the interactions between uniplanar ACL forces, we then incorporated cross-terms CT_j in modelling F_{ACL} :

$$F_{ACL} = F_{ACL}^{sag} + F_{ACL}^{front} + F_{ACL}^{trans} + \sum_j CT_j \quad (4.6)$$

where CT_j (for $j = SF, ST, FT$) represent ACL force relationships in sagittal-frontal (SF), sagittal-transverse (ST), and frontal-transversers (FT) planes.

We formulated CT_j by curve fitting to multiplanar ACL force data from [41, 62]. We used all data from [41] and a subset of the data (eleven data points) from [62] which covers different loading magnitudes (i.e., from low to high) through each plane of motion. This ensures that the model is developed by considering the entire range of the experimentally measured loads in every plane of motion as well as the combinations of these loads. Fourteen remaining data points from [62] were used to validate the model (detailed in Methods). The interactions between sagittal and frontal planes were modelled as:

$$CT_{SF} = \begin{cases} p_1 F_{ACL}^{front} e^{(p_2 F_{ACL}^{sag})} + p_3 \theta e^{(p_4 \theta)} & , if \text{ varus} \\ q_1 e^{(q_2 F_{ACL}^{front})} + q_3 \theta e^{(q_4 \theta)} & , if \text{ valgus} \end{cases} \quad (4.7)$$

where $p_1 = -0.84 \pm 8.2 \times 10^{-6}$, $p_2 = -0.004 \pm 6.9 \times 10^{-8}$, $p_3 = 2.9 \pm 1.3 \times 10^{-5}$ and $p_4 = -0.041 \pm 1.02 \times 10^{-7}$ for varus moment; and $q_1 = -39.1 \pm 1.4 \times 10^{-4}$, $q_2 = 0.002 \pm 9.7 \times 10^{-10}$, $q_3 = 8.7 \pm 1.9 \times 10^{-6}$, and $q_4 = -0.03 \pm 3.4 \times 10^{-9}$ for valgus moment (Figure 4.3A, B). Similarly, we modelled the interactions between sagittal and transverse planes as:

$$CT_{ST} = \begin{cases} v_1 F_{ACL}^{sag} F_{ACL}^{trans} + v_2 e^{(v_3 \theta)} & , if \text{ internal rotation} \\ w_1 F_{ACL}^{trans} e^{(w_2 F_{ACL}^{sag})} + w_3 e^{(w_4 \theta)} & , if \text{ external rotation} \end{cases} \quad (4.8)$$

where $v_1 = -6.8 \times 10^{-4} \pm 1.1 \times 10^{-9}$, $v_2 = -32.2 \pm 3.6 \times 10^{-3}$, and $v_3 = 0.01 \pm 1.8 \times 10^{-7}$ for internal rotation; and $w_1 = -0.81 \pm 2.8 \times 10^{-6}$, $w_2 = -0.003 \pm 1.3 \times 10^{-7}$, $w_3 = -67.9 \pm 4.3 \times 10^{-4}$, and $w_4 = -0.001 \pm 1.8 \times 10^{-7}$ for external rotation (Figure 4.3 C, D). Interactions between frontal and transverse planes CT_{SF} were found to be negligible compare to CT_{SF} and CT_{ST} (i.e., CT_{SF} was set to zero).

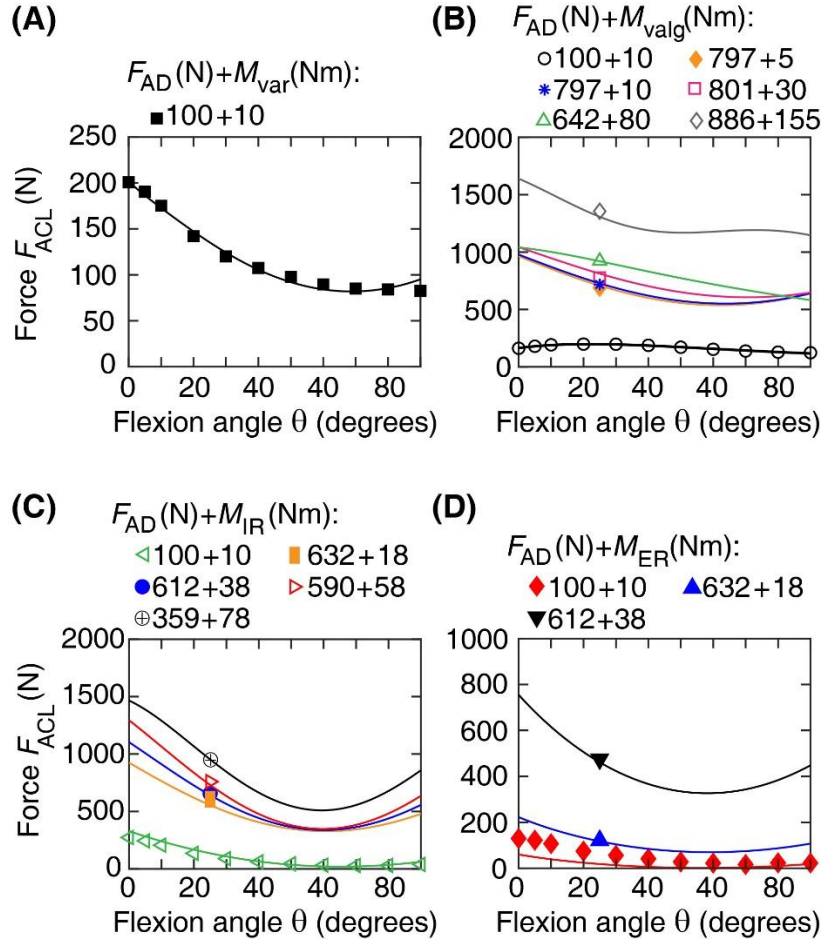


Figure 4.3. Total ACL force F_{ACL} vs knee flexion angle θ . (A) F_{ACL} in response to combined anterior drawer force F_{AD} and varus moment M_{var} . Symbols are experimental data from [41]. Continuous curve is our fit derived from Equations (4.6), (4.7). (B) F_{ACL} in response to combined F_{AD} and valgus moment M_{valg} . Open circles are experimental data [41]. Other symbols are experimental data from [62]. Continuous curves are our fits derived from Equations (4.6), (4.7). (C) F_{ACL} in response to combined F_{AD} and knee internal rotation moment M_{IR} . Left-pointing triangles are experimental data from [41]. Other symbols are experimental data from [62]. Continuous curves are our fits derived from Equations (4.6), (4.8). (D) F_{ACL} in response to combined F_{AD} and knee external rotation moment M_{ER} . Diamonds are experimental data from [41]. Other symbols are experimental data from [62]. Continuous curves are our fits derived from Equations (4.6), (4.8)

To use the ACL force model in Equation (4.6) for estimating *in vivo* ACL force during laboratory-based dynamic motor tasks, we combined the model with a neuromusculoskeletal model of the lower limb. Briefly, we used 3D motion capture,

ground reaction loads, and surface electromyography (EMG) data from laboratory testing of females performing a standardized drop-landing task, as well as previously validated neuromusculoskeletal model [27, 240, 241], to calculate knee muscle and intersegmental loading (i.e., F_{muscle} , M_{muscle} , $F_{\text{intersegmental}}$, and $M_{\text{intersegmental}}$) and knee flexion angle θ . These parameters were used to calculate F_{AD} , $M_{\text{Var/Val}}$, and $M_{\text{IR/ER}}$ (see Equations (4.1) and (4.2), and thus, total *in vivo* ACL force.

4.3.3 Model validation

Fourteen of 25 multiplanar ACL force data points from Kiapour *et al.* [62], which were not included in model development, were used to evaluate accuracy of ACL force model. Accuracy was assessed by RMSE, squared Pearson's correlation coefficient r^2 , and Bland-Altman analysis [316] (Figure 4.4).

4.3.4 *In vivo* experiment

Our combined ACL force and EMG driven neuromusculoskeletal models estimated *in vivo* ACL force during a standardised drop-landing task performed by healthy female adults in laboratory conditions at the Centre for Health, Exercise and Sports Medicine, University of Melbourne, Australia. Ethics approval was obtained by the University of Melbourne Human Research Ethics Committee (#1442604). Thirteen healthy female adults (age = 22.99 ± 2.57 years; mass = 62.11 ± 9.19 kg; height = 1.67 ± 0.07 m) completed at least three trials of standardized drop-landing task unshod. As previously described [317], the task involved hopping down from a box (30% of lower limb length) to land on one leg immediately followed by a 90° lateral jump landing on opposite leg. Three-dimensional ground reaction loads were collected at 2400 Hz using ground-embedded force platforms (AMTI, Mass, USA), and kinematic data collected at 120 Hz using a 12-camera motion capture system (Vicon Motion Systems, Oxford, UK). The

motion capture system measured 3D positions of retroreflective markers placed on specific sites of the lower-limb and head-abdomen-trunk, described in [318]. Wireless surface EMG sensors (Noraxon, AZ, USA) were secured over the rectus femoris, vastus lateralis, vastus medialis, tibialis anterior, lateral gastrocnemius, medial gastrocnemius, lateral hamstrings, and medial hamstrings muscles on the landing leg. Sensors were placed according to Surface ElectroMyoGraphy for the Non-Invasive Assessment of Muscles (SENIAM) guidelines [319] and EMG signals were recorded at 2400 Hz.

4.3.5 Signal processing

Marker trajectories and ground reaction data were filtered using a second-order, zero-lag, Butterworth filter, with low-pass cut-off frequency of 6 Hz [320]. The EMG data were band-pass filtered (30-300 Hz), full-wave rectified, and smoothed with a second-order Butterworth low-pass filter with cut-off frequency of 6 Hz to produce linear envelopes. The EMG linear envelopes were then normalized to the maximum linear envelope value of the corresponding muscle from all available motion trials.

4.3.6 Musculoskeletal modelling

Musculoskeletal modelling was performed to calculate externally applied joint moments and forces acting about planes of motion. We used a generic 37 degree-of-freedom (DOF) full-body model [303] with 80 muscle tendon unit (MTU) actuators in the OpenSim musculoskeletal modelling environment [230]. To calculate 6 generalized loads (moments and forces in three planes of motion) at ankle, knee, and hip, we modified the generic model. At the knee, we added dummy bodies of negligible mass/inertia and associated universal joints to the generic model topology [153, 321], but preserved original knee mobility: flexion/extension with abduction/adduction, internal/external rotation, superior-inferior translation, and anterior/posterior translations prescribed as

functions of knee flexion [322]. At ankle and hip, generic joints were expanded to 6 DOFs, but the newly expanded DOFs had zero mobility space. This means that ankle mobility was restricted to plantar/dorsi-flexion; whereas hip mobilities were restricted to flexion/extension, adduction/abduction, and internal/external rotations.

This modified musculoskeletal model was linearly scaled to approximate participant mass and gross dimensions. This scaling used prominent bony landmarks and hip joint centres. Hip joint centres were estimated using Harrington regression equations [323]. Scale factors were calculated as the quotient of distance between specific pairs of experimental motion capture markers placed atop prominent anatomical landmarks and their corresponding model virtual markers. Marker pairs used to compute scale factors to adjust width, height, and depth of model bodies are outlined in Table 3.4. In any dimension, where multiple marker pairs are listed, the corresponding scale factor is an average of scale factors calculated from each marker pair. Following scaling, each MTUA's tendon slack and optimal fibre lengths were optimized to preserve dimensionless force-length operating curves [306], as these are not preserved through linear scaling [324]. Each muscle's maximum isometric strength was updated and implemented as performed previously [303, 308], which estimates an individual's muscle volumes and lengths from their mass, height, and limb length.

The scaled musculoskeletal model used the laboratory data as inputs to determine joint angles, joint moments, and muscle kinematics. Inverse kinematics analysis [230] was used to determine 3D joint angles, which were then combined with ground reaction data to run inverse dynamics analysis [230] to determine model intersegmental joint loads; i.e., $F_{\text{intersegmental}}$ or $M_{\text{intersegmental}}$ for each DOF; see Equations (4.1) and (4.2). OpenSim's muscle analysis [230] was then executed to determine MTU kinematics; i.e., instantaneous lengths, moment arms, and lines of action [325].

The forces for all lower-limb muscles during drop-landing task were estimated using the calibrated EMG-informed neuromusculoskeletal modelling (CEINMS) toolbox. The CEINMS is an OpenSim plug-in which uses EMG signals and MTU parameters to drive a Hill-type muscle model and predicts muscle excitations, muscles forces, and joint moments [241]. To verify the accuracy of muscle forces predicted by CEINMS, we compared lower-limb joint moments generated by CEINMS predictions of muscle forces to their corresponding inverse dynamics values obtained from OpenSim (r^2 are 0.99 ± 0.01 , 0.94 ± 0.05 , 0.93 ± 0.04 ; and RMSE are 7.04 ± 3.99 , 11.32 ± 6.22 , 12.41 ± 4.9 Nm for knee, hip, and ankle, respectively). This neuromusculoskeletal modelling approach predicts muscle and intersegmental loading (i.e., F_{muscle} , M_{muscle} , $F_{\text{intersegmental}}$, and $M_{\text{intersegmental}}$ in Equations (4.1) and (4.2), which were used in our ACL force model.

4.4 Results and Discussion

The key prediction of our model is total ACL force F_{ACL} , which was validated by comparing with recent cadaveric experimental data [62] (Figure 4.4). Root-mean-square error (RMSE) between cadaveric data and predicted ACL forces was low (~ 55 N) and correlation was strong ($r^2 = 0.96$) (Figure 4.4 A). Bland-Altman analysis revealed good agreement between cadaveric data and predicted ACL forces, with narrow limits of agreement ~ 100 N (12%) and negligible bias (~ 44 N) across loading magnitudes (Figure 4.4 B). This agreement indicates that our ACL force model accurately estimates ACL forces in response to different knee loading magnitudes and combinations. The model can now be used to predict *in vivo* ACL loading, when combined with a neuromusculoskeletal model of muscle dynamics.

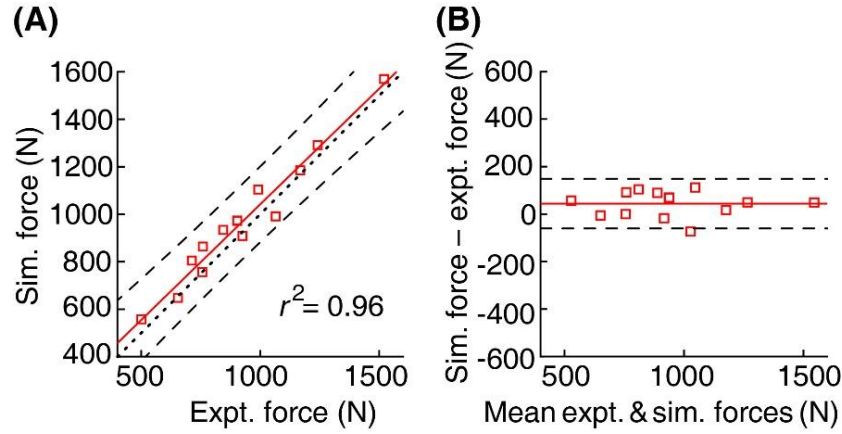


Figure 4.4. ACL force model validation. (A) Comparison of cadaveric experimental ACL force (Expt. force)[62] and simulated ACL force (Sim. force) derived from Equation (4.6). Solid line is regression line ($r^2 = 0.96$; root-mean-squared error (RMSE) = 55.04 N; $P < 0.001$), which is not significantly different from line of identity (dotted line). Dashed lines are 95% confidence intervals. (B) Bland-Altman plot for experimental and predicted ACL forces. Solid line represents mean difference (bias 44 N; $P = 0.01$), and dashed lines are 95% limits of agreement (mean difference ± 1.96 standard deviation, $n = 14$ data points).

Deploying our combined model to predict ACL forces during laboratory-based dynamic motor tasks enables us to estimate *in vivo* ACL force generated through loading in each anatomical plane of motion. We analysed stance phase of a standardized drop-landing and lateral jump movement data (Figure 4.5 A-D). We found that ACL force was mainly driven through sagittal plane, and due primarily to the action of muscles, rather than intersegmental loads (Figure 4.5 B). In frontal plane, contributions of muscle and intersegmental loads to ACL force are of opposite sign and of similar magnitude (Figure 4.5 C), resulting in small ACL forces. In transverse plane, muscle loading makes greater contribution to ACL force than intersegmental loads (Figure 4.5 D).

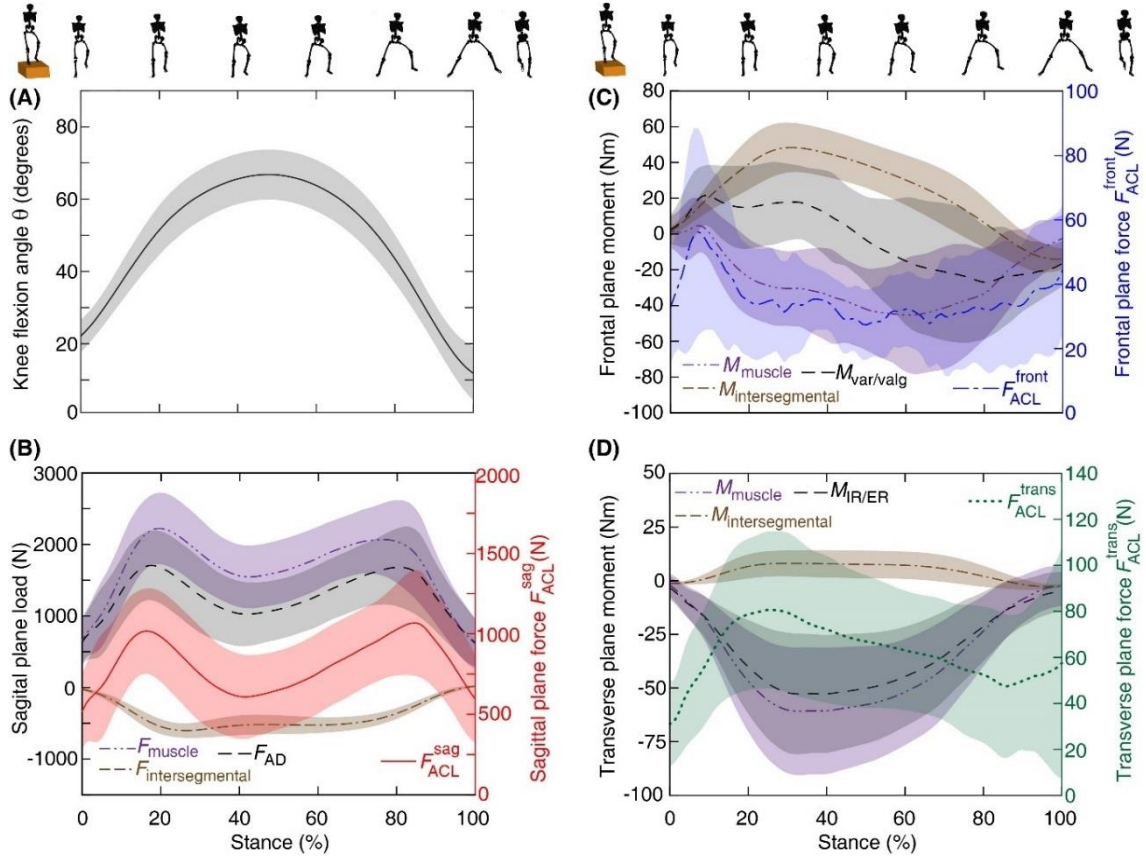


Figure 4.5. Uniplanar ACL forces across the stance phase of the drop-landing task. Silhouettes above (A, C) represent one participant during the stance phase of the task. First and last silhouettes represent the positions before and after the stance phase, respectively, shown for the clarity. (A) Knee flexion angle θ . (B) Sagittal plane knee loading and ACL force. Left axis: muscle and intersegmental forces (F_{muscle} and $F_{\text{intersegmental}}$) obtained from neuromusculoskeletal model, and net anterior drawer force F_{AD} ; see Equation (4.1). Right axis: ACL force $F_{\text{ACL}}^{\text{sag}}$ obtained from Equation(4.3). (C, D) Frontal and transverse planes knee loadings and ACL forces. Left axis: muscle and intersegmental moments (M_{muscle} and $M_{\text{intersegmental}}$), and net varus or valgus moment $M_{\text{Var/Val}}$, and internal or external rotation moment $M_{\text{IR/ER}}$; see Equation ((4.2). Right axis: ACL forces $F_{\text{ACL}}^{\text{front}}$ and $F_{\text{ACL}}^{\text{trans}}$ obtained from Equations (4.4) and ((4.5). The shaded regions are standard deviation of the forces and moments. Direction of sagittal plane knee load: anterior draw (+) and posterior draw (-); frontal plane knee moment: varus (+) and valgus (-); transverse plane knee moment: internal rotation (+) and external rotation (-).

Total ACL force F_{ACL} from multiplanar loading showed that the force applied through sagittal plane F_{ACL}^{sag} dominates contribution to F_{ACL} compared to smaller contributions from frontal and transverse planes (Figure 4.6). When ACL force reached its two local peaks, at ~17.5% and 80% of stance phase of drop-landing task, contribution through sagittal plane to ACL force was above 94%, whereas contributions from frontal or transverse planes are below 8% (Table 4.1). The first peak in ACL force occurs shortly after initial foot to ground contact (75 ± 24 ms), which is comparable to time of rupture in cadavers (54 ± 24 ms) [227]. Notably, relative contributions of uniplanar forces do not sum to 100%, due to the action of other articular soft tissues (i.e., ligaments and menisci) as well as rigid contact between femur and tibia, represented by the cross-terms in Equations (4.6)-(4.8). This contrasts with previous models where net ACL force has been formulated as the sum of multiple uniplanar forces [36, 37]. Pure summation of multiple uniplanar ACL forces results in over- and under-estimation of the total ACL force F_{ACL} depending on knee flexion angles and external loading magnitudes. This means the relationship between uniplanar loading and the force transmitted to the ACL is more complex than summation, which is unsurprising given other articular structures involved in load sharing at the knee [27].

Our estimated total and uniplanar ACL forces were physiologically plausible, as they did not include discontinuities or rapid fluctuations (Figure 4.6). In addition, estimated total ACL force was below average failure loads for young ACL specimens ~ 2160 N [326]. This result contrasts with calculations by Pflum *et al.* [32], who used single participant data and modelled the lower bound ACL force in a drop-landing task (peak ACL force was ~0.4 BW). Their predicted ACL force showed rapid fluctuations, where ACL force dropped to zero shortly after initial foot-to-ground contact, then increased sharply to its peak, and shortly dropped back to zero [32]. Such fluctuations in ACL force

do not seem physiological during landing in presence of high and continuous muscle forces. Together, we conclude that total ACL force is primarily generated through the sagittal plane F_{ACL}^{sag} mainly due to muscle loading F_{muscle} . High muscle loading through the sagittal plane is due to the anteriorly directed line of action of the quadriceps (via patellar ligament) [327] recruited to support and generate large external knee flexion and extension moments [328] during landing and push-off phases, respectively. Furthermore, many knee spanning muscles possess lines of action creating tibiofemoral compression which contributes to net sagittal plane knee loading via the posteriorly sloped tibia [329].

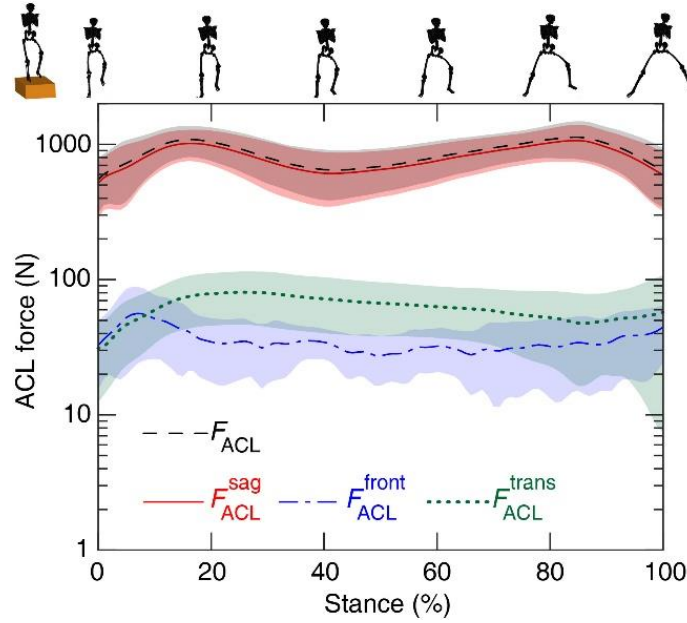


Figure 4.6. ACL force across stance phase of drop-landing. ACL forces through sagittal, F_{ACL}^{sag} , frontal, F_{ACL}^{front} , and transverse, F_{ACL}^{trans} , planes contribute to total ACL force F_{ACL} ; see Equation (4.6). Shaded regions show standard deviation of forces. Silhouettes represent one participant during stance phase of the task. First and last silhouettes are the postures before and after the stance phase, respectively, shown for the clarity.

Table 4.1. Loading parameters at peaks in ACL force during a drop-landing for $n = 13$ participants (mean \pm SD).

| Peak | ACL force (N) | ACL force (BW) | Timing of ACL force (% stance) | Contributions to ACL force from uniplanar action (%) | | |
|-----------------|------------------|----------------------|--------------------------------------|---|-----------------|-----------------|
| | | | | Sagittal | Frontal | Transverse |
| 1 st | 1137 \pm 274 | 1.90 \pm 0.57 | 17.53 \pm 4.62 | 94.32 \pm 2.36 | 7.99 \pm 2.95 | 6.23 \pm 2.52 |
| 2 nd | 1225 \pm 301 | 2.03 \pm 0.5 | 80 \pm 9.13 | 95 \pm 3.48 | 7.45 \pm 5.21 | 4.07 \pm 1.67 |

ACL: Anterior cruciate ligament; BW: body weight.

By modelling interactions between uniplanar knee loading and total ACL force using algebraic expressions, our model differs from previous models [29-37]. Earlier models used 1) explicit representations of the ACL within whole-body anatomical models, and 2) mechanical optimization to derive muscle forces. These approaches have two important limitations. First, explicit representation of the ACL requires subject-specific anatomical information of the knee and plethora articular tissues (i.e., cartilages, menisci, and capsule), as well as mechanical properties of the ACL, other knee ligaments, and articular tissues. Acquiring these data is non-trivial and there is no accepted non-invasive method to measure subject-specific mechanical properties of native knee tissues. Moreover, if there were, it would likely be resource intensive, thus limiting suitability for clinical applications. Second, mechanical optimization typically employed to determine muscle forces is unlikely to predict several empirically observed features of muscle coordination, and is insensitive to task-specific control objectives, and pathology [330, 331].

To overcome these limitations, our model does not rely on explicit representation of anatomy and mechanical parameters of the knee's articular tissues. Rather, our model is based on a set of algebraic expressions that make it easy to be evaluated in real-time [332]. This is important, because it enables ACL force to be used in biofeedback paradigms for injury prevention, training, and rehabilitation. In addition, our model

estimates muscle dynamics using neuromusculoskeletal modelling, which combines subject- and task-specific empirical measurements of muscle excitations (e.g., electromyograms) and modelled musculotendon unit kinematics (i.e., lengths and moments arms). Finally, and importantly, our model is developed and validated based on the most comprehensive available cadaveric experimental data [41, 42, 62] across a wide range of ACL force magnitudes, which are likely to occur during dynamic sporting tasks associated with ACL rupture [62] and everyday activities [41, 42]. These strengths augur well for implementation of this model into standard biomechanical studies and clinical use for people with normal ACL. Since this model is developed using normal ACL experimental data, it may not be applicable for people with a reconstructed ACL or ACL-deficiency. However, this approach can be extended to study the reconstructed ACL upon availability of relevant experimental data wherein reconstructed ACL force or strain is measured in response to multiplanar external knee loading, and/or the ACL force from the current model could be applied to the reconstructed ACL of known length and Young's modulus to estimate allograft strain.

CHAPTER 5

Mechanism of anterior cruciate ligament loading during dynamic motor tasks

Acknowledgement of co-authorship

This chapter includes a co-authored paper that has been re-formatted for this thesis. The bibliographic details/status of the co-authored paper, including all authors, are:

Nasseri, A., Lloyd, D.G., Bryant, A.L., Headrick, J., Sayer, T.A., Saxby, D.J. Mechanism of anterior cruciate ligament loading during dynamic motor tasks, *Medicine and Science in Sports and Exercise*. In Press.

I made a substantial contribution in the conception and design of this study, analysis and interpretation of data, drafting and revising of the final manuscript.

Student/ Corresponding author: Azadeh Nasseri

Principal supervisor: David G Lloyd

5.1 Abstract

Introduction: This study determined anterior cruciate ligament (ACL) force and its contributors during a standardized drop-land-lateral jump task using a validated computational model. **Methods:** Three-dimensional whole-body kinematics, ground reaction forces, and muscle activation patterns from eight knee spanning muscles were collected during dynamic tasks performed by healthy recreationally active females ($n=24$). These data were employed in a combined neuromusculoskeletal and ACL force model to determine lower limb muscle and ACL forces. **Results:** Peak ACL force (2.3 ± 0.5 BW) was observed at $\sim 14\%$ of stance during the drop-land-lateral jump. The ACL force was primarily generated through the sagittal plane and muscle was the dominant source of ACL loading. The main ACL antagonists (i.e., loaders) were the gastrocnemii and quadriceps, while the hamstrings were the main ACL agonists (i.e., supporters). **Conclusion:** Combining neuromusculoskeletal and ACL force models, the roles of muscle in ACL loading and support were determined during a challenging motor task. Results highlighted the importance of the gastrocnemius in ACL loading, which could be considered more prominently in ACL injury prevention and rehabilitation programmes.

5.2 Introduction

Rupture of the anterior cruciate ligament (ACL) is a common and debilitating knee injury. In Australia, ACL ruptures result in an annual ACL reconstruction rate of 77.4 per 100,000 individuals, which is the highest in the world, and has been increasing in adolescents and young adults over the past decades [2]. The majority of ACL ruptures do not involve direct collision, but occur during landing, sidestep cutting, and pivoting tasks common to sports such as soccer, basketball, and netball [5]. Furthermore, ACL ruptures

are 3.5-4 times more frequent in female compared to male athletes [69]. Biomechanical studies have attempted to elucidate the mechanisms of ACL loading and unloading during dynamic tasks. However, these studies have rarely examined ACL loading directly or included the individual's unique activation patterns in muscle force estimations [43, 44]. This has resulted in uncertainty regarding the roles of certain muscles, such as gastrocnemii, in loading the ACL during dynamic tasks [43, 44]. Therefore, the precise mechanisms underlying ACL loading during dynamic activities remain unclear, impeding further development of injury prevention and rehabilitation programs with personalized targets mechanistically linked to *in vivo* ACL loading.

To prevent ACL injuries it is important to study the contributions to ACL loading during tasks that likely stress the ACL, such as sidestep cutting or landing from a jump [5]. The magnitude of ACL loading may be affected by the activation and action of muscles surrounding the knee. During dynamic tasks, the central nervous system may adopt “selective” or “generalized” neural strategies to stabilize the joint [333, 334]. Selective activation predominantly activates muscles with moment arms suited to supporting the external loads. Selectivity is inferred by the magnitude of activation or ratio of activation. Examples include elevated levels of activation of gracilis to counter an external valgus moment, or co-activation of the medial hamstrings and medial quadriceps to oppose external knee valgus loading. The second strategy is generalized co-contraction [333, 334], involving coactivation of hamstring and quadriceps muscles without any selectivity of specific muscles to support specific external loads. These muscle activation patterns are thought to aid knee stabilisation by supporting externally applied loads [195], and differ based on sex, athletic skill level, and task anticipation [176, 195]. Importantly, muscle activation, as assessed by electromyography (EMG), does not directly correspond with muscle force generation [27, 335], which depends on several

additional factors including muscle physiological cross-sectional area, length, and velocity [335]. Therefore, one should not infer muscle force, nor its role in loading or unloading the ACL, from activation level alone. Studies have been conducted to directly measure (via surgically implanted instruments) ACL loading during dynamic tasks, such as jumping and landing [336-338]. However, direct measurements are invasive and cannot be conducted in large samples nor do they provide insight into the contributors to ACL loading. Alternatively, computational models enable non-invasive assessment of ACL loading and its contributors, during dynamic tasks.

A range of computational models have been developed and used to further our mechanistic understanding of ACL loading during various tasks [32-34, 36, 38, 39, 43, 44]. Shelburne and colleagues developed a sagittal-plane knee model with an elastic ACL element that demonstrated ACL loading resulted from complex interactions between muscles, ligaments, and articulating surfaces. They deployed their model to analyse isometric contractions [33], walking [34, 38, 39], and drop-landing [32], and noted that muscle-generated tibiofemoral compression contributed to ACL loading. However, the loading patterns were predicted by bespoke models developed for specific individuals and conditions and restricted to the sagittal plane [32-34, 38, 39], making generalisation to females and larger cohorts difficult.

Other studies [36, 43, 44] have used models within the free and open-source OpenSim framework [230] combined with various methods to assess ACL loading during dynamic tasks. Weinhandl and colleagues [36] studied ACL loading in sidestep cutting using their documented phenomenological ACL force model developed based on data from experiments performed on cadavers [41, 42]. However, their formulations are not consistent with direct measurements of the ACL load from [41, 42], and their musculoskeletal models employed static optimisation to synthesise muscle activation

patterns which may not account for many empirically observed features of muscle coordination. Indeed, in two studies examining drop-landing [43, 44], one reported small [43] and the other large [44] gastrocnemii contributions to ACL loading, which might be due to use of static optimization [43] and EMG-informed approaches [44] to derive muscle activation patterns. An EMG-informed model accounts for subject- and task-specific muscle activation patterns, which is important as Navacchia *et al.* demonstrated tibia anterior shear is sensitive to levels of knee muscle co-contraction [44]. Thus, incorporating EMG into computational models may clarify the role of muscle in ACL loading during tasks known to elicit high levels of co-contraction.

This study aimed to calculate ACL force during a standardized drop-land-lateral jump task in females, using a validated computational model [339]. The second aim was to determine contributions of knee muscles to ACL force. The underlying computational model incorporated subject- and task-specific muscle activation patterns using an EMG-informed neuromusculoskeletal modelling approach [339]. Females were examined due to the marked disparity between the sexes in the rates of ACL injury. It was hypothesized the ACL would receive the majority of its loading via the sagittal plane mechanism, based on previous studies of *in vivo* landing mechanics [339, 340] and experiments performed on cadavers [62]. It was also hypothesized, based on cadaveric experiments [62], the quadriceps would be the primary ACL loader (i.e., antagonists) and the hamstrings the main supporters (i.e., agonists).

5.3 Methods

This study was approved by the University of Melbourne Human Research Ethics Committee (#1442604) and data acquisition was conducted at the Centre for Health, Exercise & Sports Medicine, University of Melbourne, Australia. Twenty-four healthy

females (age: 19.9 ± 4.1 years; mass 59.8 ± 9.3 kg; height 1.65 ± 0.06 m; body mass index 21.9 ± 3.4 kg·m⁻²) volunteered to participate in this study and were recreationally active with no history of lower limb injury, knee pain, or previous ACL or meniscal injuries. All participants were classified as late/post-pubertal based on Tanner's pubertal classification system (i.e., Tanner stages IV and V). Participants, or their parents/guardians for those <18 years of age, provided their informed consent before data collection.

Each participant attended a laboratory-based testing session, wherein three trials of a standardized drop-land-lateral jump from a box and three trials of running with their natural running style (speed 2.8 to 3.2 m·s⁻¹) were performed. One drop-land-lateral jump and one running trial were subsequently used for model calibration, described in greater detail later in this section. To standardise the drop-land-lateral jump, box height was normalized to 30% of each participant's leg length (average box height (SD) = 24.6 (1.1) cm) to impose a similar task demand across individuals of different stature. For the drop-land-lateral jump, participants began by standing on their dominant leg at the centre of the box, which was positioned 10 cm from the force plate, with their hands folded across their chest. Participants were instructed to drop down and land on their dominant leg on the marked target at the centre of the force plate, and immediately perform a 90° lateral jump landing on their contralateral leg on the marked target set at a distance of 150% their lower limb length from the centre of the force plate. Participants were asked to perform the drop-land-lateral jump task as quickly as possible. This task was selected for analysis based on its similarity to single-leg landing manoeuvres performed in sports, given the majority of ACL ruptures occur during single-leg stance [341].

During the running and drop-land-lateral-jump, three-dimensional body motion (i.e., trunk, pelvis, lower limbs, and feet), ground reaction forces (GRFs), and EMG were synchronously and concurrently acquired. Three-dimensional motion was acquired using

a 12-camera motion capture system (Vicon Motion Systems, Oxford, UK) sampled at 120 Hz, while GRFs were acquired using ground embedded force platforms (AMTI, Massachusetts, USA) sampled at 2400 Hz. Muscle activations were acquired using a wireless surface EMG system (Noraxon, Arizona, USA) sampled at 2400 Hz. Each participant was outfitted with retroreflective markers mounted on specific anatomical landmarks as previously described [318]. Surface EMG electrodes were applied overlying the eight major lower limb muscles spanning the knee (i.e., rectus femoris, vastus lateralis, vastus medialis, tibialis anterior, lateral gastrocnemius, medial gastrocnemius, lateral hamstrings, and medial hamstrings) of the dominant leg, consistent with the guidelines from Surface Electromyography for the Non-Invasive Assessment of Muscles (<http://www.seniam.org/>). These muscles were selected due to their large cross-sectional area (i.e., they have substantial force generating capability), they span the knee (i.e., can directly influence knee loads), and are accessible (i.e., superficial to the leg, hence suitable for surface EMG). Data were filtered using second-order, zero-lag, Butterworth filters, where body markers and GRFs were low pass filtered with 6 Hz cut-off frequency. Raw EMG was first band-pass filtered (30-300 Hz), full-wave rectified, and then low-pass filtered with a cut-off frequency of 6 Hz to produce linear envelopes. Each EMG linear envelope was subsequently normalized to its maximum envelope value identified from all available trials.

External biomechanics as well as muscle and ACL forces were determined from comprehensive motion analysis data collected in the laboratory using the overall processing pathway presented in Figure 5.1. The external biomechanics during the drop-land-lateral jump task were determined using OpenSim [230] version 3.3. A full-body generic musculoskeletal model was used, consisting of 37 degrees-of-freedom (DOF), and 80 muscle tendon unit (MTU) actuators [303]. This generic model was modified by

adding dummy tibias of negligible mass and associated universal joints without changing the original knee mobility of flexion/extension with other motions (i.e., abduction/adduction rotation, internal/external rotation, superior-inferior translation, and anterior/posterior translation) prescribed as functions of knee flexion. This modification enabled computation of three-dimensional knee moments and tibiofemoral contact forces needed for subsequent ACL force modelling [45]. This modified generic musculoskeletal model was then linearly scaled to match gross dimensions of each participant using prominent bony landmarks and hip joint centres [339]. Following linear scaling, muscle and tendon operating ranges are not necessarily preserved [258], and, therefore, tendon slack and optimal fibre lengths for each MTU actuator were optimized to preserve the dimensionless force-length operating curves [306]. Final preparation of the musculoskeletal model for each participant involved updating maximum isometric strength of each MTU actuator using the relationships of lower limb muscle volumes with overall mass and height as per [308]. Then, OpenSim inverse kinematics, inverse dynamics, and muscle analysis tools were used to determine joints motions (i.e., general coordinates), net external joint forces and moments, and MTU kinematics, respectively [230].

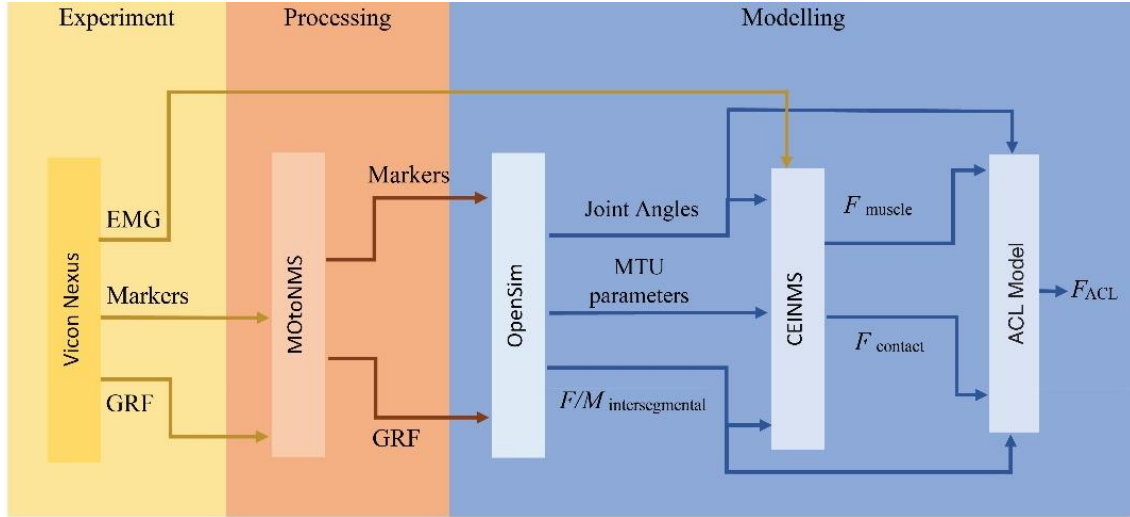


Figure 5.1. Schematic of ACL force calculation workflow composed of three main parts: experimental acquisition of movement data (yellow), data processing (orange), EMG-driven musculoskeletal modelling and ACL force calculation (blue). The box blocks represent the processing tools and the arrows represent the input/output to/from each tool. ACL: anterior cruciate ligament; EMG: electromyography; GRF: ground reaction forces; MTU: muscle tendon unit. F_{muscle} : muscle forces due to their direct line of action; $F_{contact}$: tibiofemoral contact force; F_{ACL} : force in the ACL.

The conditioned EMG, external biomechanics, and MTU kinematics, were combined to estimate lower limb muscle forces using the Calibrated EMG-informed Neuromusculoskeletal Modelling (CEINMS) toolbox [248]. For each participant, CEINMS was first run in calibration mode using one drop-land-lateral jump and one running trial. Calibration is an optimization process, whereby each participant's excitation-to-activation and MTU actuator parameters are adjusted, within physiological bounds, to minimize error between joint moments calculated from inverse dynamics and those from CEINMS. We calibrated for sagittal plane moments about the hip, knee, and ankle of the dominant (i.e., EMG instrumented) limb. Once calibrated, we used CEINMS in EMG-assisted mode [248] to estimate forces for lower limb muscles, as well as tibiofemoral contact forces, for all drop-land-lateral jump trials. In EMG-assisted mode, we used the experimentally collected EMG (i.e., from the abovementioned eight lower

limb muscles) as inputs, along with the external biomechanics, to synthesise excitations for the remaining 32 MTU of the lower limb using a neural control solution that minimally adjusted the experimentally collected EMG to match joint moments from inverse dynamics. Adjusted and synthesized excitations were achieved by minimising the following objective function:

$$E = \alpha E_{MOM} + \beta E_{EXC} + \gamma E_{EMG} \quad (5.1)$$

where, E_{MOM} is the sum of squared differences between predicted (CEINMS generated) and experimental (inverse dynamics) joint moments, E_{EXC} represents the sum of squared excitations for all MTU, and E_{EMG} is the sum of differences between adjusted EMG excitations and recorded EMG excitations. Factors α , β , and γ are positive weighting coefficients [248]. We set the values of α and β to 1, and optimised weighting of γ to minimise errors in adjusted muscle excitations and predicted joint moments.

The combined OpenSim and CEINMS modelling were used to estimate lower limb muscle, joint, and tibiofemoral contact forces, which were then incorporated into a previously validated ACL force model [339] to quantify ACL force and the biomechanical contributions to this force. The ACL force model was developed from experimental data, where a wide range of multiplanar load magnitudes and combinations were externally applied to instrumented cadaveric knees [41, 42, 62]. These loads were in the sagittal (anterior-posterior drawer and compression forces), frontal (varus/valgus moments), and transverse (internal/external rotation moments) planes. The empirical relationships between experimental multiplanar loads and ACL forces were modelled as the linear summation (equation 2) of a set of exponential functions, where the function constants were fitted to the data using a non-linear least squares method [339]. Once developed, the ACL force model was validated against a sub-set of experimental

multiplanar knee loading data [62] not used for model fitting. The ACL force model showed excellent accuracy in predicting experimentally measured ACL forces (i.e., coefficient of determination $R^2=0.96$; root-mean-squared error (RMSE)=55 N; $P<0.001$), narrow limits of agreement, and negligible bias across a wide range of loading magnitudes and combinations [339].

In brief detail, the model estimated ACL force by accounting for the multiple uniplanar loading contributions and their interactions, i.e.

$$F_{ACL} = F_{ACL}^{sag} + F_{ACL}^{front} + F_{ACL}^{trans} + \sum_j CT_j \quad (5.2)$$

where, F_{ACL}^{sag} , F_{ACL}^{front} , and F_{ACL}^{trans} are contributions to ACL force developed in sagittal, frontal, and transverse planes, respectively, while CT_j (for $j = SF, ST, FT$) represents interactions between sagittal-frontal (SF), sagittal-transverse (ST), and frontal-transverse (FT) planes loading [339]. The ACL forces in each plane (F_{ACL}^{sag} , F_{ACL}^{front} , and F_{ACL}^{trans}) and interactions (CT_j), were determined using each plane's estimated net loads. These net loads were equivalent to externally applied loads in the cadaveric studies from which ACL forces were measured, with anterior directed forces, varus moments, and internal rotation moments considered positive.

Specifically, F_{ACL}^{sag} was the ACL force due to the knee's net anterior-posterior directed forces (F_{net}^{AP}), i.e.,

$$F_{net}^{AP} = F_{muscle}^{AP} + F_{contact}^{AP} + F_{intersegmental}^{AP} \quad (5.3)$$

where F_{muscle}^{AP} were the components of the knee-spanning muscle forces acting in the anterior-posterior direction, $F_{intersegmental}^{AP}$ was the externally applied intersegmental force in anterior-posterior direction calculated by inverse dynamics, and $F_{contact}^{AP}$ was the

component of the reaction force caused by tibiofemoral compression acting in anterior-posterior direction due to the posteriorly sloped tibia (assigned average values of 7.5° and 5.2° for medial and lateral tibial plateau slopes for females, respectively) [339].

Similarly, F_{ACL}^{front} was the ACL force due to the knee's net frontal plane (varus/valgus) moments ($M_{net}^{Var/Val}$), i.e.

$$M_{net}^{Var/Val} = M_{muscle}^{Var/Val} + M_{intersegmental}^{Var/Val} \quad (5.4)$$

where $M_{net}^{var/val}$ was derived from the varus/valgus muscle moments ($M_{muscle}^{Var/Val}$) (i.e., muscle forces multiplied by their moment arms in frontal plane) and externally applied intersegmental knee varus/valgus moments calculated via inverse dynamics ($M_{intersegmental}^{Var/Val}$). Further, F_{ACL}^{trans} was the ACL force due to the knee's net transverse plane (internal/external rotation) moments ($M_{net}^{IR/ER}$), i.e.,

$$M_{net}^{IR/ER} = M_{muscle}^{IR/ER} + M_{intersegmental}^{IR/ER} \quad (5.5)$$

where $M_{net}^{IR/ER}$ was derived from the internal/external rotation muscle moments ($M_{muscle}^{IR/ER}$) (i.e., muscle forces multiplied by their moment arms in transverse plane) and externally applied intersegmental knee internal/external rotation moments calculated via inverse dynamics ($M_{intersegmental}^{IR/ER}$). Finally, the interaction terms, (CT_j), account for the increase or decrease in ACL forces determined from net uniplanar loading (Equations (5.3)-(5.5)) due to combined multiplanar loading.

Biomechanical analyses were performed across stance phase of the drop-land-lateral jump task and normalised to 101 data points. Stance phase was defined from initial to final foot-ground contact on the landing leg. For each participant, three trials of drop-land-lateral jump were analysed, then averaged to produce one curve for ACL force and

its uniplanar contributors across stance phase. From these average curves for each participant, we extracted values corresponding to two local maximums of ACL force (raw (N) and normalized to bodyweight (BW)) and the relative contributions (% of ACL force, reported as mean \pm standard deviation) from each plane of motion (Table 5.1). For conventional statistical analysis, we grouped muscles based on their commonly attributed function at the knee (e.g., extensors or flexors) and their loading effect on the ACL (i.e., elevating or lowering force through the sagittal plane mechanism) at the time of the first peak of ACL force. The first peak of ACL force is focused on, for the reason that video analysis of ACL rupture events in various sports identifies rupture to occur shortly after foot-ground (i.e., within 50 ms) [129].

One-way ANOVAs and post hoc t-tests were used to assess differences between the relative contributions of individual muscles and muscle groups to the anteriorly directed force on the tibia generated by knee spanning muscles (F_{muscle}) at the first peak of ACL force. Statistical significance was set to $p < 0.05$ for the ANOVA and then Bonferroni correction were applied to the post-hoc t-tests. All statistical analyses were performed in SPSS v25 (IBM, Armonk, NY)

5.4 Results

During the stance phase of the drop-land-lateral jump, the ACL sustained substantial (i.e., magnitudes greater than bodyweight), continuous (i.e., no instances of zero force), and smooth (i.e., no spikes) force. The magnitude of ACL force oscillated, displaying two local peaks separated by a distinct local minimum (Figure 5.2 B), with a global maximum of ~ 1370 N (~ 2.3 BW). The majority of ACL force was developed through the sagittal plane, with small contributions via frontal and transverse planes (Figure 5.2). Two peaks in the ACL force were identified at $\sim 14\%$ and $\sim 75\%$ of stance, with the first at 63.1 ± 17.4

ms following initial foot-ground contact. At the first peak, >94% of ACL force was generated through the sagittal plane, and frontal and transverse plane contributions were <8% (Table 5.1). Of note, ACL force is not equal to the sum of uniplanar contributions due to disproportionate and non-linear additive nature of multiplanar knee loading [339].

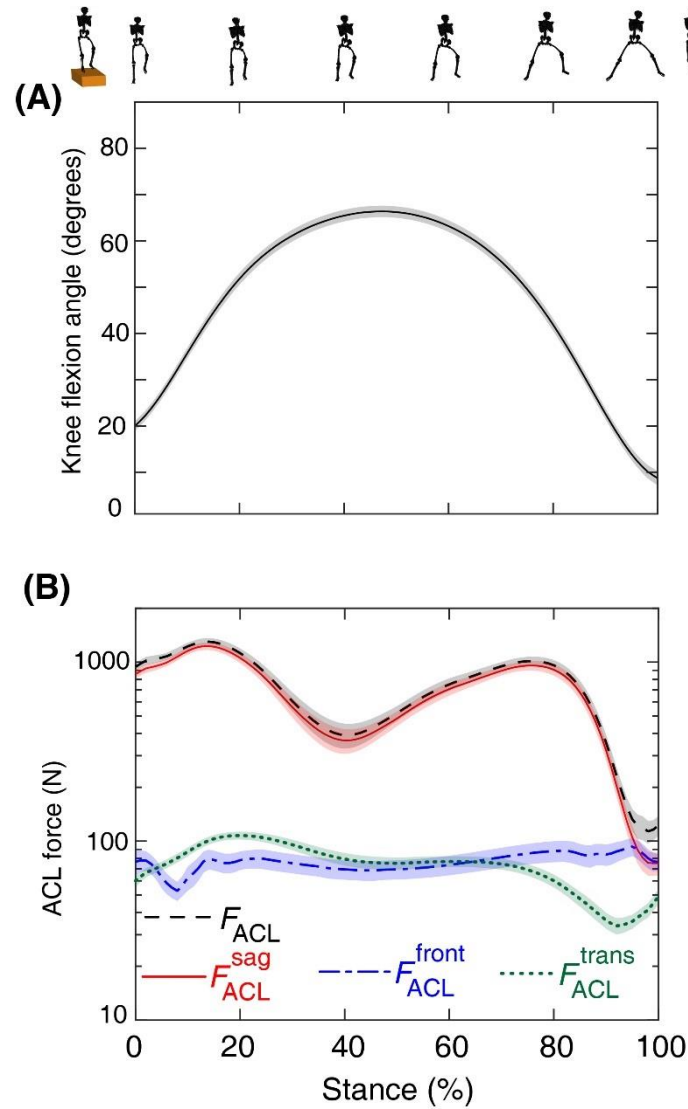


Figure 5.2. Knee flexion angle (A) and ACL force (B) across stance phase of drop-land-lateral jump. The tension in the ACL due to forces acting in the anterior-posterior direction (F_{ACL}^{sag}), the force in the ACL due to moments in frontal plane (F_{ACL}^{front}), and the force in the ACL due to moments in transverse plane (F_{ACL}^{trans}) contribute to ACL force (F_{ACL}). Shaded regions show standard error of the mean. Silhouettes represent one participant during stance phase of the task. First and last silhouettes represent posture

before and after stance, respectively, and are added to clarify the stages of the task. ACL: anterior cruciate ligament.

Table 5.1. Loading parameters at the two local peaks in the ACL force during the drop-land-lateral jump performed by twenty-four participants reported as mean \pm standard deviation.

| Peak | ACL force (N; BW) | Timing of ACL force (% stance) | Uniplanar contributions to ACL force (%) | | |
|-----------------|----------------------------------|--------------------------------------|--|---------------|---------------|
| | | | Sagittal | Frontal | Transverse |
| 1 st | 1369 \pm 308; 2.3 \pm 0.5 | 13.9 \pm 4.6 | 94.8 \pm 1.3 | 5.9 \pm 3.4 | 7.3 \pm 1.9 |
| 2 nd | 1114 \pm 255; 1.9 \pm 0.4 | 74.7 \pm 6.1 | 94.7 \pm 1.8 | 7.9 \pm 4.8 | 6.8 \pm 2.4 |

ACL: anterior cruciate ligament; BW: bodyweight.

In the sagittal plane, muscles were primary contributors to ACL force through their direct anterior-posterior lines of action and compressive contact forces applied to the posteriorly sloped tibia (Figure 5.3). Despite the posteriorly directed externally applied net intersegmental force applied to the knee, the ACL developed tension continuously throughout this task, because of the large magnitude anteriorly directed muscle and contact forces. In the frontal plane, muscles generated knee valgus moment to counter the externally applied intersegmental varus moments, which resulted in net valgus moment that had to be supported by the ACL and other soft tissues (Figure 5.4 A). In the transverse plane, muscle generated external rotation moment about the knee, to counter the externally applied intersegmental internal rotation moments, which resulted in net external rotation moment that had to be supported by the ACL and other soft tissues (Figure 5.4 B).

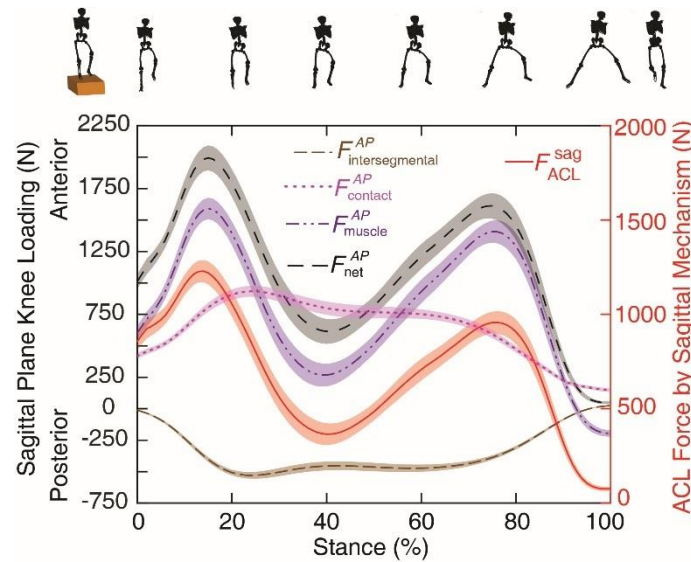


Figure 5.3. Sagittal plane knee loading (left axis) and ACL force (right axis) during stance. Left axis: muscle forces due to their direct line of action (F_{muscle}^{AP}), tibiofemoral compressive contact force ($F_{contact}^{AP}$), and intersegmental forces ($F_{intersegmental}^{AP}$). F_{net}^{AP} is the net knee joint forces acting in the anterior-posterior direction calculated as $F_{net}^{AP} = F_{muscle}^{AP} + F_{contact}^{AP} + F_{intersegmental}^{AP}$. Right axis: the tension in the ACL due to forces acting in the anterior-posterior direction (F_{ACL}^{sag}). Shaded regions show standard error of the mean. Direction of sagittal plane knee load: anteriorly (+) and posteriorly (-) directed. Silhouettes represent one participant during stance phase of the task. First and last silhouettes are before and after stance, respectively, shown to clarify the stages of the task. ACL: anterior cruciate ligament.

At the first peak of ACL force, the gastrocnemii and quadriceps were the primary muscle groups causing the anteriorly directed tibial force (Figure 5.5 A), providing $67.3 \pm 14.4\%$ and $68.2 \pm 14.4\%$ relative contributions, respectively. These contributions were not significantly different to each other ($p > 0.05$) but were significantly larger compared to the other muscle groups. The hamstring muscle group was the main contributor to posteriorly directed force, making $-30.8 \pm 17\%$ contribution. This was significantly larger (ignoring sign) ($p < 0.05$) compared to the unloading contribution from other small knee spanning muscle groups ($-4.7 \pm 4.6\%$).

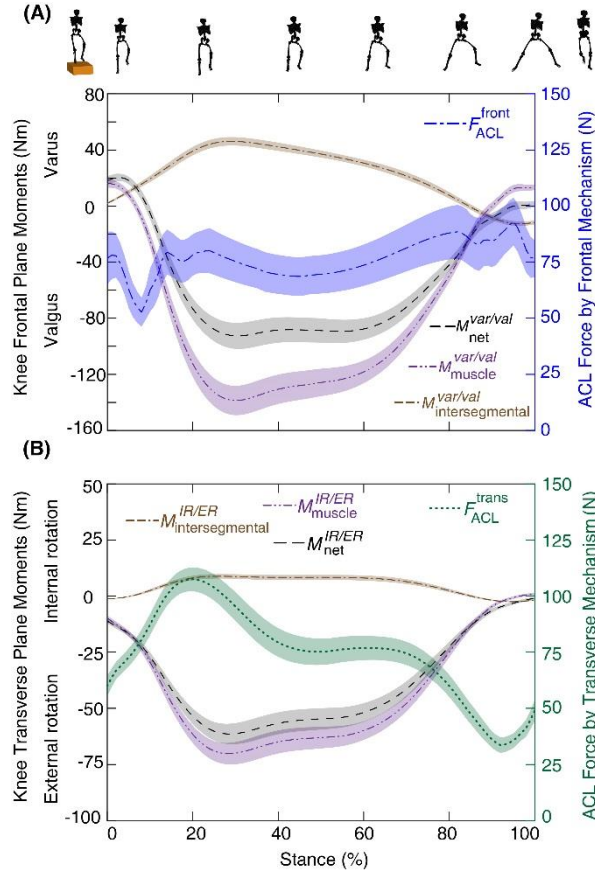


Figure 5.4. Uniplanar ACL forces across the stance phase of the drop-land-lateral jump task. **(A)** Frontal plane knee loading (left axis) and ACL force (right axis) during stance. Left axis: varus/valgus muscle moments ($M_{muscle}^{Var/Val}$) and intersegmental knee varus/valgus moments ($M_{intersegmental}^{Var/Val}$), $M_{net}^{var/val}$ is the net frontal plane (varus/valgus) moment ($M_{net}^{Var/Val}$) calculated as $M_{net}^{Var/Val} = M_{muscle}^{Var/Val} + M_{intersegmental}^{Var/Val}$. Right axis: F_{ACL}^{front} , the ACL force due to the net frontal plane (varus/valgus) moments ($M_{net}^{var/val}$). **(B)** Transverse plane knee loading (left axis) and ACL force (right axis) during stance. Left axis: internal/external rotation muscle moments ($M_{muscle}^{IR/ER}$) and intersegmental knee internal/external rotation moments ($M_{intersegmental}^{Var/Val}$), $M_{net}^{IR/ER}$ is the net transverse plane (internal/external rotation) moment calculated as $M_{net}^{IR/ER} = M_{muscle}^{IR/ER} + M_{intersegmental}^{IR/ER}$. Right axis: F_{ACL}^{trans} , the ACL force due to the net transverse plane (internal/external rotation) moments ($M_{net}^{IR/ER}$). The shaded regions represent the standard error of the mean. Direction of frontal plane knee moment: varus (+) and valgus (-) and transverse plane knee moment: internal rotation (+) and external rotation (-). Silhouettes represent one participant during the stance phase of the task. ACL: anterior cruciate ligament.

Of the individual muscle contributions (Figure 5.5 B), gastrocnemius medialis and vastus lateralis made the greatest relative contribution to anteriorly directed net muscle force at the first peak of ACL force, accounting for $51.5 \pm 12.45\%$ and $38 \pm 11.1\%$, respectively. Their contributions were not significantly different to each other ($p > 0.05$), but significantly higher than all other ACL loading muscles ($p < 0.05$). Gastrocnemius lateralis, vastus intermedius, and rectus femoris made similar contributions of $15.7 \pm 6.2\%$, $13.5 \pm 5.2\%$, and $10.2 \pm 5.2\%$, respectively, which were not significantly different to each other ($p > 0.05$). Vastus medialis made $6.4 \pm 2\%$ relative contribution to the anteriorly directed net muscle force, which was significantly lower compared to all other ACL loading muscles, except for rectus femoris ($p < 0.05$).

The semimembranosus was the main muscle generating posteriorly directed force to the tibia, making $-21.9 \pm 14.3\%$ relative contribution to the anteriorly directed net muscle force (Figure 5.5 B). Except for biceps femoris long head, contribution from semimembranosus was significantly higher compared to all the other ACL unloading muscles ($p < 0.05$). The rest of the contributions from the ACL unloading muscles were less than -5.5% (ignoring sign) and some significant differences were observed ($p < 0.05$).

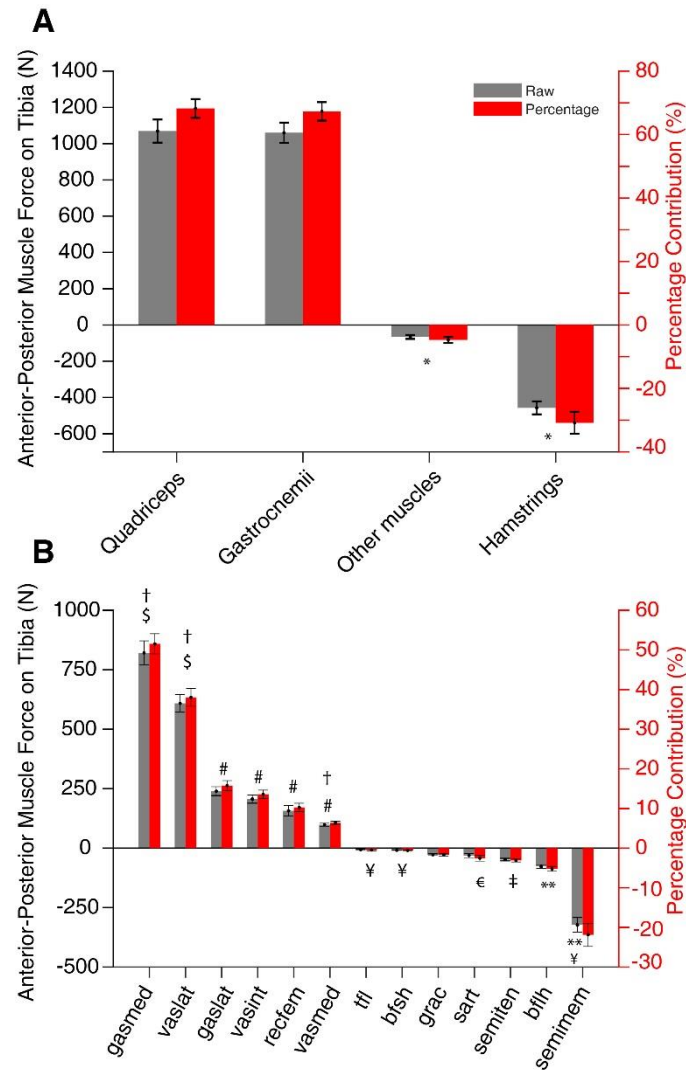


Figure 5.5. Grouped (A) and individual (B) muscle loads applied to the tibia in the sagittal plane at the first peak in ACL force. Direction of muscle forces: anteriorly (+) and posteriorly (-) directed. Left axes display the absolute muscle forces (N) and right axes display relative contributions (%) to net anterior-posterior force from all muscles (F_{muscle}). The symbols atop the bars represent significant differences. In (A), symbol * indicates significant difference from other muscle groups. In (B), the muscles that load the ACL via an anteriorly directed force are compared to each other, wherein † indicates significant difference from gaslat and vasint, # indicates significant difference from gasmed and vaslat, \$ indicates significant difference from rectfem. In (B), muscles that support load the ACL via an posteriorly directed force are compared to each other, wherein ** indicates significant difference from sart, grac, bfsh, and tfl, ¥ indicates significant difference from semiten, ‡ indicates significant difference from bfsh and tfl, € indicates significant difference from tfl. Error bars represent standard error of the mean.

ACL: anterior cruciate ligament; gasmed: gastrocnemius medial head; vaslat: vastus lateralis; gaslat: gastrocnemius lateral head; vasint: vastus intermedius; recfem: rectus femoris; vasmed: vastus medialis; bfsh: biceps femoris short head; tfl: tensor fasciae latae; grac: gracilis; sart: sartorius; semiten: semitendinosus; bflh: biceps femoris long head; semimem: semimembranosus.

5.5 Discussion

This study explored the ACL loading mechanism during an athletic task considering contributions from individual and grouped knee-spanning muscles using EMG-informed neuromusculoskeletal model incorporating a validated ACL force model. Results support the first hypothesis that the primary mechanism of ACL loading was through the sagittal plane during this task. Gastrocnemii and quadriceps groups made the greatest relative contribution to anteriorly directed tibial force, thus loading the ACL. Hamstring muscle group was the main ACL supporter, applying posteriorly directed tibial force. These findings suggest ACL force might be lowered during dynamic tasks by augmenting hamstring activation.

The finding that the ACL was loaded primarily through the sagittal plane is consistent with modelling studies of landing tasks [339, 340], but different from direct measurements taken from cadavers [62, 342, 343]. Studies performed on cadavers suggest knee internal rotation, varus, and valgus moments make large contributions, in addition to sagittal plane forces, to loading the ACL. The discrepancy between results from modelling and cadaveric studies may be due to the different knee kinematics and loads in live humans compared to cadaveric experiments. In recent cadaveric experiments [62, 342], the femur was mounted on an instrumented rig, in which multiplanar external knee and artificial muscle loads were applied to the shank with an axial compressive impact superimposed. This resulted in considerable non-sagittal knee motions (e.g., 27° valgus and 38° tibial rotation), which do not occur during non-injurious dynamic tasks such as

those performed in a motion capture laboratory. Moreover, the anterior force applied to the cadaver tibia was considerably smaller in magnitude (e.g., 268 N) compared to the net anterior-posterior knee load estimated by our model of the dynamic motor task (e.g., ~ 2000 N). Furthermore, in the current study there was considerable muscular support of the externally applied varus and internal rotation moments, possibly greater than used in the cadaveric studies. Together, these differences may account for the relatively small contributions from anterior tibia force to ACL loading compared to valgus and internal rotation moments found in experiments conducted on cadavers. On the other hand, the contribution to ACL force from frontal plane loading might increase if the performed activity induced greater external valgus knee moments than those generated by the task in the current study, which involved predominantly sagittal motions of the drop-landing leg, with relatively small frontal plane loading that did not involve large external valgus knee moments.

Contrary to the second hypothesis, the gastrocnemii and quadriceps made the greatest contributions to the anteriorly directed force applied to the tibia (Figure 5.5). The large gastrocnemii contribution is consistent with a previous study that used an EMG-informed method to determine muscle forces and their contributions to knee loading during a drop landing task [44]. In contrast, Mokhatrzadeh *et al.* [43] reported small gastrocnemii contribution to ACL loading during a landing task. This discrepancy in the role of the gastrocnemii is potentially due to use of static optimization [43], compared to EMG-informed methods, to determine muscle forces [43], underestimating gastrocnemius activation and its role in ACL loading. Together with results of Navacchia *et al* [44], our findings highlight the importance of the gastrocnemii in ACL loading, which may have been previously overlooked. Indeed, many previous studies focused on the roles of the quadriceps and hamstrings in ACL injury risk [344] or loading [32, 33].

However, recent studies have shown the ankle spanning muscles are highly recruited to generate the torque and power essential to task performance during demanding dynamic single-leg tasks (e.g., side-step cutting) [345]. In this study, we observed moderate knee flexion ($37\pm 11^\circ$) at the first peak of ACL force and at this position the gastrocnemii can apply substantial posteriorly directed force to the femur due to their anterior-posterior lines-of-action as well as their compression forces applied to a posteriorly sloped tibia [346]. Overall, we found muscle contributions to anteriorly directed force on the tibia, and thus ACL force, through their anterior-posterior lines of action was greater than that from compression of the posteriorly sloped tibia. Nevertheless, both mechanisms were found important contributors to ACL loading and should be considered when investigating risk of ACL injury.

The hamstrings were the primary knee-spanning muscles generating posteriorly directed force to the tibia, supporting our second hypothesis and consistent with previous findings [43]. Hamstrings can apply a posteriorly directed force to the tibia to support the ACL when the knee is moderately flexed, as we observed at the peak ACL force during this task. However, their ACL support is partially offset by the hamstrings having lines of actions with vectors components perpendicular to the tibial plateau, which generate tibiofemoral compression and consequently anterior force due to the posteriorly sloped tibia. Hamstrings likely provide better restraint of the tibia at greater knee flexion as their contribution to tibiofemoral compression diminishes [347]. However, at greater knee flexion, medial and lateral hamstrings have diminished capacity to support varus and valgus knee moments, potentially increasing the ACL loading from these frontal plane moments. Suffice to say, any muscle's contribution to ACL loading or support varies with changes in lower limb kinematics which alter the muscle's line of action and force generating capacity. Thus, modelling as performed in this and similar studies can

delineate the role of muscle in loading or unloading the ACL.

In this study, the largest ACL force across participants (~1845 N), was below average ACL failure loads (~2160 N) reported in young specimens [326]. The presence of such elevated ACL force might suggest that the individual was approaching ACL failure strength, our modelling overestimated ACL force, or ACL failure load is higher than that reported in the literature. However, average peak ACL force in this study is higher compared to previous direct measurement from strain gauges (if a conversion from strain to force is made) [147] and indirect measurement from medical imaging-based approaches [204, 226]. This might be due to the different motor tasks examined in previous studies, where individuals performed single-leg hopping [147] and single-leg vertical jump [204] from the ground or double-leg jump-landing from a box [226]. These tasks might have been less demanding compared to the task performed in this study, where individuals dropped from a considerable height (30% of leg length) onto one leg, followed immediately by a nested motor task in the form of a lateral bound. In addition, these past studies were performed on male participants [147, 204, 226], while the current study examined females.

Compared with a prior modelling study [30] examining a stop-jump task performed by young females, our peak ACL force (1369 N; ~2.3 BW) is of similar magnitude (1150 N; ~2 BW) and timing (~14% and ~17% of stance, respectively) [30]. However, our estimated peak ACL force is higher compared to other prior models' estimations [43, 348], which may have several explanations. First, prior models focused exclusively on the sagittal plane ACL loading mechanism, despite empirical evidence showing that estimation of ACL forces based on multiplanar loading mechanisms can result in smaller or greater ACL forces compared to ACL forces estimated from uniplanar loading alone [41, 62]. Indeed, ACL loading depends on knee posture, external loading

magnitudes and specific combinations, as well as muscles' actions in the different loading planes. Second, previous studies examined single or double-leg drop-jumps confined to the sagittal plane [43, 348], whereas the task performed in the current study involved some out-of-sagittal-plane motion to perform the lateral-jump, likely causing larger frontal and transverse plane loading which in-turn prompted high-levels of muscular co-contraction about the knee to stabilize the joint [195]. Third, we found considerable gastrocnemii contribution to ACL loading using an EMG-informed neuromusculoskeletal modelling approach that respected the individual's muscle activation patterns, whereas gastrocnemii contributions were very small when static optimization was used for muscle force estimation [43].

In the present study, two local ACL force peaks were observed, corresponding with absorption and push-off, respectively. The local minimum separating the peaks roughly aligned with peak knee flexion. The first peak occurred shortly after foot-ground contact ($\sim 14\%$ of stance, 63.1 ± 17.4 ms), similar to the previous simulations [43] after correcting for between-study differences in the definition of movement phases. The timing of the peak ACL force in this study is similar to the time of rupture (54 ± 24 ms) measured in cadaveric experiments [227]. In contrast, *in vivo* measures of ACL strain [204, 226] reported peak strain ~ 50 ms before initial foot-ground contact during a jump and land task. However, video analyses of sport-related ACL injury indicate rupture occurs after initial foot-ground contact, which is supported by results of destructive experiments performed on cadavers [62, 227]. Potentially, the jump and land task monitored through *in vivo* measurement methods was not demanding enough to reproduce the timing of ACL loading seen during rupture events.

In general, ACL loading is driven by complex interplay between muscle forces, body and inertial loads, joint contact forces, and the other passive soft tissues at the knee.

Based on our findings, the hamstrings primarily support the ACL, thus hamstring recruitment is a viable target for reducing ACL load, as found previously [349]. Indeed, high levels of hamstring activation could protect the ACL by reducing the anterior shear forces on tibia [44]. On the other hand, gastrocnemius and quadriceps were the primary loaders of the ACL. Therefore, in theory, lowering the activation of these muscle groups could protect the ACL. However, it is not clear how individual, or group-level muscle recruitment can readily be increased or decreased by training and retained during dynamic tasks without affecting the task performance. Some studies have shown isometric strength or balance training is ineffective in increasing hamstring-to-quadriceps co-contraction [350, 351]. Others suggest specific strength training can increase quadriceps-to-hamstring co-contraction and potentially benefit ACL injury prevention and rehabilitation [352]. Thus, the selection, intensity, and biofeedback of exercises might be important when focusing on ACL injury prevention, as suggested by earlier studies [353, 354]. However, the effects of muscle activation and forces on ACL loads are complex, and therefore, using real-time modelling of ACL force for biofeedback would enable personalized strategies for ACL force reduction and may eventually reduce risk of ACL injury.

A limitation of this study may be the use of scaled musculoskeletal model in the simulations. A higher-fidelity anatomical and neuromuscular representation of the individual will provide more accurate prediction of internal body mechanics, but the effects of increasing model personalization on ACL force estimates is unclear. Second, in our musculoskeletal model, knee varus/valgus rotations, internal/external rotations, and translations are prescribed as functions of knee flexion, and not independent model mobilities resolved via inverse kinematics. Analysing secondary knee motions might provide useful information, since the drop-land-lateral jump task has non-sagittal plane motions. However, analysis of non-sagittal knee motion via three dimensional motion

capture with skin surface markers carries considerable error [167]. Secondary knee joint motions can be accurately recorded via dynamic radiography [355], yet infeasible for large cohorts. Third, the box height from which the participants jumped was normalized to create a similar neuromuscular demand between participants of different heights. However, the kinetic energy at ground impact is also influenced by participant mass, which was not considered in the normalization of the box height and may have contributed to variability in ACL loading between participants. However, the height and mass variations in our sample were small, thus it seems unlikely it would have confounded our interpretation of the results. Fourth, the role of non-knee spanning muscles which might influence the intersegmental loads through the dynamic coupling in multi-body systems, were not considered in this study. Finally, due to higher rates of ACL injury in females, we studied only healthy young female participants. Therefore, the conclusions from this study may not be extended to males. In future, studying both sexes could reveal sex-specific ACL loading mechanisms. Finally, being recreationally active (i.e., performing at least 30 minutes of moderate or vigorous daily physical activity) was one of the inclusion criteria of this study. However, we did not further control for the strength or sporting experience of the participants who met the eligibility criteria which may have affected the jump landing technique. Despite these limitations, our study found timing of peak ACL force consistent with video analysis of injury and destructive cadaveric testing. Importantly, our analysis clarifies how ACL forces are generated during a standardized movement task, which provides further understanding of the ACL loading mechanisms.

In conclusion, the ACL was loaded primarily through the sagittal plane during a standardized drop-land-lateral jump task. Muscles generated substantial forces directed anteriorly to the tibia, hence causing ACL force through their anterior-posterior lines of

action, outweighing smaller contributions made through tibiofemoral compression. The gastrocnemii and quadriceps were the main ACL loaders, while the hamstrings were the major supporter of the ACL. Results highlight the important role of the gastrocnemii in ACL loading, which may have previously been overlooked and may be considered more prominently in ACL injury prevention and rehabilitation programmes.

CHAPTER 6

Effects of pubertal maturation on anterior cruciate ligament forces during a landing task in females

Acknowledgement of co-authorship

This chapter includes a co-authored paper that has been re-formatted for this thesis. The bibliographic details/status of the co-authored paper, including all authors, are:

Nasseri, A., Lloyd, D.G., Minahan, C., Sayer, T.A., Paterson, K., C.J., Vertullo, Bryant, A.L, Saxby, D.J. Effects of pubertal maturation on anterior cruciate ligament forces during a landing task in females. *American Journal of Sports Medicine*. Under review.

I made a substantial contribution in the conception and design of this study, analysis and interpretation of data, drafting and revising of the final manuscript.

Student/ Corresponding author: Azadeh Nasseri

Principal supervisor: David G Lloyd

6.1 Abstract

Background: Rates of anterior cruciate ligament (ACL) rupture in young people have increased by more than seventy percent over the past decades. Adolescent and young adult females are at higher risk of ACL injury compared to their pre-pubertal counterparts.

Purpose: To determine ACL loading and its causes during a standardized drop-land-lateral jump in females at different stages of pubertal maturation.

Study Design: Cross-sectional descriptive laboratory study.

Methods: Based on Tanner's classification system, 19 pre-pubertal, 19 early/mid-pubertal, 24 late/post-pubertal females performed standardized drop-land-lateral jump while three-dimensional body motion, ground reaction forces, and surface electromyography were acquired. These data were used to model external biomechanics, lower limb muscle forces, and knee contact forces, which were subsequently used in a validated computational model to estimate the ACL loading. Statistical parametric mapping analysis of variance was used to compare ACL force, and its causal contributors, between the three pubertal maturation groups during stance phase of the task.

Results: Compared to pre- and early/mid-pubertal females, late/post-pubertal females had significantly higher ACL force (mean differences 482 N and 355 N during 3%-30% and 55%-89% of stance; and 381 N and 296 N during 3%-25% and 62%-85% of stance, respectively), which overlapped peaks in ACL force. At the peak point of ACL force, contributions from the sagittal, and transverse plane loading mechanisms to ACL force were higher in late/post pubertal group compared to pre and early/mid pubertal groups (medium effect sizes ranging from 0.44 to 0.77). No differences were found between pre- and early/mid-pubertal groups in ACL force or its contributors.

Conclusion: The highest ACL forces were observed in late/post-pubertal females (aged 14-25 years), consistent with recently reported rises of ACL injury rates in females aged 15-19 years.

Clinical relevance: Growth of ACL volume plateaus around 10 years of age, prior to pubertal maturation. Compared to their less mature counterparts, late/post-pubertal females are heavier but have a similarly sized ACL. Combined with our finding that ACL force is higher in late/post-pubertal females, these factors may explain the higher rates of ACL injuries in females aged 15-19 years.

6.2 Introduction

Anterior cruciate ligament (ACL) rupture is a common and debilitating knee injury resulting in direct societal health care costs (i.e., surgical care and physical therapy) and elevated risk of early onset knee osteoarthritis [7]. Rates of ACL rupture in young people have increased dramatically over past decades [2]. with the resultant burden of trauma-induced knee osteoarthritis falling most heavily on the young. Age- and sex-specific differences in rates of ACL rupture have been observed [2]. There is two to four times greater risk of sustaining ACL injury in females athletes compared to male athletes [8-10]. and late- to post-pubertal young women compared to pre-pubertal girls [10], possibly due to younger females having lower proprioceptive acuity [11] and using muscle activation patterns less suited to knee stabilization [12-14], potentially antagonizing the ACL [13]. Further, postural and anatomical changes associated with pubertal maturation, such as increased knee valgus alignment and internally rotated hips [356], potentially contribute to higher ACL strain sustained by female cadavers compared to male cadaveric specimens subjected to similar external loading [357]. However, conclusive causal mechanism(s) have yet to be presented.

Increased rates of ACL reconstruction in females aged 15 to 19 years have been reported [2], possibly due to higher rates of ACL rupture in that cohort, however, the reason remains unclear. Prior literature [11-14] indicates neuromuscular control deteriorates as females progress through puberty, suggesting changes in the contributions from body and inertia, muscle, and articular contact forces to ACL force. As females reach latter stages of pubertal maturation, they land with straighter knees [15], and experience larger ground reaction forces [16] and external knee moments [17-20], potentially placing the ACL under greater load compared to less mature females [40, 62]. Anatomical changes occurring across mid-to-late pubertal maturation stages, such as rapid lower limb growth [21] and deteriorating neuromuscular control [11-14], may conspire to increase ACL force in young women. Moreover, a plethora of studies speculate about the role of puberty-related changes to anatomy [22], external joint biomechanics [20], force generation [23], and neuromuscular control [24, 25] in increased rates of ACL rupture. However, a validated causal model of ACL forces in live humans has not been performed. Recently, a computational model of ACL force has been developed and validated to estimate ACL force during dynamic tasks [339]. This model could be used to study females at different stages of pubertal maturation to reveal causal effects of maturation on ACL force.

The purpose of this study was to use a validated model to determine ACL force during a dynamic motor task likely to load the ACL in females across stages of pubertal maturation. We used an EMG-informed neuromusculoskeletal model [241] in combination with a validated phenomenological model of ACL loading [339] to estimate ACL force, and its causes, during a standardized drop-land-jump task. We hypothesized that, across pubertal maturation, ACL force would increase and contributors to ACL force would vary.

6.3 Methods

6.3.1 Participants

In a cross-sectional study design, 93 healthy females were recruited from local universities, schools, sporting facilities, and community centres between June 2015 and May 2016. Given the lack of data pertaining to ACL loading during single-limb landing and female pubertal development, the sample size calculation was based on knee abduction moment data [358] (Figure 6.1). Inclusion criteria were as follows: aged 7-25 years, body mass index less than $30 \text{ kg}\cdot\text{m}^{-2}$ and recreationally active (i.e., at least 30 minutes of moderate or vigorous daily physical activity). The time spent in moderate and vigorous physical activity identified via a self-reported modified Children's Leisure Activity Study Survey [359]. History of lower limb injury, knee pain, medical condition affecting sporting tasks, previous ACL or meniscal injury, or biphasic or triphasic oral contraceptive pill use were the exclusion criteria. We excluded those using bi- or tri-phasic oral contraceptive pill to eliminate effects of estrogen fluctuations, produced by these contraceptives, on lower limb biomechanics [22]. All participants, together with parents/guardians of those <18 years of age, provided their written informed consent prior to testing. This study was approved by the University of Melbourne Human Research Ethics Committee (#1442604).

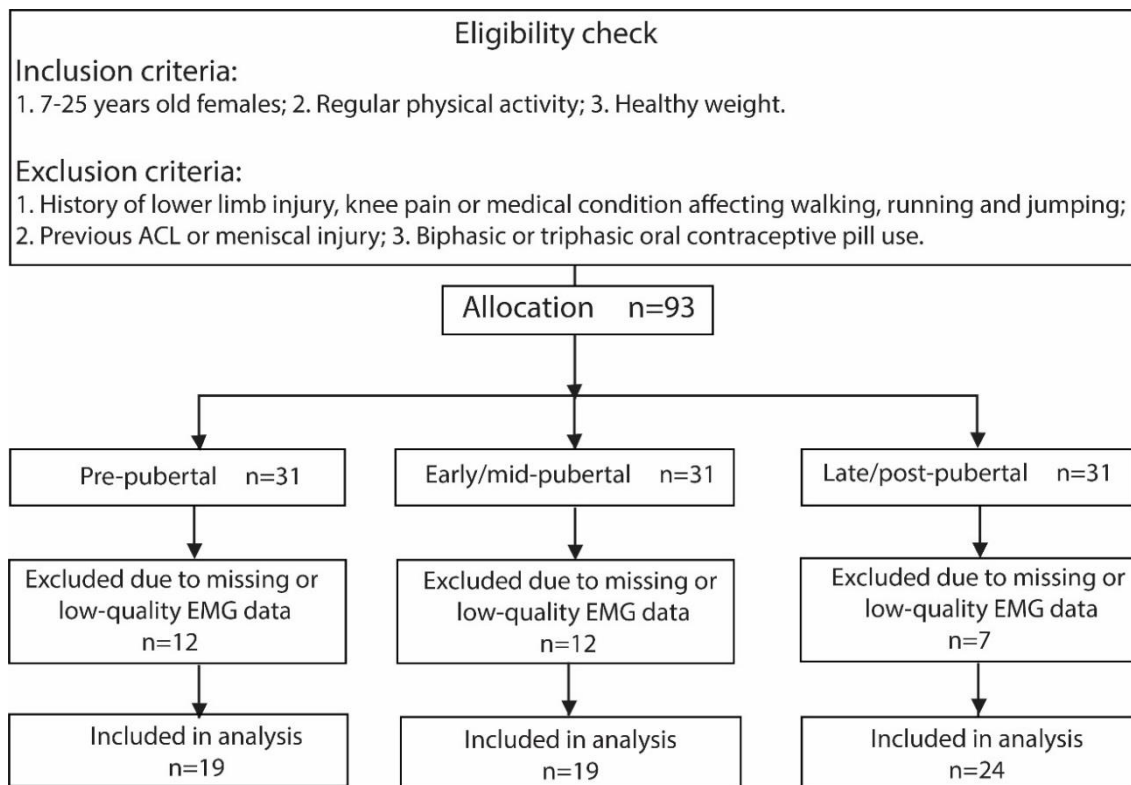


Figure 6.1. CONSORT flow diagram that illustrates the grouping and flow of the participants. ACL – anterior cruciate ligament; EMG – electromyography.

Participants were categorised into three pubertal maturation groups based on self-rated Tanner staging for breast development, growth spurt (i.e., 7.5-9.0 cm growth in the past 6 months), and menarche (i.e., first occurrence of menstruation) [21, 290]. The groups were pre-pubertal (Tanner stage 1), early/mid-pubertal (Tanner stages 2 and 3 and either growth spurt or menarche), or late/post-pubertal (Tanner stages 4 and 5, both growth spurt and menarche). Participants provided their pubertal assessment information by completing an online, de-identified questionnaire containing pictures and modified diagrams [290]. For participants younger than 12 years of age, a parent or guardian provided pubertal assessment information.

6.3.2 Hormonal considerations

Salivary concentrations of endogenous estrogen (5 mL, Nutripath Integrative Pathology, Melbourne, Australia) were measured from each participant to ensure all underwent

biomechanical testing with low levels of estrogen. Saliva samples were stored at -20°C and subsequently analysed via enzyme immunoassay according to the manufacturer's instructions. Low levels were defined as estradiol concentration $<18\text{ pmol/L}$, based on reference ranges for the follicular phase. This was done because higher levels of estrogen during and after puberty might influence external knee biomechanics [22]. Eumenorrheic participants not using a monophasic oral contraceptive pill were tested within their early follicular phase (i.e., first 7 days of menstrual cycle). For those using a monophasic oral contraceptive pill or had not yet experienced menarche, testing was performed at their convenience any time during their menstrual cycle.

6.3.3 Dynamic motor task

Each participant completed one laboratory-based testing session. Therein, participants performed three repeated trials of straight running and three repeated trials of a standardized drop-land-lateral jump. Participants were afforded opportunity to familiarize themselves with both tasks. The standardized drop-land-lateral jump consisted of a drop landing onto a single-leg from a box (OEM Engineering Pty Ltd, Melbourne, Australia) height of 30% of the participants lower limb length, measured from the outermost lateral aspect of the greater trochanter to the floor. Box height was normalized to create similar neuromuscular demand between participants of different heights given that jump and landing height increases during adolescence [360]. Participants stood on their dominant leg at the centre of the box. They dropped off the box, landed on their dominant leg atop a marked target 10 cm from the centre of the box. Immediately following landing, they performed a 90° lateral jump, landing on their contralateral leg at 150% of their leg length. In addition to the drop-land-lateral-jump, participants were instructed to complete running trials using their natural running style at preferred pace. For the purposes of this paper, running trials at the speed range of 2.8 to $3.2\text{ m}\cdot\text{s}^{-1}$ were used for subsequent

biomechanical model calibration (detailed later) only while all the biomechanical analysis were performed on drop-land-lateral jump as a closer representation of ACL injury incidence events.

6.3.4 Biomechanical data acquisition

During the movement task, three-dimensional body motion, ground reaction forces (GRF), and surface electromyography (EMG) were acquired concurrently and synchronously. Participants were prepared for testing by placing retroreflective markers on the skin-surface atop specific anatomical landmarks [318]. Further, surface EMG electrodes were mounted atop the eight major muscles of the lower limb (i.e., rectus femoris, vastus lateralis, vastus medialis, tibialis anterior, lateral gastrocnemius, medial gastrocnemius, lateral hamstrings, and medial hamstrings) of the dominant leg. For the EMG electrode placement, anatomical sites were identified and prepared consistent with the guidelines from Surface Electromyography for the Non-Invasive Assessment of Muscles [319]. A 12-camera motion capture system (Vicon Motion Systems, Oxford, UK) sampling at 120 Hz, ground embedded force platform (AMTI, Massachusetts, USA) sampling at 2400 Hz, and wireless surface EMG system (Noraxon, Arizona, USA) sampling at 2400 Hz were used to acquire whole-body motions, body-ground interaction (i.e., GRF), and muscle activations, respectively. Second-order, zero-lag, infinite impulse response digital Butterworth filters[361] were applied to all data, with correct phase adjustment [320], in the following way. Motion and GRF data were low pass filtered with cut-off frequency of 6 Hz. Muscle activations were first band-pass filtered (30-300 Hz), full-wave rectified, and then low-pass filtered with a cut-off frequency of 6 Hz to produce linear envelopes. Each linear envelope was subsequently normalized to its maximum envelope value identified from all trials.

6.3.5 Biomechanical modelling

To determine ACL force during the drop-land-lateral jump, we used a three-step approach. First, we determined external biomechanics by performing musculoskeletal modelling in OpenSim [230] version 3.3. We modified a generic full-body musculoskeletal model consisting of 37 degrees of freedom (DOF) and 80 muscle tendon unit (MTU) actuators [303] by adding ankle and hip rotational mobilities, a dummy 6 DOF tibia [339], and both medial and lateral condylar contact bodies [153]. To personalise the musculoskeletal model, prominent bony landmarks and hip joint centres were used to linearly scale the model to each participant's gross dimensions, mass, and inertia. This was followed by morphometric scaling to preserve fibre and tendon operating ranges [306], and lastly we updated each muscle's maximum isometric strength based on the Handsfield equations [308]. After model preparation, we determined motions, joint forces and moments, and MTU kinematics (i.e., moment arms, lengths, and lines of action) using the inverse kinematics, inverse dynamics, and muscle analysis tools of OpenSim, respectively [230].

The second step was to use the modelled external biomechanics in conjunction with muscle activation patterns (i.e., EMG linear envelopes) to estimate lower limb muscle dynamics through the Calibrated EMG-informed Neuromusculoskeletal Modelling (CEINMS) toolbox [248]. The CEINMS was used to synthesize 32 excitations corresponding to the lower limb MTU for which we did not have EMG. Once synthesized, CEINMS was calibrated against the sagittal plane moments of the hip, knee, and ankle during one running and one drop-land-lateral jump trial for each participant. Consistent with prior modelling studies, we used biomechanical data from multiple motor tasks in calibration to prevent model over-fitting and enhance its predictive capacity [240, 362, 363]. Once calibrated, CEINMS was used in EMG-informed mode to estimate lower limb

muscle and tibiofemoral contact forces. Lower limb muscle forces and moments were determined by multiplying muscle forces (estimated through CEINMS) by their respective lines of action [364] (for translational loads) or moment arms (for rotational loads). Collectively, OpenSim and CEINMS modelling outputs included external biomechanics and MTU kinematics, as well as lower limb muscle and tibiofemoral contact forces.

The third and final step was to determine ACL force by incorporating the lower limb biomechanics from OpenSim and CEINMS into a validated ACL force model [339]. This ACL force model was developed using the most relevant, complete, and accessible cadaveric data from the literature and shows excellent correspondence (i.e., minimal error, strong correlation, and narrow limits of agreement with minimal bias) to experimental measures of ACL loading during complex knee loading [339]. For each participant, we determined the ACL force (N), and its uniplanar causal contributors (N and % contribution), throughout the stance phase of the drop-land-lateral jump. Stance was defined as the period between first and last instances of foot to ground contact detected by force plate measurement of greater than 40 N. The ACL forces were not normalized to body mass for the different pubertal groups as it has been reported that ACL cross-sectional area to length ratio remains unchanged across pubertal maturation in females [365]. For each trial, ACL force data were normalized to 100% of the stance, averaged for each participant, and ensemble averaged for pubertal groups.

6.3.6 Statistical analysis

Descriptive statistics were used to report participant demographic and anthropometric data. Between-group differences in demographic and anthropometric data were tested using one-way ANOVA and *post-hoc* independent t-tests. To analyse ACL force in a time-continuous manner, statistical parametric mapping (SPM) was used. We used the

open-source SPM1d software (v0.4, www.spm1d.org), implemented in MATLAB (R2018a, MathWorks, Inc., MA), to conduct our analysis [366]. First, the normality of the data was verified in SPM1d, and based on the outcome, statistical non-parametric mapping (SnPM) ANOVA were used to compare ACL force during stance, and its contributors, generated by the different pubertal groups. Results for these comparisons were reported as SnPM{F} curves. Where a statistically significant SnPM ANOVA result was found, *post-hoc* comparisons between groups were undertaken using SnPM t-tests with Bonferroni correction. Thus, a conservative alpha of 0.0170 was used to determine statistical significance. For the comparison of uniplanar contributions at the peak ACL force, non-parametric equivalent of one-way ANOVA (Kruskal-Wallis) with Bonferroni corrections for pair-wise comparisons were performed. Then, the effect size was calculated using the *Cohen's d_z* formula. The effect size can be interpreted as small ($d = 0.2$), medium ($d=0.5$) and large ($d=0.8$) [367].

6.4 Results

Data from 31 participants (12, from each of pre- and early /mid pubertal groups and 7 from late/post pubertal group) were excluded from biomechanical analysis due to missing or low-quality EMG. Those excluded were not significantly different to those retained in each group in terms of age, weight, and height. Overall, 62 participants (19 from each of pre- and early /mid pubertal groups and 24 from late/post pubertal group) were included for analysis. Compared to pre- and early/mid-pubertal groups, late/post-pubertal group was significantly older, taller, and heavier. The early/mid pubertal group was significantly taller compared to the pre-pubertal group (Table 6.1).

Table 6.1. *Characteristics of the different pubertal groups.*

| | Pre-pubertal | Early/mid-pubertal | Late/post-pubertal |
|-------------|--------------|----------------------|--------------------------|
| n | 19 | 19 | 24 |
| Age (years) | 9.8±1.1 | 11±1.3 | 19.9±4.1 ^{*,**} |
| Weight (kg) | 30.9±4.5 | 37.4±5.6 | 59.8±9.3 ^{*,**} |
| Height (m) | 1.4±0.1 | 1.5±0.1 [*] | 1.6±0.1 ^{*,**} |

All variables are reported as mean ± standard deviation. *Significantly different to pre-pubertal group (P<0.05). **Significantly different to early/mid-pubertal group (P<0.05).

The SnPM ANOVA revealed ACL force during the drop-land-lateral jump was significantly different across maturation (Figure 6.2 A). Compared to the pre-pubertal group, the late/post-pubertal group generated significantly higher ACL force (mean differences of 471 N and 356 N during first 30% and 48%-85% of stance, respectively). Compared to the early/mid-pubertal group, the late/post-pubertal group generated significantly higher ACL force (mean differences of 343 N and 274 N during first 24% and 59%-81% of stance, respectively). The periods of stance when these differences were found overlapped the instances of peaks in the ACL force. No significant difference in ACL force was observed between pre- and early/mid-pubertal groups (Figure 6.2 B).

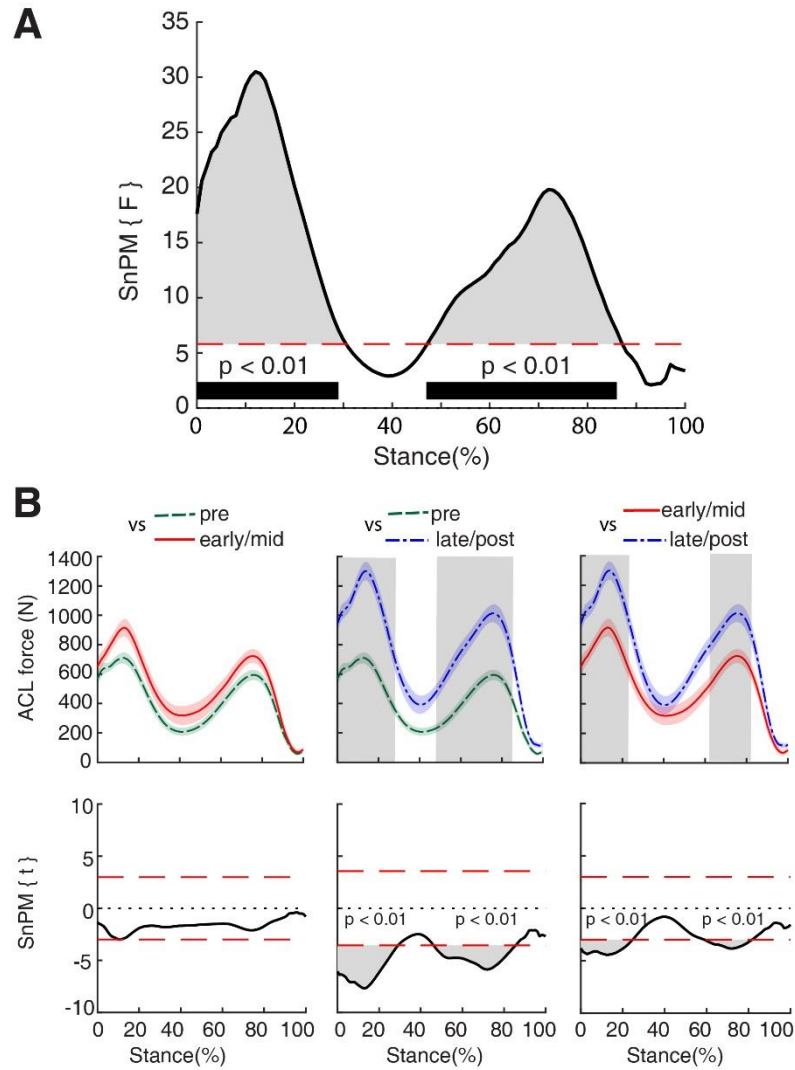


Figure 6.2. Comparisons of the ACL force generated during the stance phase of the drop-land-lateral jump between pre-, early/mid-, and late/post-pubertal females performed with statistical parametric mapping (SPM). **(A)** The SPM ANOVA across 100% of the stance phase. The bold black line is the computed F-curve, the dashed (red) line indicates the critical threshold calculated at $\alpha=0.05$, and the thick black bars correspond to the regions of statistical significance. **(B)** The ACL force for each pubertal group is plotted (pre in even dash green, early/mid in solid red, and late/post in alternating dash blue) with standard error of the mean shown as translucent areas. Shaded grey columns in each plot indicate regions of significant difference in the ACL force between pubertal groups. In the bottom row, the respective post-hoc paired t-tests are plotted, with grey shaded regions corresponding to regions of significant difference. The associated p statistic is listed. ACL – anterior cruciate ligament; SPM – statistical parametric mapping.

The SnPM ANOVA was also used to examine if contributors to ACL force changed between pubertal maturation groups. We found ACL force developed through the sagittal plane was significantly higher in late/post-pubertal compared to pre-pubertal (mean differences of 427 N and 321 N during first 28% and 48%-85% of stance) and early/mid-pubertal (mean differences of 305 N and 254 N during first 22% and 67%-77% of stance) groups (Figure 6.3). The ACL force developed through the transverse plane was significantly higher in the late/post-pubertal group compared to the other pubertal groups, and differences were observed over almost all of stance (Figure 6.4). For very small periods of stance, we observed significant differences in ACL force developed through the frontal plane (Figure 6.5). We found no significant differences in uniplanar contributions to ACL force between pre- and early/mid-pubertal groups.

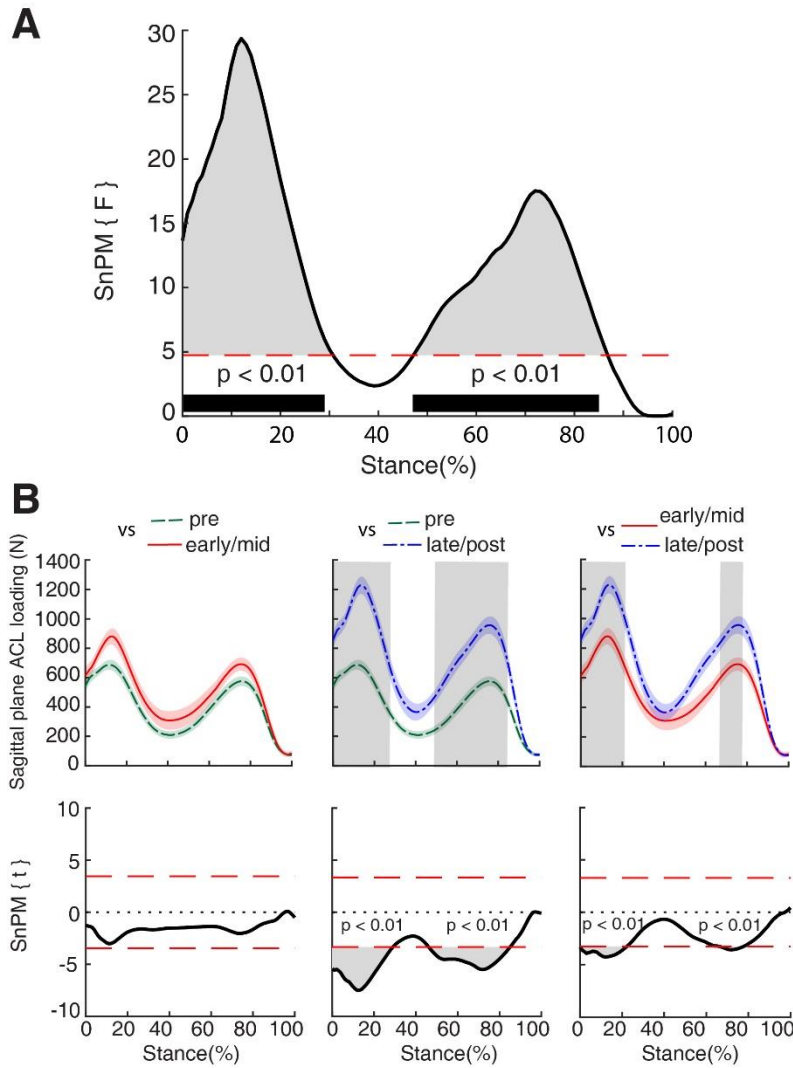


Figure 6.3. Comparisons of the ACL force developed through the sagittal plane during the stance phase of the drop-land-lateral jump between pre-, early/mid-, and late/post-pubertal females performed using statistical parametric mapping (SPM). **(A)** The SPM ANOVA across 100% of the stance phase. The bold black line is the computed F-curve, the dashed (red) line indicates the critical threshold calculated at $\alpha=0.05$, and the thick black bars correspond to the regions of statistical significance. **(B)** The ACL force developed through the sagittal plane for each pubertal group is plotted (pre in even dash green, early/mid in solid red, and late/post in alternating dash blue) with standard error of the mean shown as translucent areas. Shaded grey columns indicate regions of significant difference between the pubertal groups. In the bottom row, the respective post-hoc paired t-tests are plotted, with grey shaded regions corresponding to regions of significant difference. The associated p statistic is listed. ACL – anterior cruciate ligament; SPM – statistical parametric mapping.

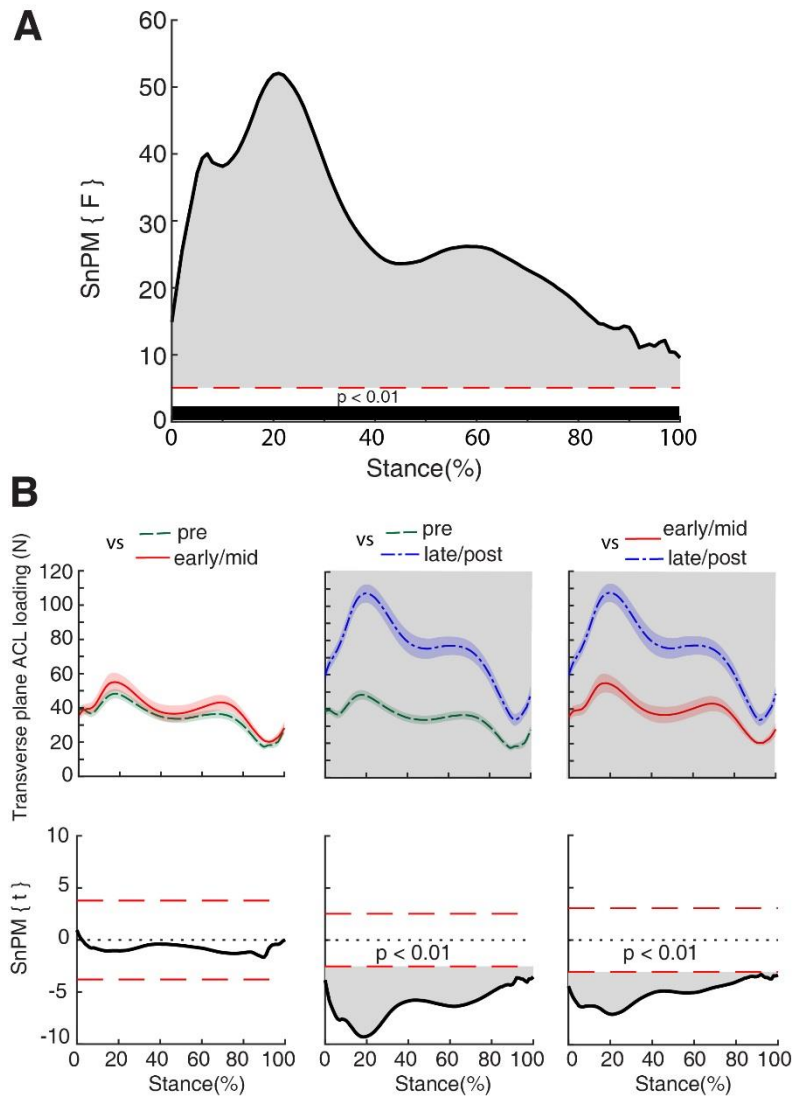


Figure 6.4. Comparisons of the ACL force developed through the transverse plane during the stance phase of the drop-land-lateral jump between pre-, early/mid-, and late/post-pubertal females performed using statistical parametric mapping (SPM). (A) The SPM ANOVA across 100% of the stance phase. The bold black line is the computed F-curve, the dashed (red) line indicates the critical threshold calculated at $\alpha=0.05$, and the thick black bars correspond to the regions of significant difference. (B) The ACL force developed through the transverse plane in each pubertal group is plotted (pre in even dash green, early/mid in solid red, and late/post in alternating dash blue) with standard error of the mean shown as translucent areas. Shaded grey columns indicate regions of significant difference between the pubertal groups. In the bottom row, the respective post-hoc paired t-tests are plotted, with grey shaded regions corresponding to regions of significant difference. The associated p statistic is listed. ACL – anterior cruciate ligament; SPM – statistical parametric mapping.

At the instance of peak ACL force, absolute contributions from sagittal and transverse planes were significantly higher in the late/post-pubertal group compared to the other pubertal groups with medium effect sizes (*Cohen's dz (r)* ranging from 0.44 to 0.77). However, when relative (%) contributions were analysed, the sagittal plane contribution to ACL force was lower in the late/post-pubertal group compared to the pre-pubertal group (mean difference of %-1.53, $r = -0.49$), whereas transverse plane contribution was greater in late/post pubertal group compared to early/mid pubertal group (mean difference of % 1.75, $r = -0.47$). No significant differences were observed in relative contributions between pre-and early/mid-pubertal groups (Figure 6.6).

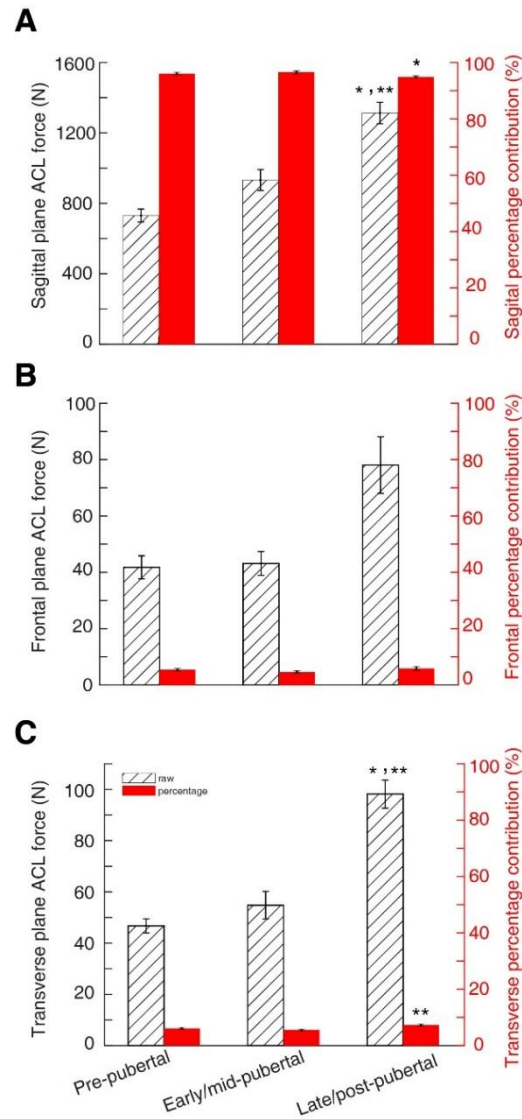


Figure 6.6. Uniplanar contributions to ACL force at the time of peak ACL force. Left axes display the absolute uniplanar contributions (N) and right axes display relative contributions (%). (A) sagittal plane absolute contribution was greater in late/post pubertal group compared to pre and early/mid maturation groups ($P < .001$, $r = -0.75$; $P < .001$, $r = -0.55$; respectively) whereas it's relative contribution was smaller compared to pre maturation group ($P = .003$, effect size (r) = -0.49), (B) in frontal plane there were no between group differences in absolute or relative contributions, and (C) transverse plane absolute contribution was greater in late/post pubertal group compared to pre and early/mid maturation groups ($P < .001$, $r = -0.77$; $P < .001$, $r = -0.64$; respectively), and the relative contribution was greater compared to early/mid pubertal group ($P = .008$, $r = -0.47$). *Significantly different to pre-pubertal group ($P < 0.05$). **Significantly different to early/mid-pubertal group ($P < 0.05$). Error bars, 1 SEM.

6.5 Discussion

To understand the ACL injury mechanism in girls and young women, the effects of pubertal maturation on female anatomy, external biomechanics, and muscle function have previously been examined. As females mature, they perform landing and cutting tasks with decreased knee flexion [15, 189] and generate larger knee moments [17, 18, 20], but show no significant change in muscle strength adjusted to body weight [24]. Although external biomechanics (e.g., knee motion and generalized loads) may help identify conditions surrounding injury and statistically associate with injury risk [54], external biomechanics are not indicative of internal biomechanics [153, 368, 369]. Previous studies have speculated how biomechanical and neuromuscular changes incurred by female pubertal maturation might influence ACL loading, but this is the first study to directly examine pubertal maturation effects on ACL loading. We overcame many prior limitations by combining body motion and external loading with subject- and task-specific muscle activation patterns to determine ACL force using validated computational models. Our findings indicate late- and post-pubertal females generate larger ACL force during drop-land-lateral jump compared to those in earlier maturation stages. The sagittal plane was the dominant contributor to ACL force across pubertal maturation, but its relative contribution decreased. It is unknown if ACL loading during dynamic tasks can be modulated through targeted intervention, which warrants urgent study.

We assessed a standardized drop-land-lateral jump task and found that late/post-pubertal females generated larger magnitude ACL forces across the majority of stance in comparison to early/mid- and pre-pubertal females. However, the ACL forces developed by early/mid-pubertal females were not larger in comparison to pre-pubertal females. The results partially support our hypothesis that pubertal maturation would increase ACL force magnitude during a dynamic motor task. Importantly, ACL rupture occurs when the

tissue's stresses exceed its ultimate tensile strength, which depends on the ACL cross sectional area and material properties. It has been reported that the increases in ACL volume and length plateaus at approximately 10 [370], and 15 [365] years of age, respectively. In contrast, ACL cross-sectional area to length ratio remains unchanged across pubertal maturation in females [365]. This suggests the female ACL does not necessarily grow larger through pubertal maturation, despite increases in ACL forces reported in the current study. We are unaware of literature indicating subsequent changes in ACL material properties once female pubertal maturation is complete. Therefore, larger forces applied to a structure of fixed size and material properties increases mechanical risk of failure, which may explain increases in ACL ruptures in late/post-pubertal females.

The greater ACL forces in the late/post-pubertal females are obviously due to their 75% larger body mass, rather than dropping from greater box heights (~7% intergroup stature differences), compared to pre- and early/mid-pubertal cohorts. However, this “mass x acceleration” influence on ACL forces was affected differently around knee rotational planes across maturation. The sagittal and transverse plane increased significantly in late/post-pubertal females compare to those in earlier stages of maturation but remained the dominant mechanism of ACL loading. Interestingly, the frontal plane had increased significant contributions in only a few small phases of stance. Uniplanar contributions to ACL forces as predicted by the ACL model are not strictly summative due to interaction terms [339], which are sensitive to knee position and the specific multiplanar external and internal knee loads. Consistent with prior literature that reported changes in external biomechanics with pubertal maturation [15, 17, 18, 189], our results also suggest maturational effects on load sharing between muscle, rigid contact, and passive soft tissues (including the ACL) is complex, non-linear, and dynamical.

Notably, larger magnitude ACL forces found in late/post-pubertal compared to pre- and early/mid-pubertal females were generated by a relative decrease in the contribution from the sagittal plane ($P = .003$, $r = -0.49$) and marginal relative increases from transverse ($P = .008$, $r = -0.47$) and frontal plane (not statistically significant) mechanisms. These results partially support and provide an underlying mechanism for speculations drawn from longitudinal studies that found statistical links between ACL injury risk and decreased neuromuscular control in females as they mature pubertally [20, 24]. We did not find significant increases in the contribution to ACL forces through the frontal plane, i.e., varus - valgus, across pubertal maturation in females as previously suggested in literature [20, 24, 25, 54]. However, this is likely due to the specific task we assessed, that first deaccelerated whole-body motion relative to drop-landing leg/foot in predominantly sagittal and transverse planes, and then involved small increases in frontal plane motion, which did not involve particularly large valgus knee moments. However, it is still unclear if the changes in ACL force we identified across pubertal maturation can be inferred from only external biomechanical measures. A more challenging motor task, such as a reactive cutting task that imposes much larger non-sagittal loading, might reveal larger pubertal maturation effects on the relative contribution of multiplanar loading to ACL force.

In this study, we examined moderately sized cohorts of females across maturation with respect to their ACL force generation in dynamic tasks. We used validated neuromusculoskeletal and computational models to quantify ACL force across maturation to directly address our research question rather than using proxy biomechanical measures. Nonetheless, there are limitations to consider. First, we did not use experimental measures of muscle strength (e.g., through dynamometers) to personalize our models. However, relative muscle strength has been reported not to

change significantly across maturation in females [24] and we did adjust our modelled muscle strength for each participant based on population estimates of the relationship between stature and mass with strength [308]. Additionally, we lineally scaled a generic model to each participant's gross dimensions, mass, and inertia. Highly personalized musculoskeletal models, created from medical imaging, will produce better anatomical and neuromuscular fidelity. However, the groups of different pubertal maturation were modelled using the same framework, thus, the limitation of linearly scaled models should not affect comparisons made in this study.

In conclusion, we present for the first time ACL force generation in females across the stages of pubertal maturation. This study revealed that, during a standardized drop-land-lateral jump, late/post-pubertal females generate higher ACL forces compared to less mature females across a large percentage of stance, including instances of peak forces. Furthermore, the sagittal plane was the primary contributor to ACL force in all maturation groups but made relatively lower contribution in the late/post-pubertal group compared to less mature females. The current study indicates ACL forces increase across pubertal maturation in females, and, given the cessation of ACL growth at ~10 years of age, may explain the dramatic rise in ACL rupture sustained by females 15-19 years of age.

CHAPTER 7

General discussion

This chapter will highlight the main findings of the thesis and discuss the implications for ACL injury prevention, particularly in females. Further, the limitations of the conducted research will be noted, and future research directions will be suggested.

7.1 Brief thesis summary

The overarching aim of this thesis was to elucidate the mechanisms of ACL loading during dynamic motor tasks in females across pubertal maturation stages. To achieve this aim, first a computational model of ACL loading was developed and validated, then mechanistic contributors to ACL forces were explored, and finally ACL loading and its biomechanical contributors were examined across the three pubertal maturation stages.

In study one (Chapter 4), a computational ACL force model was developed using the most relevant, complete, and accessible cadaveric data from the literature, where ACL response to uniplanar and multiplanar knee loading was measured. The model was then validated against a subset of the novel experimental data (i.e., the data which was not utilised in model development) showing strong statistical correlation ($r^2=0.96$ and $P<0.001$), minimal bias, and narrow limits of agreement. The developed computational ACL force model was combined with EMG-informed neuromusculoskeletal model to illustrate its functionality by estimating *in vivo* ACL force during the drop-land-lateral jump task performed by female participants.

In study two (Chapter 5), biomechanical contributions to ACL loading were further investigated by determining the role of knee spanning muscles in ACL force of late/post pubertal female participants during the drop-land-lateral jump task. The results highlighted the important role of gastrocnemius muscle in ACL loading, which should be considered more prominently in ACL injury prevention and rehabilitation programmes.

In study three (Chapter 6), the ACL loading during a drop-land-lateral jump task was compared between females across three different pubertal maturation stages. The relative contributions to ACL force from three planes of motion (sagittal, frontal, and transverse) were also compared. Females in late/post pubertal group (age range 14-20 yrs.) experienced significantly higher ACL forces during a large percentage of the stance phase compared to their counterparts at earlier stages of maturation. This important result may partially explain the higher rate of ACL injury in females aged 15-19 years, which has been reported in incidence studies over the last couple of decades. Furthermore, it has been shown that ACL growth plateaus at the age of 10, prior to full pubertal maturation and cessation in growth of stature. Thus, compared to their less sexually mature counterparts, females in late/post pubertal group have similar sized ACL, but are heavier and thereby experience greater ACL loading as shown in the final study. These are possible reasons for the higher rate of ACL injury observed in this group.

7.2 External biomechanics or ligament loading?

The incidence of ACL injury has increased dramatically in adolescent and young adult populations, and particularly in females, over the past couple of decades [2, 371]. Since the majority of ACL injuries are non-contact, this suggests that ACL injuries are in some sense self-inflicted, and therefore, might also be preventable [54] if the causal mechanisms could be understood and modified. Hence, considerable biomechanical

research has focused on potentially modifiable risk factors of the ACL injury. Although some physical training programs targeted to prevent ACL injuries have demonstrated encouraging results [354, 372-374], others have been less successful (reviewed in [69]). Moreover, the success achieved in longitudinal studies, have not been incorporated at the population level to address the current rapidly rising rates of non-contact ACL injuries. Indeed, it is unclear if these programs “could” be scaled to curb population ACL injury incidence rates without technological progress.

Nevertheless, the ultimate goal of ACL injury reduction can only be achieved if the mechanisms of ACL injury are clearly elaborated. It has been argued that the reasons for the lack of clarity surrounding the ACL injury mechanisms may be due to the lack of validated methods to directly assess ACL loading, and the neuromusculoskeletal factors contributing to this loading, while also being viable for cohort analysis. This thesis attempted to address these issues.

A considerable amount of research has focused on the external biomechanics of the individual during task performance, including knee joint motion and net loading. Knee joint motion can be assessed, but may be not precisely measured, during actual game play and injury incidence events. Knee net loading, however, can be assessed in the laboratory [45, 153, 198] and potentially with the aid of artificial intelligence methods in the field [375-377]. Critically, these external biomechanics are only surrogate measures of either ACL loading, or for ACL injury risk assessment to identify gender and age-based differences during sports specific movements [172, 174]. However, the loading in the ACL during dynamic movement is a result of complex interaction between many neuromusculoskeletal and biomechanical factors including the forces and moments that are applied to the knee joint, the position and orientation of the lower limbs, and the muscle activation patterns and the subsequent action of muscles in loading or unloading

the ACL. Consequently, the major current focus on external biomechanics as measures of ACL injury risk is hindering a causal, mechanistic focused approach that would directly address the issue of “too much force through the ACL breaks it” [46].

Unsurprisingly, the findings regarding ACL loading mechanism driven from external biomechanics measures are conflicting. Some studies suggest increased knee valgus [54, 145] and internal rotation moments [55, 59] can be considered as important contributors to ACL loading, particularly in females compared to males [172, 174]. However, others have found no sex-specific differences in knee joint kinematics when the skill level of individual was considered [173, 175, 378]. These conflicting results are probably due, in part, to external biomechanics measures only being surrogates of ACL load. Indeed, it can be argued that ACL injury risk can be modified only if the ACL forces can be estimated, since the ultimate mechanism of the ACL injury is that the load applied to the ACL is greater than it’s tolerance to withstand that load [46].

During dynamic motor tasks the knee is subject to complex multiplanar loading that is shared across multiple interacting internal passive (i.e., ligaments, articulating contact forces) and active (i.e., muscles) structures. This complex system should be quantified, as previously argued, given the importance of understanding ACL loading mechanisms. However, there is only sparse *in vivo* ACL load data acquired from dynamic high-risk activities [147, 204]. The *in vivo* ACL force has been measured directly through implanted strain gauge [147], but the invasiveness of this technique severely limits its applicability and more generalisable use in studying *in vivo* human joint loading. Biplanar radiography, a technique capable of capturing a portion of the motion cycle near ground impact has been used as an alternative approach to directly and non-invasively measure ACL strain [204]. However, this approach carries its own limitations including the use of ionizing radiation, potential for operator-tracking errors, a small field of view [379], as

well as time intensive data processing [380]. Overall, these *in vivo* measurements of the ACL loading, if external biomechanics and muscle activations were not concurrently acquired, only provide an estimate of the ACL loading magnitude during specific tasks and are not particularly valuable in understanding the ACL loading mechanisms.

Detailed knee joint computational models such as finite element and elasto-structural models can be used to estimate *in vivo* ACL force/stain [34, 38, 40, 58]. However, these methods are computationally demanding and time consuming. For example, a finite element knee model, may take days or even weeks to solve under quasi-static conditions [278]. Thus, joint mechanics are often resolved only at specific instances in a movement. Therefore, mathematical models of knee function that can rapidly estimate the empirical relationships between the ACL force and external knee loads should be introduced to biomechanical studies to estimate the ACL force as a feasible approach for large scale research and clinical applications [31, 36]. However, to date this empirical mathematical modelling approach has been limited in use and inadequately implemented.

The motivation for the development of multiplanar ACL force model in this thesis was to address the limitations of the existing mathematical formulations. Current models either employ uniplanar models that do not consider the multiplanar mechanisms of ACL loading [31], nor do the multiplanar mathematical formulations [36] incorporate multiplanar loading interactions, and therefore fail to reproduce the ACL force values recorded in cadaveric studies. For example, in loading scenarios of 100 N anterior force combined with 10 Nm of external rotation, internal rotation, or varus moments at the knee flexion angle of 60°, the currently published model estimations of the ACL forces are approximately 400 N, -800N and -200 N, respectively [36], whereas the experimentally

measured ACL forces in response to the same loading scenarios were approximately 10 N, 30 N and 100 N, respectively [41]. This is a major obvious shortcoming.

These aforementioned ACL models rely on estimates of muscle forces that are generated by neuromusculoskeletal biomechanical models. However, the neuromusculoskeletal models employed may not estimate physiologically plausible muscle forces [381]. Therefore, in this thesis, a computational framework of combined EMG-informed neuromusculoskeletal and ACL force models was used. In this framework both external (i.e., knee kinematics and net loads) and internal (muscle, tibiofemoral contact, and ACL forces) loads were determined for the entire motion of a dynamic drop-land-lateral jump.

The action of muscles in ACL loading and injury needs to be considered as muscles are the only active contractile knee stabilizers [65] and generate the majority of internal loading [382]. Indeed, internal knee biomechanics are highly sensitive to muscle forces [209]. However, determining a set muscle forces that satisfy the rigid multibody physics, respect neural patterns of muscle activation, and physiological muscle dynamics is a highly non-trivial task. The majority of the ACL modelling studies have determined muscle forces using some form of static optimization, and much less commonly, EMG-informed approaches. The issue with the static optimization approaches are that net-intersegmental forces and moments are solved quasi-statically by minimizing a criteria governing muscle activation or stress [383]. Although static optimization can be readily implemented and is computationally efficient, it cannot predict many well documented neural patterns of muscle coordination, such as antagonistic co-contraction [384], force-sharing loops [385], control-task sensitivity [251], training-sensitivity [386], pathology-sensitivity [253, 387], and, importantly, activation patterns directed to stabilise joints [388]. In contrast to static optimization, EMG-informed methods, which directly

incorporate experimental measures of muscle activation, are therefore sensitive to the subject- and task-specific nature of muscle coordination. Crucially, EMG-informed models may produce more physiologically plausible muscle activation patterns and muscle force estimates [237, 249]. Thus, in this thesis an EMG-informed approach was used for muscle force estimation, which represents an important addition to the prior literature where muscle contributions to ACL loading rested on the assumptions of static optimization and other purely mechanical approaches for muscle forces estimation [31, 36].

7.3 Role of muscles in loading the anterior cruciate ligament across pubertal maturation in females

Most ACL ruptures are non-contact in nature and are likely influenced by poor neuromuscular control and movement technique. Indeed, experiments on cadavers, *in vivo* measurements, and computational modelling all indicate posture and muscle activation influence force production in knee spanning muscles [54, 389, 390], and hence ACL force both in terms of magnitude and timing. Adolescent and young adult female athletes are more likely to sustain a non-contact ACL injury during sport compared to similar aged male and older females counterparts [391-394]. So, where in this mechanistic neuromusculoskeletal and biomechanical pathway to ACL loading do adolescent females exhibit risk of ACL injury?

Compared to male athletes, it has been reported that female athletes may demonstrate higher quadriceps activation during landing and cutting manoeuvres [395-399], and higher gastrocnemii activation during cutting tasks [178]. However, increased activation of these muscles does not equate to increased muscle forces and action thereby the effects on ACL loading are not obvious. This is critical, and the findings of this thesis

for the first time indicate that the quadriceps and gastrocnemii are primary loaders of the ACL during the drop-land-lateral jump task in females. This thesis has shown elevated activations in combination with the specific dynamics of this motor task result in elevated muscle forces, thereby causing high levels of anterior tibia shear force, by their direct action and joint compression. This may contribute to the elevated risk of non-contact ACL injury observed in female athletes. Further, female athletes demonstrate different kinematic profiles such as less knee flexion angles during landings and side-step cutting tasks compared to their male counterparts [171, 395, 398]. The higher gastrocnemii activity in females may be used to enhance joint stability in knee flexion [179] by of compressing both compartments of the tibiofemoral joint [153, 198, 400]. Large concurrent force generation by the knee extensors and gastrocnemii in extended knee postures during demanding tasks such as landing are typically present in females, affecting high ACL loading, and may explain the high rates of ACL injury.

The results of this thesis indicated hamstrings were the main supporters of the ACL generating posteriorly directed forces on the tibia. This finding showed direct evidence of the previously inferred role of the hamstrings in stabilizing and protecting the ACL during landing and side-cutting tasks [401, 402]. Compared to males, females demonstrate reduced hamstring activation in the early contact phase of cutting tasks, and reduced hamstring-to-quadriceps co-activation ratio during landing and cutting tasks [401, 403-405], potentially reducing restraint of the tibia. It has been opined that this muscle activation pattern is likely adopted by female athletes as it would favour a more explosive jumping movement [344]. However, and again, lower levels of hamstring activity do not directly result in reduced hamstring forces or lower support of the ACL, countering this muscle groups' beneficial provision of dynamic knee joint stability in females. In this thesis ACL force was only estimated for females, with no direct

comparison of ACL force between sexes. Nevertheless, when compared to prior reports of ACL loading in males [147, 204, 226], lower hamstring forces and greater ACL forces were observed in our females. Thus, this thesis supports the prior speculation in the literature based on indirect measures (i.e., activation, knee posture, etc) by providing direct quantification of the muscular contributions to ACL loading in females. However, this does not directly explain the role of sexual maturation in ACL loading.

The neuromuscular differences between the sexes (e.g., power, strength and coordination) appear to emerge during sexual maturation since these differences are not evident before puberty [24, 183, 184]. Indeed, strength and performance differences exist between the sexes in adult athletes; however, these differences are not apparent among immature children [406]. Across sexual maturation, males dramatically gain lower limb muscle strength proportional to body mass, while females do not [15]. In addition to sex differences in lower limb strength, sexual maturation leads to decreased hamstring-to-quadriceps strength ratio in females[407], which could increase ACL loading.

The results of this thesis indicated late/post pubertal females experience significantly higher ACL force compared to their less sexually mature female counterparts, while there were no differences in ACL force between pre- and early/mid pubertal females. The majority of ACL forces were generated through muscular action, which might confirm the hypothesis of poor neuromuscular control [24] following pubertal maturation. Neuromuscular control is seen in terms of muscle activation patterns, segment and joint kinematics, and external joint loading. Interestingly, the results of this thesis do not support the theories of high knee valgus moments as the primary contributor to ACL loading in general, and in late/post pubertal females in particular [20, 54, 183]. The contribution to ACL loading from varus/valgus knee moments were considerably smaller (<8%) than the contribution from anterior-posterior knee forces (>94%).

Furthermore, when compared across pubertal stages, there were no significant differences in varus/valgus knee moments contributions to ACL force, although this might be due to the specific task assessed in this thesis. This task involved predominantly sagittal motion of the drop-landing leg, with small increases in frontal plane motion, which did not involve particularly large valgus knee moments. However, it is unlikely the changes in ACL force identified across pubertal maturation can be inferred from external biomechanical measures only. A more challenging motor task, such as a reactive cutting task that imposes much larger non-sagittal loading, might reveal larger pubertal maturation effects on the relative contribution of multiplanar loading to ACL. This requires future research.

The muscle forces in anterior-posterior direction appeared to play the primary role in ACL loading in late/post pubertal females. This is due to their anterior-posterior lines of action, exerting forces onto the tibia drawing it anteriorly or posteriorly and thus increasing or decreasing the ACL tension, respectively. Additionally, muscles are also the main contributors to joint compression forces. Due to the posterior tibia slope, joint compression forces create a reaction force pushing the femur posteriorly (hence the tibia anteriorly) and thus loading the ACL. The results of this thesis support the contention that it is poor neuromuscular control [24], affecting the action of muscles and knee joint postures, causing increased ACL forces, which subsequently leads to elevated risk of ACL injury observed in young adult females [15, 54, 178, 397].

In summary, during the single-leg drop-land-lateral jump examined for females in this thesis, quadriceps and gastrocnemius were equally the primary ACL loaders. Furthermore, the ability of hamstrings muscles to restrain anterior tibia translation was the most important protective mechanism to reduce ACL force. This suggests that increasing hamstring muscle activity during landing, while avoiding non-optimal muscle

activation patterns (e.g., highly activated quadriceps and gastrocnemii) could represent an important neuromuscular adaptation target for the ACL injury prevention trainings and thus reducing the incidence of non-contact ACL injury in young female athletes. These findings could help healthcare professionals (e.g., physiotherapists and exercise physiologists), coaches and physical trainers to design and implement more efficient exercise programs for ACL injury prevention in young female athletes. Importantly, the *in vivo* ACL force measurements could be used to inform neuromuscular training programs on avoiding motions and muscle activation patterns that predispose the ACL to injury and to identify individuals who are at high risk for injury and could be targeted for intervention.

7.4 Limitations

In the Chapters 4-6 of this thesis, limitations related to methodology and underlying assumptions have already been presented and will not be repeated here. Rather, comments on the limitations warranting further consideration will be presented.

The ACL force model was developed based on the empirical relationships between experimental multiplanar loads applied to the knee and the resulting ACL forces. These “input-output” relationships were modelled as the summation of a set of exponential functions where the function coefficients were fitted to the experimental measurements taken from cadaveric experiments using a non-linear least squares method. The experimental data used for model fitting were in form of ACL force and ACL strain. Thus, these data were first unified by transforming ACL strain to ACL force. Since the geometry and mechanical properties of the cadaver specimen were not available, average literature values for ACL cross-sectional area (CSA) and Young’s modulus (E) were used along with the reported strain to be converted to force via the simple expression, force =

$CSA \times E \times \text{strain}$. These assumptions are reasonable since both the ACL resultant load, geometry and mechanical properties of the ACL are average data. Further, linear elastic behaviour was assumed for the ACL, which is insensitive to the rate of loading. In future, upon the availability comprehensive experimental loading rate data, the ACL force model could be improved to incorporate the dynamical aspect of the ACL loading.

Although the explicit representation of the ACL (e.g., geometry and mechanical properties) are not considered, the model showed excellent accuracy in predicting novel experimentally measured ACL forces (i.e., a sub-set of experimental multiplanar knee loading data not used in model fitting). Thus, this model is a non-invasive and computationally inexpensive approach to quantify ACL loading, which makes it a feasible approach for large cohort analysis given it can be easily implemented by replication of the methodology presented in this thesis.

The experimental data selected from the literature to develop the ACL force model represented a wide range of ACL loading magnitudes and combinations to avoid model over-fitting and predictive bias. However, there might be some *in vivo* loading conditions that are not represented by these data. Nevertheless, with the data available, the predictive bias in the model was ~ 44 N or less that 2.75 % of maximum experimental data point.

Due to lack of published paediatric musculoskeletal models, a full-body generic adult musculoskeletal model (i.e., Rajagopal model [303]) was linearly scaled for all participants in the current study, including children. Further to model geometry, the internal MTU parameters (i.e., optimal fibre and tendon slack lengths) were optimised via a morphometric scaling approach [306], followed by scaling of the muscles maximal isometric strength [308]. The morphometric scaling process aims to preserve the dimensionless operating ranges of muscle and tendon, which seems appropriate given the

ratio of tendon slack and muscle tendon unit lengths are preserved during growth [307]. Likewise, scaling maximum isometric force for each muscle was performed using the regression equations [308] developed based on cadaveric data of specimens as young as 12 years of age. Thus, these scaling processes can be considered reasonable to be used for a healthy paediatric and adolescent population. Although this approach could be improved in the future with subject-specific measures of anatomy (i.e., bone and muscle morphology), the effects of such set of input parameters on the ACL model predictions have not been established. Moreover, even if limited subject-specificity in the modelling process affected the accuracy of ACL force prediction, it may not affect comparisons across maturation since all participants were modelled via the same process.

Lastly, surface EMG signals were collected from only eight lower limb muscles. Consequently, in the EMG-assisted approach, the excitations of the muscles with no experimental data were synthesized. These additional muscle excitations were mapped from existing experimental EMG data with the assumption that muscles with same innervation have the same activation patterns [242]. Further, even if more EMG channels were used, there are still many muscles in the lower limb that are inaccessible through surface EMG, thus, using an EMG-assisted approach that is combining EMG and mechanical optimization appears an effective compromise between physiologically (i.e., those that actually reflect the experimental muscle activations) and mechanically (i.e., well match the rigid body physics) plausible solutions in analysis of dynamic tasks [408].

7.5 Future research directions

Based on the findings and limitation of this thesis, several directions can be suggested for future work. First, the ACL force model was developed based on healthy ligaments behaviour. Future work might focus on extending the current ACL force model by

including experimental data acquired from reconstructed ACL, which would broaden the use of this model in clinical problems such as rehabilitation following ACL reconstruction. Indeed, secondary ACL injury is a major concern and if an ACL reconstruction model could be created it might be used as a tool to monitor the force in the reconstructed ACL, assess the effects of certain interventions or exercises.

In addition, the ability of the model to estimate ACL force in a computationally inexpensive way may facilitate investigation of the ACL force magnitude and loading mechanism in real-time. This would enable immediate feedback for individuals in the field or clinical environments by providing the real-time effects of changes in technique (in athletes), equipment (in soldiers and athletes), orthoses (in patients), and exercises (in athletes, soldiers and patients) on ACL loading [265, 409].

Future work should also consider applying the model in other populations such as males and pathological populations. These could include people with muscle strains or muscles compromised by surgery, e.g., after ACL reconstruction. It should be noted that the current thesis chose to exclusively study females, due to their higher rates of ACL injury compared to males. Indeed, the approach developed in this thesis should follow on from previous studies that have examined and shown differences in indirect measures (external biomechanics, EMG etc) between the sexes [172, 174, 178, 395-399]. However, just because there are differences between males and females by indirect measures it does not necessarily mean that these differences affect ACL loading and risk of injury. It is only when all the sex differences are evaluated in terms of ACL loading can clear mechanistic cause and affect be established. Moreover, it is only through this approach that insight into if and how the sex differences in neuromuscular function and external biomechanics affect ACL loading will provide guidance toward to more effective population specific countermeasures to prevent ACL injuries maybe attained. Potentially,

the specific muscle function (e.g., quadriceps to hamstring strength and activation patterns) involved in the direct mechanisms of high ACL loading by females during dynamic tasks will provide mechanically causative targets for re-training or other physical intervention aimed at lowering ACL force. Importantly, this does not need to be done in comparison to males, since these are mechanistic means to lower ACL loading and risk of injury in females.

In this thesis we attempted to standardize the task to anthropometry by normalizing the box height and distance away from the box to lower limb length. However, these parameters may not equally affect the ACL loading. The landing height may affect the ACL loading dependent upon the participants mass and internal strength, whereas, the distance away they land from the box would be influenced by anthropometry. Since there are many tasks designed to mimic in field loading of the ACL in the literature, future work should verify the effects of landing height on ACL loading by comparing the identical to standardized box heights conditions [410]. Furthermore, to have a truly ecologically valid test, more in-field measurements of ACL loading should be developed.

The findings of this thesis highlighted the importance of gastrocnemii muscles in ACL loading during a landing task. However, currently most of the research has focused on the role of quadriceps and hamstring muscle groups in ACL loading or supporting. Future work should investigate the effects of exercise interventions which target all muscle groups on ACL force during high-demand sporting manoeuvres, such as sidestep cutting and single-leg landing. Further, computational modelling that can accurately capture ACL force during dynamic movements, should systematically analyse the influence of changes in the timing and the magnitude of various muscle-tendon forces on ACL loading in different populations (e.g., different sex and maturation status), to

improve the current understanding of the ACL loading mechanisms, which ultimately can inform targeted injury preventive programmes (e.g., optimal muscle activation patterns) in a population specific framework.

7.6 Conclusions

In conclusion, this thesis entailed development and validation of a new computational ACL force model which provided a platform for integration of external biomechanics, muscle forces, and joint contact forces to calculate ACL force *in silico*. This ACL force model enabled examination of the ACL loading mechanism by exploring the main contributors to the ACL loading and revealed the primary role of sagittal plane knee loadings. Further examination of mature females during the drop-land-lateral jump task, supported previous findings of the importance of the quadriceps and hamstrings as ACL loaders and supporters, respectively and revealed the critical role of the gastrocnemii as ACL loaders. For the first time in the literature, the effects of female sexual maturation on ACL loading was examined, revealing a significant increase in ACL force at late/post sexual maturation compared to females at earlier stages of pubertal maturation. The inter-individual variability in both ACL force and its contributors suggests computational models capable of estimating ACL force are essential if one aims to understand the ACL injury mechanisms and design individualised ACL injury prevention programs, rather than relying on external biomechanics used as surrogates of ACL loading.

References

1. Moffat, K.L., et al., *Characterization of the structure-function relationship at the ligament-to-bone interface*. Proc Natl Acad Sci U S A, 2008. **105**(23): p. 7947-52.
2. Zbrojkiewicz, D., C. Vertullo, and J.E. Grayson, *Increasing rates of anterior cruciate ligament reconstruction in young Australians, 2000-2015*. Med J Aust, 2018. **208**(8): p. 354-358.
3. Gianotti, S.M., et al., *Incidence of anterior cruciate ligament injury and other knee ligament injuries: a national population-based study*. J Sci Med Sport, 2009. **12**(6): p. 622-7.
4. Kiapour, A.M. and M.M. Murray, *Basic science of anterior cruciate ligament injury and repair*. Bone Joint Res, 2014. **3**(2): p. 20-31.
5. Boden, B.P., et al., *Noncontact anterior cruciate ligament injuries: mechanisms and risk factors*. J Am Acad Orthop Surg, 2010. **18**(9): p. 520-7.
6. Ajuied, A., et al., *Anterior cruciate ligament injury and radiologic progression of knee osteoarthritis: a systematic review and meta-analysis*. Am J Sports Med, 2014. **42**(9): p. 2242-52.
7. Lie, M.M., et al., *What's the rate of knee osteoarthritis 10 years after anterior cruciate ligament injury? An updated systematic review*. Br J Sports Med, 2019.
8. Beynnon, B.D., et al., *The effects of level of competition, sport, and sex on the incidence of first-time noncontact anterior cruciate ligament injury*. American Journal of Sports Medicine, 2014. **42**(8): p. 1806-1812.
9. Prodromos, C.C., et al., *A meta-analysis of the incidence of anterior cruciate ligament tears as a function of gender, sport, and a knee injury-reduction regimen*. Arthroscopy, 2007. **23**(12): p. 1320-1325 e6.
10. Shea, K.G., et al., *Anterior cruciate ligament injury in pediatric and adolescent soccer players: an analysis of insurance data*. J Pediatr Orthop, 2004. **24**(6): p. 623-8.
11. Lee, S.J., et al., *Pivoting neuromuscular control and proprioception in females and males*. Eur J Appl Physiol, 2015. **115**(4): p. 775-84.
12. Del Bel, M.J., et al., *A hierarchy in functional muscle roles at the knee is influenced by sex and anterior cruciate ligament deficiency*. Clin Biomech (Bristol, Avon), 2018. **57**: p. 129-136.
13. Flaxman, T.E., A.J. Smith, and D.L. Benoit, *Sex-related differences in neuromuscular control: Implications for injury mechanisms or healthy stabilisation strategies?* Journal of Orthopaedic Research, 2014. **32**(2): p. 310-7.
14. Hughes, G. and N. Dally, *Gender difference in lower limb muscle activity during landing and rapid change of direction*. Science & Sports, 2015. **30**(3): p. 163-168.
15. DiStefano, L.J., et al., *Maturation and Sex Differences in Neuromuscular Characteristics of Youth Athletes*. J Strength Cond Res, 2015. **29**(9): p. 2465-73.
16. Leppänen, M., et al., *Stiff Landings Are Associated With Increased ACL Injury Risk in Young Female Basketball and Floorball Players*. Am J Sports Med, 2017. **45**(2): p. 386-393.
17. Westbrook, A.E., et al., *Effects of maturation on knee biomechanics during cutting and landing in young female soccer players*. PLoS One, 2020. **15**(5): p. e0233701.

18. Sayer, T.A., et al., *Differences in Hip and Knee Landing Moments across Female Pubertal Development*. Med Sci Sports Exerc, 2019. **51**(1): p. 123-131.
19. Leppänen, M., et al., *Sagittal Plane Hip, Knee, and Ankle Biomechanics and the Risk of Anterior Cruciate Ligament Injury: A Prospective Study*. Orthop J Sports Med, 2017. **5**(12): p. 2325967117745487.
20. Hewett, T.E., et al., *Longitudinal Increases in Knee Abduction Moments in Females during Adolescent Growth*. Med Sci Sports Exerc, 2015. **47**(12): p. 2579-85.
21. Tanner, J.M. and P.S. Davies, *Clinical longitudinal standards for height and height velocity for North American children*. J Pediatr, 1985. **107**(3): p. 317-29.
22. Wild, C.Y., J.R. Steele, and B.J. Munro, *Why do girls sustain more anterior cruciate ligament injuries than boys?: a review of the changes in estrogen and musculoskeletal structure and function during puberty*. Sports Med, 2012. **42**(9): p. 733-49.
23. Quatman, C.E., et al., *Maturation leads to gender differences in landing force and vertical jump performance: a longitudinal study*. Am J Sports Med, 2006. **34**(5): p. 806-13.
24. Hewett, T.E., G.D. Myer, and K.R. Ford, *Decrease in neuromuscular control about the knee with maturation in female athletes*. J Bone Joint Surg Am, 2004. **86**(8): p. 1601-8.
25. Ford, K.R., G.D. Myer, and T.E. Hewett, *Longitudinal effects of maturation on lower extremity joint stiffness in adolescent athletes*. Am J Sports Med, 2010. **38**(9): p. 1829-37.
26. Quatman, C.E., C.C. Quatman-Yates, and T.E. Hewett, *A 'plane' explanation of anterior cruciate ligament injury mechanisms: a systematic review*. Sports Med, 2010. **40**(9): p. 729-46.
27. Lloyd, D.G., T.S. Buchanan, and T.F. Besier, *Neuromuscular biomechanical modeling to understand knee ligament loading*. Med Sci Sports Exerc, 2005. **37**(11): p. 1939-47.
28. Maniar, N., et al., *Non-knee-spanning muscles contribute to tibiofemoral shear as well as valgus and rotational joint reaction moments during unanticipated sidestep cutting*. Sci Rep, 2018. **8**(1): p. 2501.
29. Kar, J. and P.M. Quesada, *A numerical simulation approach to studying anterior cruciate ligament strains and internal forces among young recreational women performing valgus inducing stop-jump activities*. Ann Biomed Eng, 2012. **40**(8): p. 1679-91.
30. Kar, J. and P.M. Quesada, *A musculoskeletal modeling approach for estimating anterior cruciate ligament strains and knee anterior-posterior shear forces in stop-jumps performed by young recreational female athletes*. Ann Biomed Eng, 2013. **41**(2): p. 338-48.
31. Kernozek, T.W. and R.J. Ragan, *Estimation of anterior cruciate ligament tension from inverse dynamics data and electromyography in females during drop landing*. Clin Biomech (Bristol, Avon), 2008. **23**(10): p. 1279-86.
32. Pflum, M.A., et al., *Model prediction of anterior cruciate ligament force during drop-landings*. Med Sci Sports Exerc, 2004. **36**(11): p. 1949-58.
33. Shelburne, K.B. and M.G. Pandy, *A musculoskeletal model of the knee for evaluating ligament forces during isometric contractions*. J Biomech, 1997. **30**(2): p. 163-76.
34. Shelburne, K.B., et al., *Pattern of anterior cruciate ligament force in normal walking*. J Biomech, 2004. **37**(6): p. 797-805.

35. Shin, C.S., A.M. Chaudhari, and T.P. Andriacchi, *The influence of deceleration forces on ACL strain during single-leg landing: a simulation study*. J Biomech, 2007. **40**(5): p. 1145-52.
36. Weinhandl, J.T., et al., *Anticipatory effects on anterior cruciate ligament loading during sidestep cutting*. Clin Biomech (Bristol, Avon), 2013. **28**(6): p. 655-63.
37. Weinhandl, J.T., et al., *Reduced hamstring strength increases anterior cruciate ligament loading during anticipated sidestep cutting*. Clin Biomech (Bristol, Avon), 2014. **29**(7): p. 752-9.
38. Shelburne, K.B., M.R. Torry, and M.G. Pandy, *Muscle, ligament, and joint-contact forces at the knee during walking*. Med Sci Sports Exerc, 2005. **37**(11): p. 1948-56.
39. Shelburne, K.B., M.R. Torry, and M.G. Pandy, *Contributions of muscles, ligaments, and the ground-reaction force to tibiofemoral joint loading during normal gait*. J Orthop Res, 2006. **24**(10): p. 1983-90.
40. Navacchia, A., et al., *Knee Abduction and Internal Rotation Moments Increase ACL Force During Landing Through the Posterior Slope of the Tibia*. J Orthop Res, 2019. **37**(8): p. 1730-1742.
41. Markolf, K.L., et al., *Combined knee loading states that generate high anterior cruciate ligament forces*. J Orthop Res, 1995. **13**(6): p. 930-5.
42. Markolf, K.L., et al., *Direct measurement of resultant forces in the anterior cruciate ligament. An in vitro study performed with a new experimental technique*. J Bone Joint Surg Am, 1990. **72**(4): p. 557-67.
43. Mokhtarzadeh, H., et al., *Contributions of the soleus and gastrocnemius muscles to the anterior cruciate ligament loading during single-leg landing*. J Biomech, 2013. **46**(11): p. 1913-20.
44. Navacchia, A., et al., *EMG-Informed Musculoskeletal Modeling to Estimate Realistic Knee Anterior Shear Force During Drop Vertical Jump in Female Athletes*. Ann Biomed Eng, 2019. **47**(12): p. 2416-2430.
45. Lenton, G.K., et al., *Tibiofemoral joint contact forces increase with load magnitude and walking speed but remain almost unchanged with different types of carried load*. PloS one, 2018. **13**(11): p. e0206859-e0206859.
46. Lloyd, D.G., *Rationale for training programs to reduce anterior cruciate ligament injuries in Australian football*. J Orthop Sports Phys Ther, 2001. **31**(11): p. 645-54; discussion 661.
47. Marieswaran, M., et al., *A Review on Biomechanics of Anterior Cruciate Ligament and Materials for Reconstruction*. Appl Bionics Biomech, 2018. **2018**: p. 4657824.
48. Markatos, K., et al., *The anatomy of the ACL and its importance in ACL reconstruction*. European Journal of Orthopaedic Surgery and Traumatology, 2013. **23**(7): p. 747-752.
49. Kraeutler, M.J., et al., *Anatomy and Biomechanics of the Native and Reconstructed Anterior Cruciate Ligament: Surgical Implications*. JBJS, 2017. **99**(5): p. 438-445.
50. Kweon, C., E.S. Lederman, and A. Chhabra, *Anatomy and Biomechanics of the Cruciate Ligaments and Their Surgical Implications*, in *The Multiple Ligament Injured Knee: A Practical Guide to Management*, G.C. Fanelli, Editor. 2013, Springer New York: New York, NY. p. 17-27.
51. Markatos, K., et al., *The anatomy of the ACL and its importance in ACL reconstruction*. European Journal of Orthopaedic Surgery & Traumatology, 2013. **23**(7): p. 747-752.

52. Clark, J.M. and J.A. Sidles, *The interrelation of fiber bundles in the anterior cruciate ligament*. J Orthop Res, 1990. **8**(2): p. 180-8.
53. Sakane, M., et al., *In situ forces in the anterior cruciate ligament and its bundles in response to anterior tibial loads*. J Orthop Res, 1997. **15**(2): p. 285-93.
54. Hewett, T.E., et al., *Biomechanical measures of neuromuscular control and valgus loading of the knee predict anterior cruciate ligament injury risk in female athletes: a prospective study*. Am J Sports Med, 2005. **33**(4): p. 492-501.
55. Meyer, E.G. and R.C. Haut, *Anterior cruciate ligament injury induced by internal tibial torsion or tibiofemoral compression*. J Biomech, 2008. **41**(16): p. 3377-83.
56. Shin, C.S., A.M. Chaudhari, and T.P. Andriacchi, *Valgus plus internal rotation moments increase anterior cruciate ligament strain more than either alone*. Medicine & Science in Sports and Exercise, 2011. **43**(8): p. 1484-1491.
57. Markolf, K.L., D.C. Wascher, and G.A. Finerman, *Direct in vitro measurement of forces in the cruciate ligaments. Part II: The effect of section of the posterolateral structures*. J Bone Joint Surg Am, 1993. **75**(3): p. 387-94.
58. Shelburne, K.B., M.G. Pandy, and M.R. Torry, *Comparison of shear forces and ligament loading in the healthy and ACL-deficient knee during gait*. J Biomech, 2004. **37**(3): p. 313-9.
59. Meyer, E.G., et al., *Tibiofemoral contact pressures and osteochondral microtrauma during anterior cruciate ligament rupture due to excessive compressive loading and internal torque of the human knee*. Am J Sports Med, 2008. **36**(10): p. 1966-77.
60. Shin, C.S., A.M. Chaudhari, and T.P. Andriacchi, *Valgus plus internal rotation moments increase anterior cruciate ligament strain more than either alone*. Med Sci Sports Exerc, 2011. **43**(8): p. 1484-91.
61. Hame, S.L., D.A. Oakes, and K.L. Markolf, *Injury to the anterior cruciate ligament during alpine skiing: a biomechanical analysis of tibial torque and knee flexion angle*. Am J Sports Med, 2002. **30**(4): p. 537-40.
62. Kiapour, A.M., et al., *Strain Response of the Anterior Cruciate Ligament to Uniplanar and Multiplanar Loads During Simulated Landings: Implications for Injury Mechanism*. Am J Sports Med, 2016. **44**(8): p. 2087-96.
63. Rust, D.A., C.J. Gilmore, and G. Treme, *Injury patterns at a large Western United States ski resort with and without snowboarders: the Taos experience*. Am J Sports Med, 2013. **41**(3): p. 652-6.
64. Boeth, H., et al., *Anterior cruciate ligament-deficient patients with passive knee joint laxity have a decreased range of anterior-posterior motion during active movements*. Am J Sports Med, 2013. **41**(5): p. 1051-7.
65. Hsieh, H.H. and P.S. Walker, *Stabilizing mechanisms of the loaded and unloaded knee joint*. J Bone Joint Surg Am, 1976. **58**(1): p. 87-93.
66. Arendt, E.A., J. Agel, and R. Dick, *Anterior Cruciate Ligament Injury Patterns among Collegiate Men and Women*. Journal of Athletic Training, 1999. **34**(2): p. 86-92.
67. Boden, B.P., et al., *Mechanisms of anterior cruciate ligament injury*. Orthopedics, 2000. **23**(6): p. 573-578.
68. Cochrane, J.L., et al., *Characteristics of anterior cruciate ligament injuries in Australian football*. Journal of Science and Medicine in Sport, 2007. **10**(2): p. 96-104.
69. Voskanian, N., *ACL Injury prevention in female athletes: review of the literature and practical considerations in implementing an ACL prevention program*. Curr Rev Musculoskelet Med, 2013. **6**(2): p. 158-63.

70. Maffulli, N., et al., *Long-term health outcomes of youth sports injuries*. British Journal of Sports Medicine, 2010. **44**(1): p. 21-25.
71. Shea, K.G., et al., *Anterior cruciate ligament injury in pediatric and adolescent soccer players: An analysis of insurance data*. Journal of Pediatric Orthopaedics, 2004. **24**(6): p. 623-628.
72. Caine, D., J. DiFiori, and N. Maffulli, *Physcal injuries in children's and youth sports: Reasons for concern?* British Journal of Sports Medicine, 2006. **40**(9): p. 749-760.
73. Grimmer, K.A., D. Jones, and J. Williams, *Prevalence of adolescent injury from recreational exercise: An Australian perspective*. Journal of Adolescent Health, 2000. **27**(4): p. 266-272.
74. Olsen, O.E., et al., *Exercises to prevent lower limb injuries in youth sports: Cluster randomised controlled trial*. British Medical Journal, 2005. **330**(7489): p. 449-452.
75. Fu, F.H., et al., *Current trends in anterior cruciate ligament reconstruction. Part 1: Biology and biomechanics of reconstruction*. Am J Sports Med, 1999. **27**(6): p. 821-30.
76. Chambat, P., et al., *The evolution of ACL reconstruction over the last fifty years*. Int Orthop, 2013. **37**(2): p. 181-6.
77. Armour, T., et al., *Isokinetic evaluation of internal/external tibial rotation strength after the use of hamstring tendons for anterior cruciate ligament reconstruction*. Am J Sports Med, 2004. **32**(7): p. 1639-43.
78. Lohmander, L.S., et al., *The long-term consequence of anterior cruciate ligament and meniscus injuries: osteoarthritis*. Am J Sports Med, 2007. **35**(10): p. 1756-69.
79. Pinczewski, L.A., et al., *A 10-year comparison of anterior cruciate ligament reconstructions with hamstring tendon and patellar tendon autograft: a controlled, prospective trial*. Am J Sports Med, 2007. **35**(4): p. 564-74.
80. Riediger, M.D., et al., *ACL Reconstruction with Augmentation: a Scoping Review*. Curr Rev Musculoskelet Med, 2019. **12**(2): p. 166-172.
81. Granan, L.P., et al., *The Scandinavian ACL registries 2004-2007: baseline epidemiology*. Acta Orthop, 2009. **80**(5): p. 563-7.
82. Lekkas, C., et al., *Feasibility of establishing an Australian ACL registry: a pilot study by the Australian Orthopaedic Association National Joint Replacement Registry (AOANJRR)*. Knee Surg Sports Traumatol Arthrosc, 2017. **25**(5): p. 1510-1516.
83. Orchard, J.W., L. Engebretsen, and J.A. Feller, *The rate of anterior cruciate ligament reconstruction in Australia is high: a national registry is needed*. Med J Aust, 2018. **208**(8): p. 341-342.
84. Lewis, D.A., et al., *Comparison of four alternative national universal anterior cruciate ligament injury prevention programme implementation strategies to reduce secondary future medical costs*. Br J Sports Med, 2018. **52**(4): p. 277-282.
85. Janssen, K.W., et al., *High incidence and costs for anterior cruciate ligament reconstructions performed in Australia from 2003-2004 to 2007-2008: time for an anterior cruciate ligament register by Scandinavian model?* Scand J Med Sci Sports, 2012. **22**(4): p. 495-501.
86. Moses, B., J. Orchard, and J. Orchard, *Systematic Review: Annual Incidence of ACL Injury and Surgery in Various Populations*. Research in Sports Medicine, 2012. **20**(3-4): p. 157-179.

87. Mouarbes, D., et al., *Anterior Cruciate Ligament Reconstruction: A Systematic Review and Meta-analysis of Outcomes for Quadriceps Tendon Autograft Versus Bone–Patellar Tendon–Bone and Hamstring–Tendon Autografts*. The American Journal of Sports Medicine, 2019. **47**(14): p. 3531-3540.
88. Magnussen, R.A., et al., *Graft Size and Patient Age Are Predictors of Early Revision After Anterior Cruciate Ligament Reconstruction With Hamstring Autograft*. Arthroscopy: The Journal of Arthroscopic & Related Surgery, 2012. **28**(4): p. 526-531.
89. Snaebjörnsson, T., et al., *Graft Diameter and Graft Type as Predictors of Anterior Cruciate Ligament Revision: A Cohort Study Including 18,425 Patients from the Swedish and Norwegian National Knee Ligament Registries*. JBJS, 2019. **101**(20): p. 1812-1820.
90. Rahardja, R., et al., *Effect of Graft Choice on Revision and Contralateral Anterior Cruciate Ligament Reconstruction: Results From the New Zealand ACL Registry*. The American Journal of Sports Medicine, 2019. **48**(1): p. 63-69.
91. Kirwan, G.W., et al., *Graft tensioning practices in anterior cruciate ligament reconstruction amongst orthopaedic surgeons in Australia: a national survey*. Arch Orthop Trauma Surg, 2015. **135**(12): p. 1733-41.
92. Grassi, A., et al., *New Trends in Anterior Cruciate Ligament Reconstruction: A Systematic Review of National Surveys of the Last 5 Years*. Joints, 2018. **6**(3): p. 177-187.
93. Cimino, F., B.S. Volk, and D. Setter, *Anterior cruciate ligament injury: diagnosis, management, and prevention*. American Family Physician, 2010. **82**(8): p. 917-22.
94. Risberg, M.A., M. Lewek, and L. Snyder-Mackler, *A systematic review of evidence for anterior cruciate ligament rehabilitation: How much and what type?* Physical Therapy in Sport, 2004. **5**(3): p. 125-145.
95. Janssen, K.W., et al., *High incidence and costs for anterior cruciate ligament reconstructions performed in Australia from 2003-2004 to 2007-2008: Time for an anterior cruciate ligament register by Scandinavian model?* Scandinavian Journal of Medicine and Science in Sports, 2012. **22**(4): p. 495-501.
96. Hunter, D.J., D. Schofield, and E. Callander, *The individual and socioeconomic impact of osteoarthritis*. Nat Rev Rheumatol, 2014. **10**(7): p. 437-41.
97. Cross, M.J., et al., *Regeneration of the semitendinosus and gracilis tendons following their transection for repair of the anterior cruciate ligament*. Am J Sports Med, 1992. **20**(2): p. 221-3.
98. Suijkerbuijk, M.A.M., et al., *Hamstring Tendon Regeneration After Harvesting: A Systematic Review*. The American Journal of Sports Medicine, 2014. **43**(10): p. 2591-2598.
99. Janssen, R.P., et al., *Regeneration of hamstring tendons after anterior cruciate ligament reconstruction*. Knee Surg Sports Traumatol Arthrosc, 2013. **21**(4): p. 898-905.
100. Simonian, P.T., et al., *Assessment of morbidity of semitendinosus and gracilis tendon harvest for ACL reconstruction*. Am J Knee Surg, 1997. **10**(2): p. 54-9.
101. Nikolaou, V.S., N. Efstathiopoulos, and T. Wredmark, *Hamstring tendons regeneration after ACL reconstruction: an overview*. Knee Surg Sports Traumatol Arthrosc, 2007. **15**(2): p. 153-60.
102. Bryant, A.L., R.A. Clark, and Y.H. Pua, *Morphology of hamstring torque-time curves following ACL injury and reconstruction: mechanisms and implications*. J Orthop Res, 2011. **29**(6): p. 907-14.

103. Burks, R.T., et al., *The effects of semitendinosus and gracilis harvest in anterior cruciate ligament reconstruction*. Arthroscopy, 2005. **21**(10): p. 1177-85.
104. Eriksson, K., et al., *Semitendinosus muscle in anterior cruciate ligament surgery: Morphology and function*. Arthroscopy, 2001. **17**(8): p. 808-17.
105. Karagiannidis, E., et al., *Semitendinosus muscle architecture during maximum isometric contractions in individuals with anterior cruciate ligament reconstruction and controls*. Muscles Ligaments Tendons J, 2017. **7**(1): p. 147-151.
106. Konrath, J.M., et al., *Morphologic Characteristics and Strength of the Hamstring Muscles Remain Altered at 2 Years After Use of a Hamstring Tendon Graft in Anterior Cruciate Ligament Reconstruction*. Am J Sports Med, 2016. **44**(10): p. 2589-2598.
107. Lindstrom, M., et al., *Functional and muscle morphometric effects of ACL reconstruction. A prospective CT study with 1 year follow-up*. Scand J Med Sci Sports, 2013. **23**(4): p. 431-42.
108. Macleod, T.D., et al., *Early regeneration determines long-term graft site morphology and function after reconstruction of the anterior cruciate ligament with semitendinosus-gracilis autograft: a case series*. International journal of sports physical therapy, 2013. **8**(3): p. 256-268.
109. Messer, D.J., et al., *Hamstring muscle activation and morphology are significantly altered 1–6 years after anterior cruciate ligament reconstruction with semitendinosus graft*. Knee Surgery, Sports Traumatology, Arthroscopy, 2019.
110. Nakamura, E., et al., *Three-dimensional computed tomography evaluation of semitendinosus harvest after anterior cruciate ligament reconstruction*. Arthroscopy, 2004. **20**(4): p. 360-5.
111. Nomura, Y., R. Kuramochi, and T. Fukubayashi, *Evaluation of hamstring muscle strength and morphology after anterior cruciate ligament reconstruction*. Scand J Med Sci Sports, 2015. **25**(3): p. 301-7.
112. Snow, B.J., et al., *Evaluation of Muscle Size and Fatty Infiltration with MRI Nine to Eleven Years Following Hamstring Harvest for ACL Reconstruction*. JBJS, 2012. **94**(14): p. 1274-1282.
113. Takeda, Y., et al., *Hamstring muscle function after tendon harvest for anterior cruciate ligament reconstruction: evaluation with T2 relaxation time of magnetic resonance imaging*. Am J Sports Med, 2006. **34**(2): p. 281-8.
114. Tsifountoudis, I., et al., *The natural history of donor hamstrings unit after anterior cruciate ligament reconstruction: a prospective MRI scan assessment*. Knee Surg Sports Traumatol Arthrosc, 2017. **25**(5): p. 1583-1590.
115. Williams, G.N., et al., *Muscle and tendon morphology after reconstruction of the anterior cruciate ligament with autologous semitendinosus-gracilis graft*. J Bone Joint Surg Am, 2004. **86-A**(9): p. 1936-46.
116. Yasuda, K., et al., *Graft site morbidity with autogenous semitendinosus and gracilis tendons*. Am J Sports Med, 1995. **23**(6): p. 706-14.
117. Nishino, A., et al., *Knee-flexion torque and morphology of the semitendinosus after ACL reconstruction*. Med Sci Sports Exerc, 2006. **38**(11): p. 1895-900.
118. Aune, A.K., et al., *Four-strand hamstring tendon autograft compared with patellar tendon-bone autograft for anterior cruciate ligament reconstruction. A randomized study with two-year follow-up*. Am J Sports Med, 2001. **29**(6): p. 722-8.

119. Nakamura, N., et al., *Evaluation of active knee flexion and hamstring strength after anterior cruciate ligament reconstruction using hamstring tendons*. Arthroscopy, 2002. **18**(6): p. 598-602.
120. Viola, R.W., et al., *Internal and external tibial rotation strength after anterior cruciate ligament reconstruction using ipsilateral semitendinosus and gracilis tendon autografts*. Am J Sports Med, 2000. **28**(4): p. 552-5.
121. Wiggins, A.J., et al., *Risk of Secondary Injury in Younger Athletes After Anterior Cruciate Ligament Reconstruction: A Systematic Review and Meta-analysis*. Am J Sports Med, 2016. **44**(7): p. 1861-76.
122. Messer, D., et al., *Eccentric Knee Flexor Strength and Hamstring Injury Risk in Athletes with History of Anterior Cruciate Ligament Reconstruction*. Br J Sports Med, 2017. **51**(4): p. 363.1-363.
123. Finch, C.F., J.L. Kemp, and A.J. Clapperton, *The incidence and burden of hospital-treated sports-related injury in people aged 15+ years in Victoria, Australia, 2004-2010: a future epidemic of osteoarthritis? Osteoarthritis Cartilage*, 2015. **23**(7): p. 1138-43.
124. Carter, C.W., et al., *Sex-based Differences in Common Sports Injuries*. J Am Acad Orthop Surg, 2018. **26**(13): p. 447-454.
125. Fulstone, D., et al., *Continued Sex-Differences in the Rate and Severity of Knee Injuries among Collegiate Soccer Players: The NCAA Injury Surveillance System, 2004–2009*. Int J Sports Med, 2016. **37**(14): p. 1150-1153.
126. Gupta, A.S., et al., *Sex-Based Differences in Anterior Cruciate Ligament Injuries Among United States High School Soccer Players: An Epidemiological Study*. Orthop J Sports Med, 2020. **8**(5): p. 2325967120919178.
127. Lin, C.Y., et al., *Sex Differences in Common Sports Injuries*. PM and R, 2018. **10**(10): p. 1073-1082.
128. Stanley, L.E., et al., *Sex Differences in the Incidence of Anterior Cruciate Ligament, Medial Collateral Ligament, and Meniscal Injuries in Collegiate and High School Sports: 2009-2010 Through 2013-2014*. The American Journal of Sports Medicine, 2016. **44**(6): p. 1565-1572.
129. Dai, B.Y., et al., *Anterior cruciate ligament injuries in soccer: Loading mechanisms, risk factors, and prevention programs*. Journal of Sport and Health Science, 2014. **3**(4): p. 299-306.
130. Joseph, A.M., et al., *A multisport epidemiologic comparison of anterior cruciate ligament injuries in high school athletics*. Journal of Athletic Training, 2013. **48**(6): p. 810-817.
131. Morgan, M.D., et al., *Fifteen-Year Survival of Endoscopic Anterior Cruciate Ligament Reconstruction in Patients Aged 18 Years and Younger*. Am J Sports Med, 2016. **44**(2): p. 384-92.
132. Waldén, M., et al., *The epidemiology of anterior cruciate ligament injury in football (soccer): a review of the literature from a gender-related perspective*. Knee Surg Sports Traumatol Arthrosc, 2011. **19**(1): p. 3-10.
133. Theisen, D., et al., *Injury risk is different in team and individual youth sport*. Journal of Science and Medicine in Sport, 2013. **16**(3): p. 200-204.
134. Thelin, N., S. Holmberg, and A. Thelin, *Knee injuries account for the sports-related increased risk of knee osteoarthritis*. Scandinavian Journal of Medicine and Science in Sports, 2006. **16**(5): p. 329-333.
135. Johnston, J.T., et al., *Video Analysis of Anterior Cruciate Ligament Tears in Professional American Football Athletes*. Am J Sports Med, 2018. **46**(4): p. 862-868.

136. Montgomery, C., et al., *Mechanisms of ACL injury in professional rugby union: a systematic video analysis of 36 cases*. Br J Sports Med, 2018. **52**(15): p. 994-1001.
137. Grassi, A., et al., *Mechanisms and situations of anterior cruciate ligament injuries in professional male soccer players: a YouTube-based video analysis*. Eur J Orthop Surg Traumatol, 2017. **27**(7): p. 967-981.
138. Walden, M., et al., *Three distinct mechanisms predominate in non-contact anterior cruciate ligament injuries in male professional football players: a systematic video analysis of 39 cases*. Br J Sports Med, 2015. **49**(22): p. 1452-60.
139. Olsen, O.E., et al., *Injury mechanisms for anterior cruciate ligament injuries in team handball: a systematic video analysis*. Am J Sports Med, 2004. **32**(4): p. 1002-12.
140. Cochrane, J.L., et al., *Characteristics of anterior cruciate ligament injuries in Australian football*. J Sci Med Sport, 2007. **10**(2): p. 96-104.
141. Carlson, V.R., F.T. Sheehan, and B.P. Boden, *Video Analysis of Anterior Cruciate Ligament (ACL) Injuries: A Systematic Review*. JBJS Rev, 2016. **4**(11).
142. Stuelcken, M.C., et al., *Mechanisms of anterior cruciate ligament injuries in elite women's netball: a systematic video analysis*. J Sports Sci, 2016. **34**(16): p. 1516-22.
143. Weir, G., et al., *A Reliable Video-based ACL Injury Screening Tool for Female Team Sport Athletes*. Int J Sports Med, 2019. **40**(3): p. 191-199.
144. Krosshaug, T., et al., *Mechanisms of anterior cruciate ligament injury in basketball: video analysis of 39 cases*. Am J Sports Med, 2007. **35**(3): p. 359-67.
145. Koga, H., et al., *Mechanisms for noncontact anterior cruciate ligament injuries: knee joint kinematics in 10 injury situations from female team handball and basketball*. Am J Sports Med, 2010. **38**(11): p. 2218-25.
146. Bates, N.A., et al., *Sex-based differences in knee ligament biomechanics during robotically simulated athletic tasks*. J Biomech, 2016. **49**(9): p. 1429-1436.
147. Cerulli, G., et al., *In vivo anterior cruciate ligament strain behaviour during a rapid deceleration movement: case report*. Knee Surg Sports Traumatol Arthrosc, 2003. **11**(5): p. 307-11.
148. Markolf, K.L., et al., *Combined knee loading states that generate high anterior cruciate ligament forces*. Journal of Orthopaedic Research, 1995. **13**(6): p. 930-935.
149. Hame, S., D. Oakes, and K. Markolf, *Injury to the ACL during alpine skiing: A biomechanical analysis of tibial torque and knee flexion angle*. Am J Sports Med, 2002. **30**: p. 537-540.
150. Li, Y., et al., *Posterior tibial slope influences static anterior tibial translation in anterior cruciate ligament reconstruction: a minimum 2-year follow-up study*. Am J Sports Med, 2014. **42**(4): p. 927-33.
151. Wascher, D.C., et al., *Direct in vitro measurement of forces in the cruciate ligaments. Part I: The effect of multiplane loading in the intact knee*. J Bone Joint Surg Am, 1993. **75**(3): p. 377-86.
152. Markolf, K., et al., *Effects of tibiofemoral compression on ACL forces and knee kinematics under combined knee loads*. J Orthop Res, 2019. **37**(3): p. 631-639.
153. Saxby, D.J., et al., *Tibiofemoral contact forces during walking, running and sidestepping*. Gait Posture, 2016. **49**: p. 78-85.
154. Holden, S., C. Boreham, and E. Delahunt, *Sex Differences in Landing Biomechanics and Postural Stability During Adolescence: A Systematic Review with Meta-Analyses*. Sports Med, 2016. **46**(2): p. 241-53.

155. Lamontagne, M. and M.J. Kennedy, *The biomechanics of vertical hopping: a review*. Res Sports Med, 2013. **21**(4): p. 380-94.
156. Dos'Santos, T., et al., *The effect of limb dominance on change of direction biomechanics: A systematic review of its importance for injury risk*. Phys Ther Sport, 2019. **37**: p. 179-189.
157. Hay, J.G., *The biomechanics of the triple jump: a review*. J Sports Sci, 1992. **10**(4): p. 343-78.
158. Lees, A., et al., *The biomechanics of kicking in soccer: a review*. J Sports Sci, 2010. **28**(8): p. 805-17.
159. Fox, A.S., et al., *What is normal? Female lower limb kinematic profiles during athletic tasks used to examine anterior cruciate ligament injury risk: a systematic review*. Sports Med, 2014. **44**(6): p. 815-32.
160. Bruton, M.R., N. O'Dwyer, and R. Adams, *Sex differences in the kinematics and neuromuscular control of landing: biological, environmental and sociocultural factors*. J Electromyogr Kinesiol, 2013. **23**(4): p. 747-58.
161. Ford, K.R., et al., *Longitudinal sex differences during landing in knee abduction in young athletes*. Medicine and Science in Sports and Exercise, 2010. **42**(10): p. 1923-1931.
162. Mendiguchia, J., et al., *Sex differences in proximal control of the knee joint*. Sports Medicine, 2011. **41**(7): p. 541-557.
163. Hewett, T.E., G.D. Myer, and K.R. Ford, *Decrease in neuromuscular control about the knee with maturation in female athletes*. Journal of Bone and Joint Surgery - Series A, 2004. **86**(8): p. 1601-1608.
164. Carson, D.W. and K.R. Ford, *Sex differences in knee abduction during landing: a systematic review*. Sports Health, 2011. **3**(4): p. 373-82.
165. Cronstrom, A., et al., *Gender differences in knee abduction during weight-bearing activities: A systematic review and meta-analysis*. Gait Posture, 2016. **49**: p. 315-328.
166. Benoit, D.L., et al., *Effect of skin movement artifact on knee kinematics during gait and cutting motions measured in vivo*. Gait Posture, 2006. **24**(2): p. 152-64.
167. Benoit, D.L., et al., *In vivo knee kinematics during gait reveals new rotation profiles and smaller translations*. Clin Orthop Relat Res, 2007. **454**(454): p. 81-8.
168. Stagni, R., et al., *Quantification of soft tissue artefact in motion analysis by combining 3D fluoroscopy and stereophotogrammetry: a study on two subjects*. Clin Biomech (Bristol, Avon), 2005. **20**(3): p. 320-9.
169. Piazza, S.J. and P.R. Cavanagh, *Measurement of the screw-home motion of the knee is sensitive to errors in axis alignment*. J Biomech, 2000. **33**(8): p. 1029-1034.
170. Besier, T.F., et al., *Repeatability of gait data using a functional hip joint centre and a mean helical knee axis*. J Biomech, 2003. **36**(8): p. 1159-68.
171. Schmitz, R.J., et al., *Sex differences in lower extremity biomechanics during single leg landings*. Clin Biomech (Bristol, Avon), 2007. **22**(6): p. 681-8.
172. Seymore, K.D., et al., *Sex and limb impact biomechanics associated with risk of injury during drop landing with body borne load*. PLoS One, 2019. **14**(2): p. e0211129.
173. Cleather, D.J. and M.B. Czasche, *Knee Forces During Landing in Men and Women*. J Hum Kinet, 2019. **68**: p. 177-192.

174. Sigward, S.M., C.D. Pollard, and C.M. Powers, *The influence of sex and maturation on landing biomechanics: implications for anterior cruciate ligament injury*. Scand J Med Sci Sports, 2012. **22**(4): p. 502-9.
175. Butler, R.J., et al., *Gender differences in landing mechanics vary depending on the type of landing*. Clin J Sport Med, 2013. **23**(1): p. 52-7.
176. Flaxman, T.E., A.J. Smith, and D.L. Benoit, *Sex-related differences in neuromuscular control: Implications for injury mechanisms or healthy stabilisation strategies?* J Orthop Res, 2014. **32**(2): p. 310-7.
177. Stearns-Reider, K.M. and C.M. Powers, *Rate of Torque Development and Feedforward Control of the Hip and Knee Extensors: Gender Differences*. J Mot Behav, 2018. **50**(3): p. 321-329.
178. Landry, S.C., et al., *Gender differences exist in neuromuscular control patterns during the pre-contact and early stance phase of an unanticipated side-cut and cross-cut maneuver in 15-18 years old adolescent soccer players*. J Electromyogr Kinesiol, 2009. **19**(5): p. e370-9.
179. Huston, L.J. and E.M. Wojtys, *Neuromuscular performance characteristics in elite female athletes*. Am J Sports Med, 1996. **24**(4): p. 427-36.
180. Fleming, B.C., et al., *The gastrocnemius muscle is an antagonist of the anterior cruciate ligament*. J Orthop Res, 2001. **19**(6): p. 1178-84.
181. Griffin, L.Y., et al., *Understanding and preventing noncontact anterior cruciate ligament injuries: a review of the Hunt Valley II meeting, January 2005*. Am J Sports Med, 2006. **34**(9): p. 1512-32.
182. Myer, G.D., et al., *Longitudinal assessment of noncontact anterior cruciate ligament injury risk factors during maturation in a female athlete: a case report*. J Athl Train, 2009. **44**(1): p. 101-9.
183. Ford, K.R., et al., *Longitudinal sex differences during landing in knee abduction in young athletes*. Med Sci Sports Exerc, 2010. **42**(10): p. 1923-31.
184. Roemmich, J.N. and A.D. Rogol, *Physiology of growth and development. Its relationship to performance in the young athlete*. Clin Sports Med, 1995. **14**(3): p. 483-502.
185. Read, P.J., et al., *Hopping and Landing Performance in Male Youth Soccer Players: Effects of Age and Maturation*. Int J Sports Med, 2017. **38**(12): p. 902-908.
186. Read, P.J., et al., *Landing Kinematics in Elite Male Youth Soccer Players of Different Chronologic Ages and Stages of Maturation*. J Athl Train, 2018. **53**(4): p. 372-378.
187. Fort-Vanmeerhaeghe, A., et al., *Sex and Maturation Differences in Performance of Functional Jumping and Landing Deficits in Youth Athletes*. J Sport Rehabil, 2019. **28**(6): p. 606-613.
188. DiCesare, C.A., et al., *Lower Extremity Biomechanics Are Altered Across Maturation in Sport-Specialized Female Adolescent Athletes*. Front Pediatr, 2019. **7**: p. 268.
189. Holden, S., et al., *Sex differences in sagittal plane control emerge during adolescent growth: a prospective investigation*. Knee Surg Sports Traumatol Arthrosc, 2019. **27**(2): p. 419-426.
190. Myer, G.D., K.R. Ford, and T.E. Hewett, *Rationale and Clinical Techniques for Anterior Cruciate Ligament Injury Prevention Among Female Athletes*. J Athl Train, 2004. **39**(4): p. 352-364.

191. Ford, K.R., et al., *The effects of age and skill level on knee musculature co-contraction during functional activities: a systematic review*. Br J Sports Med, 2008. **42**(7): p. 561-6.
192. Oliver, J.L. and P.M. Smith, *Neural control of leg stiffness during hopping in boys and men*. J Electromyogr Kinesiol, 2010. **20**(5): p. 973-9.
193. Besier, T.F., et al., *Anticipatory effects on knee joint loading during running and cutting maneuvers*. Med Sci Sports Exerc, 2001. **33**(7): p. 1176-81.
194. Brown, S.R., M. Brughelli, and P.A. Hume, *Knee mechanics during planned and unplanned sidestepping: a systematic review and meta-analysis*. Sports Med, 2014. **44**(11): p. 1573-88.
195. Besier, T.F., D.G. Lloyd, and T.R. Ackland, *Muscle activation strategies at the knee during running and cutting maneuvers*. Med Sci Sports Exerc, 2003. **35**(1): p. 119-27.
196. Besier, T.F., et al., *External loading of the knee joint during running and cutting maneuvers*. Medicine & Science in Sports & Exercise, 2001. **33**(7): p. 1168-1175.
197. Besier, T.F., et al., *Anticipatory effects on knee joint loading during running and cutting maneuvers*. Medicine & Science in Sports & Exercise, 2001. **33**(7): p. 1176-1181.
198. Killen, B.A., et al., *Individual muscle contributions to tibiofemoral compressive articular loading during walking, running and sidestepping*. J Biomech, 2018. **80**: p. 23-31.
199. Weir, G., et al., *Coordination and variability during anticipated and unanticipated sidestepping*. Gait Posture, 2019. **67**: p. 1-8.
200. Lee, M.J., et al., *Effects of different visual stimuli on postures and knee moments during sidestepping*. Med Sci Sports Exerc, 2013. **45**(9): p. 1740-8.
201. Dai, B., et al., *The effect of a secondary cognitive task on landing mechanics and jump performance*. Sports Biomech, 2018. **17**(2): p. 192-205.
202. Almonroeder, T.G., et al., *Cognitive Demands Influence Lower Extremity Mechanics During a Drop Vertical Jump Task in Female Athletes*. J Orthop Sports Phys Ther, 2018. **48**(5): p. 381-387.
203. Kim, J.H., et al., *Effect of Anticipation on Lower Extremity Biomechanics During Side- and Cross-Cutting Maneuvers in Young Soccer Players*. Am J Sports Med, 2014. **42**(8): p. 1985-92.
204. Englander, Z.A., et al., *In Vivo Anterior Cruciate Ligament Deformation During a Single-Legged Jump Measured by Magnetic Resonance Imaging and High-Speed Biplanar Radiography*. Am J Sports Med, 2019. **47**(13): p. 3166-3172.
205. Kernozek, T.W., M.R. Torry, and M. Iwasaki, *Gender differences in lower extremity landing mechanics caused by neuromuscular fatigue*. Am J Sports Med, 2008. **36**(3): p. 554-65.
206. Markolf, K.L., et al., *Effects of applied quadriceps and hamstrings muscle loads on forces in the anterior and posterior cruciate ligaments*. Am J Sports Med, 2004. **32**(5): p. 1144-9.
207. Hug, F., P.W. Hodges, and K. Tucker, *Muscle force cannot be directly inferred from muscle activation: Illustrated by the proposed imbalance of force between the vastus medialis and vastus lateralis in people with patellofemoral pain*. Journal of Orthopaedic and Sports Physical Therapy, 2015. **45**(5): p. 360-365.
208. Bergmann, G., et al., *Standardized loads acting in knee implants*. PLoS One, 2014. **9**(1): p. e86035.
209. Fregly, B.J., et al., *Grand challenge competition to predict in vivo knee loads*. J Orthop Res, 2012. **30**(4): p. 503-13.

210. Bergmann, G., et al., *Standardized Loads Acting in Hip Implants*. PLoS One, 2016. **11**(5): p. e0155612.
211. Damm, P., et al., *Total hip joint prosthesis for in vivo measurement of forces and moments*. Med Eng Phys, 2010. **32**(1): p. 95-100.
212. Fukashiro, S., et al., *In vivo Achilles tendon loading during jumping in humans*. Eur J Appl Physiol Occup Physiol, 1995. **71**(5): p. 453-8.
213. Komi, P.V., et al., *In Vivo Registration of Achilles Tendon Forces in Man*. Int J Sports Med, 1987. **08**(S 1): p. S3-S8.
214. Beynnon, B., et al., *The measurement of anterior cruciate ligament strain in vivo*. Int Orthop, 1992. **16**(1): p. 1-12.
215. Beynnon, B.D., et al., *Anterior cruciate ligament strain behavior during rehabilitation exercises in vivo*. Am J Sports Med, 1995. **23**(1): p. 24-34.
216. Beynnon, B.D., et al., *The strain behavior of the anterior cruciate ligament during squatting and active flexion-extension. A comparison of an open and a closed kinetic chain exercise*. Am J Sports Med, 1997. **25**(6): p. 823-9.
217. Fleming, B.C., et al., *An in vivo comparison of anterior tibial translation and strain in the anteromedial band of the anterior cruciate ligament*. J Biomech, 1993. **26**(1): p. 51-8.
218. Fleming, B.C., et al., *The strain behavior of the anterior cruciate ligament during stair climbing: an in vivo study*. Arthroscopy, 1999. **15**(2): p. 185-91.
219. Fleming, B.C., et al., *The strain behavior of the anterior cruciate ligament during bicycling. An in vivo study*. Am J Sports Med, 1998. **26**(1): p. 109-18.
220. Fleming, B.C., et al., *The effects of compressive load and knee joint torque on peak anterior cruciate ligament strains*. Am J Sports Med, 2003. **31**(5): p. 701-7.
221. Fleming, B.C., et al., *The effect of weightbearing and external loading on anterior cruciate ligament strain*. J Biomech, 2001. **34**(2): p. 163-70.
222. Heijne, A., et al., *Strain on the anterior cruciate ligament during closed kinetic chain exercises*. Med Sci Sports Exerc, 2004. **36**(6): p. 935-41.
223. Howe, J.G., et al., *Arthroscopic strain gauge measurement of the normal anterior cruciate ligament*. Arthroscopy, 1990. **6**(3): p. 198-204.
224. Englander, Z.A., et al., *In vivo attachment site to attachment site length and strain of the ACL and its bundles during the full gait cycle measured by MRI and high-speed biplanar radiography*. J Biomech, 2020. **98**: p. 109443.
225. Englander, Z.A., et al., *Automatic registration of MRI-based joint models to high-speed biplanar radiographs for precise quantification of in vivo anterior cruciate ligament deformation during gait*. J Biomech, 2018. **81**: p. 36-44.
226. Taylor, K.A., et al., *Measurement of in vivo anterior cruciate ligament strain during dynamic jump landing*. J Biomech, 2011. **44**(3): p. 365-71.
227. Kiapour, A.M., et al., *Timing sequence of multi-planar knee kinematics revealed by physiologic cadaveric simulation of landing: implications for ACL injury mechanism*. Clin Biomech (Bristol, Avon), 2014. **29**(1): p. 75-82.
228. Fleming, B.C. and B.D. Beynnon, *In vivo measurement of ligament/tendon strains and forces: a review*. Ann Biomed Eng, 2004. **32**(3): p. 318-28.
229. Smith, C.R., et al., *Influence of Ligament Properties on Tibiofemoral Mechanics in Walking*. J Knee Surg, 2016. **29**(2): p. 99-106.
230. Delp, S.L., et al., *OpenSim: open-source software to create and analyze dynamic simulations of movement*. IEEE Trans Biomed Eng, 2007. **54**(11): p. 1940-50.
231. Jin, Z., *Computational Modelling of Biomechanics and Biotribology in the Musculoskeletal System: Biomaterials and Tissues*. Computational Modelling of

- Biomechanics and Biotribology in the Musculoskeletal System: Biomaterials and Tissues. 2014. 1-525.
232. Kadaba, M.P., H.K. Ramakrishnan, and M.E. Wootten, *Measurement of lower extremity kinematics during level walking*. J Orthop Res, 1990. **8**(3): p. 383-92.
 233. Kainz, H., et al., *Joint kinematic calculation based on clinical direct kinematic versus inverse kinematic gait models*. J Biomech, 2016. **49**(9): p. 1658-1669.
 234. Lu, T.W. and J.J. O'Connor, *Bone position estimation from skin marker coordinates using global optimisation with joint constraints*. J Biomech, 1999. **32**(2): p. 129-34.
 235. Anderson, F.C. and M.G. Pandy, *Static and dynamic optimization solutions for gait are practically equivalent*. J Biomech, 2001. **34**(2): p. 153-61.
 236. Crowninshield, R.D. and R.A. Brand, *A physiologically based criterion of muscle force prediction in locomotion*. J Biomech, 1981. **14**(11): p. 793-801.
 237. Hoang, H.X., et al., *A calibrated EMG-informed neuromusculoskeletal model can appropriately account for muscle co-contraction in the estimation of hip joint contact forces in people with hip osteoarthritis*. J Biomech, 2019. **83**: p. 134-142.
 238. Kainz, H., et al., *Selective dorsal rhizotomy improves muscle forces during walking in children with spastic cerebral palsy*. Clin Biomech (Bristol, Avon), 2019. **65**: p. 26-33.
 239. Kautz, S.A., R.R. Neptune, and F.E. Zajac, *General coordination principles elucidated by forward dynamics: minimum fatigue does not explain muscle excitation in dynamic tasks*. Motor Control, 2000. **4**(1): p. 75-80; discussion 97-116.
 240. Lloyd, D.G. and T.F. Besier, *An EMG-driven musculoskeletal model to estimate muscle forces and knee joint moments in vivo*. J Biomech, 2003. **36**(6): p. 765-76.
 241. Pizzolato, C., et al., *CEINMS: A toolbox to investigate the influence of different neural control solutions on the prediction of muscle excitation and joint moments during dynamic motor tasks*. J Biomech, 2015. **48**(14): p. 3929-36.
 242. Sartori, M., et al., *EMG-driven forward-dynamic estimation of muscle force and joint moment about multiple degrees of freedom in the human lower extremity*. PLoS One, 2012. **7**(12): p. e52618.
 243. Hill, A.V., *The heat of shortening and the dynamic constants of muscle*. Proceedings of the Royal Society Series B-Biological Sciences, 1938. **126**(843): p. 136-195.
 244. Falisse, A., et al., *EMG-Driven Optimal Estimation of Subject-SPECIFIC Hill Model Muscle-Tendon Parameters of the Knee Joint Actuators*. IEEE Trans Biomed Eng, 2017. **64**(9): p. 2253-2262.
 245. Hoang, H.X., et al., *Subject-specific calibration of neuromuscular parameters enables neuromusculoskeletal models to estimate physiologically plausible hip joint contact forces in healthy adults*. J Biomech, 2018. **80**: p. 111-120.
 246. Meyer, A.J., C. Patten, and B.J. Fregly, *Lower extremity EMG-driven modeling of walking with automated adjustment of musculoskeletal geometry*. PLoS One, 2017. **12**(7): p. e0179698.
 247. Shao, Q., et al., *An EMG-driven model to estimate muscle forces and joint moments in stroke patients*. Comput Biol Med, 2009. **39**(12): p. 1083-8.
 248. Sartori, M., D. Farina, and D.G. Lloyd, *Hybrid neuromusculoskeletal modeling to best track joint moments using a balance between muscle excitations derived from electromyograms and optimization*. J Biomech, 2014. **47**(15): p. 3613-21.

249. Veerkamp, K., et al., *The effects of electromyography-assisted modelling in estimating musculotendon forces during gait in children with cerebral palsy*. J Biomech, 2019. **92**: p. 45-53.
250. Aeles, J., et al., *Revealing the unique features of each individual's muscle activation signatures*. bioRxiv, 2020: p. 2020.07.23.217034.
251. Buchanan, T.S. and D.G. Lloyd, *Muscle activity is different for humans performing static tasks which require force control and position control*. Neurosci Lett, 1995. **194**(1-2): p. 61-4.
252. Tax, A.A., J.J. Denier van der Gon, and C.J. Erkelens, *Differences in coordination of elbow flexor muscles in force tasks and in movement tasks*. Exp Brain Res, 1990. **81**(3): p. 567-72.
253. Besier, T.F., et al., *Knee muscle forces during walking and running in patellofemoral pain patients and pain-free controls*. J Biomech, 2009. **42**(7): p. 898-905.
254. Menegaldo, L.L. and L.F. Oliveira, *An EMG-driven model to evaluate quadriceps strengthening after an isokinetic training*. Iutam Symposium on Human Body Dynamics, 2011. **2**: p. 131-141.
255. Norton, J.A. and M.A. Gorassini, *Changes in cortically related intermuscular coherence accompanying improvements in locomotor skills in incomplete spinal cord injury*. J Neurophysiol, 2006. **95**(4): p. 2580-9.
256. Panizzolo, F.A., et al., *Muscle size explains low passive skeletal muscle force in heart failure patients*. PeerJ, 2016. **4**: p. e2447.
257. Gerus, P., et al., *Subject-specific knee joint geometry improves predictions of medial tibiofemoral contact forces*. J Biomech, 2013. **46**(16): p. 2778-86.
258. Winby, C.R., D.G. Lloyd, and T.B. Kirk, *Evaluation of different analytical methods for subject-specific scaling of musculotendon parameters*. J Biomech, 2008. **41**(8): p. 1682-8.
259. Assila, N., et al., *EMG-Assisted Algorithm to Account for Shoulder Muscles Co-Contraction in Overhead Manual Handling*. Applied Sciences-Basel, 2020. **10**(10).
260. Kian, A., et al., *Static optimization underestimates antagonist muscle activity at the glenohumeral joint: A musculoskeletal modeling study*. J Biomech, 2019. **97**: p. 109348.
261. Saxby, D.J., et al., *Tibiofemoral contact forces in the anterior cruciate ligament-reconstructed knee*. Medicine and Science in Sports and Exercise, 2016. **48**(11): p. 2195-2206.
262. Saxby, D.J., et al., *Relationships Between Tibiofemoral Contact Forces and Cartilage Morphology at 2 to 3 Years After Single-Bundle Hamstring Anterior Cruciate Ligament Reconstruction and in Healthy Knees*. Orthopaedic Journal of Sports Medicine, 2017. **5**(8).
263. Wellsandt, E., et al., *Decreased Knee Joint Loading Associated With Early Knee Osteoarthritis After Anterior Cruciate Ligament Injury*. Am J Sports Med, 2016. **44**(1): p. 143-51.
264. Diamond, L.E., et al., *Individuals with mild-to-moderate hip osteoarthritis walk with lower hip joint contact forces despite higher levels of muscle co-contraction compared to healthy individuals*. Osteoarthritis Cartilage, 2020. **28**(7): p. 924-931.
265. Saxby, D.J., et al., *Machine learning methods to support personalized neuromusculoskeletal modelling*. Biomech Model Mechanobiol, 2020.

266. Sahu, N.K. and A.K. Kaviti, *A Review of Use FEM Techniques in Modeling of Human Knee Joint*. Journal of Biomimetics, Biomaterials and Biomedical Engineering, 2016. **28**: p. 14-25.
267. Weiss, J.A. and J.C. Gardiner, *Computational modeling of ligament mechanics*. Crit Rev Biomed Eng, 2001. **29**(3): p. 303-71.
268. Naghibi Beidokhti, H., et al., *The influence of ligament modelling strategies on the predictive capability of finite element models of the human knee joint*. J Biomech, 2017. **65**: p. 1-11.
269. Hosseini Nasab, S.H., et al., *Length-Change Patterns of the Collateral Ligaments During Functional Activities After Total Knee Arthroplasty*. Ann Biomed Eng, 2020. **48**(4): p. 1396-1406.
270. Ng, K.C., et al., *Hip Joint Stresses Due to Cam-Type Femoroacetabular Impingement: A Systematic Review of Finite Element Simulations*. PLoS One, 2016. **11**(1): p. e0147813.
271. Smith, C.R., et al., *Efficient Computation of Cartilage Contact Pressures within Dynamic Simulations of Movement*. Comput Methods Biomech Biomed Eng Imaging Vis, 2018. **6**(5): p. 491-498.
272. Imeni, M., et al., *Constitutive modeling of menisci tissue: a critical review of analytical and numerical approaches*. Biomech Model Mechanobiol, 2020.
273. Guess, T.M. and S. Razu, *Loading of the medial meniscus in the ACL deficient knee: A multibody computational study*. Med Eng Phys, 2017. **41**: p. 26-34.
274. Wakeling, J.M., et al., *The Energy of Muscle Contraction. I. Tissue Force and Deformation During Fixed-End Contractions*. Front Physiol, 2020. **11**: p. 813.
275. Hinckel, B.B., et al., *The Effect of Mechanical Varus on Anterior Cruciate Ligament and Lateral Collateral Ligament Stress: Finite Element Analyses*. Orthopedics, 2016. **39**(4): p. e729-36.
276. Chaudhari, A.M. and T.P. Andriacchi, *The mechanical consequences of dynamic frontal plane limb alignment for non-contact ACL injury*. J Biomech, 2006. **39**(2): p. 330-8.
277. Xie, F., et al., *A study on construction three-dimensional nonlinear finite element model and stress distribution analysis of anterior cruciate ligament*. J Biomech Eng, 2009. **131**(12): p. 121007.
278. Kazemi, M., Y. Dabiri, and L.P. Li, *Recent advances in computational mechanics of the human knee joint*. Comput Math Methods Med, 2013. **2013**: p. 718423.
279. Brandon, S.C.E., C.R. Smith, and D.G. Thelen, *Simulation of soft tissue loading from observed movement dynamics*, in *Handbook of Human Motion*. 2018. p. 395-428.
280. Brito da Luz, S., et al., *Feasibility of using MRIs to create subject-specific parallel-mechanism joint models*. J Biomech, 2017. **53**: p. 45-55.
281. Pandy, M.G. and K. Sasaki, *A Three-Dimensional Musculoskeletal Model of the Human Knee Joint. Part 2: Analysis of Ligament Function*. Comput Methods Biomech Biomed Engin, 1998. **1**(4): p. 265-283.
282. Pandy, M.G., K. Sasaki, and S. Kim, *A Three-Dimensional Musculoskeletal Model of the Human Knee Joint. Part 1: Theoretical Construct*. Comput Methods Biomech Biomed Engin, 1998. **1**(2): p. 87-108.
283. Serpas, F., T. Yanagawa, and M. Pandy, *Forward-dynamics simulation of anterior cruciate ligament forces developed during isokinetic dynamometry*. Comput Methods Biomech Biomed Engin, 2002. **5**(1): p. 33-43.

284. Barzan, M., et al., *Development and validation of subject-specific pediatric multibody knee kinematic models with ligamentous constraints*. J Biomech, 2019. **93**: p. 194-203.
285. Guess, T.M., et al., *A subject specific multibody model of the knee with menisci*. Med Eng Phys, 2010. **32**(5): p. 505-15.
286. Koo, S. and T.P. Andriacchi, *A comparison of the influence of global functional loads vs. local contact anatomy on articular cartilage thickness at the knee*. J Biomech, 2007. **40**(13): p. 2961-6.
287. Sancisi, N. and V. Parenti-Castelli, *A New Kinematic Model of the Passive Motion of the Knee Inclusive of the Patella*. Journal of Mechanisms and Robotics-Transactions of the Asme, 2011. **3**(4).
288. Shelburne, K.B. and M.G. Pandy, *A dynamic model of the knee and lower limb for simulating rising movements*. Comput Methods Biomech Biomed Engin, 2002. **5**(2): p. 149-59.
289. Bernstein, N.A., *The Co-Ordination and Regulation of Movements*. 1967, Oxford: Pergamon Press.
290. Tanner, J.M., *Normal growth and techniques of growth assessment*. Clin Endocrinol Metab, 1986. **15**(3): p. 411-51.
291. Tanner, J.M., et al., *The adolescent growth spurt of boys and girls of the Harpenden growth study*. Ann Hum Biol, 1976. **3**(2): p. 109-26.
292. Davies, P.L. and J.D. Rose, *Motor skills of typically developing adolescents: awkwardness or improvement?* Phys Occup Ther Pediatr, 2000. **20**(1): p. 19-42.
293. Chan, N.P., et al., *Reliability of pubertal self-assessment in Hong Kong Chinese children*. J Paediatr Child Health, 2008. **44**(6): p. 353-8.
294. Pereira, A., et al., *Breast bud detection: A validation study in the Chilean Growth Obesity Cohort Study*. BMC Women's Health, 2014. **14**(1): p. 96.
295. Balachandar, V., et al., *Effects of the menstrual cycle on lower-limb biomechanics, neuromuscular control, and anterior cruciate ligament injury risk: a systematic review*. Muscles Ligaments Tendons J, 2017. **7**(1): p. 136-146.
296. Meldrum, D., et al., *Test-retest reliability of three dimensional gait analysis: including a novel approach to visualising agreement of gait cycle waveforms with Bland and Altman plots*. Gait Posture, 2014. **39**(1): p. 265-71.
297. Merletti, R., *Surface electromyography: The SENIAM project*. Europa Medicophysica, 2000. **36**(4): p. 167-169.
298. Coren, S., *The Lateral Preference Inventory for Measurement of Handedness, Footedness, Eyedness, and Earedness - Norms for Young-Adults*. Bulletin of the Psychonomic Society, 1993. **31**(1): p. 1-3.
299. Schache, A.G. and R. Baker, *On the expression of joint moments during gait*. Gait and Posture, 2007. **25**(3): p. 440-452.
300. Mantoan, A., et al., *MOtoNMS: A MATLAB toolbox to process motion data for neuromusculoskeletal modeling and simulation*. Source Code Biol Med, 2015. **10**: p. 12.
301. Robertson, D.G.E. and J.J. Dowling, *Design and responses of Butterworth and critically damped digital filters*. Journal of Electromyography and Kinesiology, 2003. **13**(6): p. 569-573.
302. Harrington, M.E., et al., *Prediction of the hip joint centre in adults, children, and patients with cerebral palsy based on magnetic resonance imaging*. J Biomech, 2007. **40**(3): p. 595-602.
303. Rajagopal, A., et al., *Full-Body Musculoskeletal Model for Muscle-Driven Simulation of Human Gait*. IEEE Trans Biomed Eng, 2016. **63**(10): p. 2068-79.

304. Zelik, K.E., K.Z. Takahashi, and G.S. Sawicki, *Six degree-of-freedom analysis of hip, knee, ankle and foot provides updated understanding of biomechanical work during human walking*. J Exp Biol, 2015. **218**(Pt 6): p. 876-86.
305. Kainz, H., et al., *Accuracy and Reliability of Marker-Based Approaches to Scale the Pelvis, Thigh, and Shank Segments in Musculoskeletal Models*. J Appl Biomech, 2017. **33**(5): p. 354-360.
306. Modenese, L., et al., *Estimation of musculotendon parameters for scaled and subject specific musculoskeletal models using an optimization technique*. J Biomech, 2016. **49**(2): p. 141-8.
307. O'Brien, T.D., et al., *In vivo measurements of muscle specific tension in adults and children*. Exp Physiol, 2010. **95**(1): p. 202-10.
308. Handsfield, G.G., et al., *Relationships of 35 lower limb muscles to height and body mass quantified using MRI*. J Biomech, 2014. **47**(3): p. 631-8.
309. Mantoan, A. and M. Reggiani, *BOPS v0.9*. 2015.
310. Manal, K. and T.S. Buchanan, *Subject-specific estimates of tendon slack length: A numerical method*. Journal of Applied Biomechanics, 2004. **20**(2): p. 195-203.
311. Frobell, R.B., et al., *The acutely ACL injured knee assessed by MRI: are large volume traumatic bone marrow lesions a sign of severe compression injury?* Osteoarthritis Cartilage, 2008. **16**(7): p. 829-36.
312. Viskontas, D.G., et al., *Bone bruises associated with ACL rupture: correlation with injury mechanism*. Am J Sports Med, 2008. **36**(5): p. 927-33.
313. Kiapour, A.M., et al., *Uni-directional coupling between tibiofemoral frontal and axial plane rotation supports valgus collapse mechanism of ACL injury*. J Biomech, 2015. **48**(10): p. 1745-51.
314. Takeda, Y., et al., *Biomechanical function of the human anterior cruciate ligament*. Arthroscopy, 1994. **10**(2): p. 140-147.
315. Chandrashekar, N., et al., *Sex-based differences in the tensile properties of the human anterior cruciate ligament*. J Biomech, 2006. **39**(16): p. 2943-50.
316. Altman, D.G. and J.M. Bland, *Measurement in Medicine - the Analysis of Method Comparison Studies*. Journal of the Royal Statistical Society Series D-the Statistician, 1983. **32**(3): p. 307-317.
317. Sayer, T.A., et al., *Effect of high and low-supportive footwear on female tri-planar knee moments during single limb landing*. J Foot Ankle Res, 2018. **11**: p. 51.
318. Schache, A.G. and R. Baker, *On the expression of joint moments during gait*. Gait Posture, 2007. **25**(3): p. 440-52.
319. Hermens, H.J., et al., *Development of recommendations for SEMG sensors and sensor placement procedures*. J Electromyogr Kinesiol, 2000. **10**(5): p. 361-74.
320. Robertson, D.G. and J.J. Dowling, *Design and responses of Butterworth and critically damped digital filters*. J Electromyogr Kinesiol, 2003. **13**(6): p. 569-73.
321. Hall, M., et al., *Immediate effects of valgus knee bracing on tibiofemoral contact forces and knee muscle forces*. Gait Posture, 2019. **68**: p. 55-62.
322. Walker, P.S., J.S. Rovick, and D.D. Robertson, *The effects of knee brace hinge design and placement on joint mechanics*. J Biomech, 1988. **21**(11): p. 965-74.
323. Harrington, M.E., et al., *Prediction of the hip joint centre in adults, children, and patients with cerebral palsy based on magnetic resonance imaging*. Journal of Biomechanics, 2007. **40**(3): p. 595-602.
324. Ward, S.R., L.H. Smallwood, and R.L. Lieber. *Scaling of human lower extremity muscle architecture to skeletal dimensions (Abstract)*. in ISB XXth Congress. 2005. Cleveland, Ohio.

325. van Arkel, R.J., et al., *Hip abduction can prevent posterior edge loading of hip replacements*. J Orthop Res, 2013. **31**(8): p. 1172-9.
326. Woo, S.L., et al., *Tensile properties of the human femur-anterior cruciate ligament-tibia complex. The effects of specimen age and orientation*. Am J Sports Med, 1991. **19**(3): p. 217-25.
327. Herzog, W. and L.J. Read, *Lines of action and moment arms of the major force-carrying structures crossing the human knee joint*. J Anat, 1993. **182** (Pt 2): p. 213-30.
328. Ward, S.H., et al., *Deficits in Quadriceps Force Control After Anterior Cruciate Ligament Injury: Potential Central Mechanisms*. J Athl Train, 2019. **54**(5): p. 505-512.
329. Meyer, E.G. and R.C. Haut, *Excessive compression of the human tibio-femoral joint causes ACL rupture*. J Biomech, 2005. **38**(11): p. 2311-6.
330. Fregly, B.J., M.L. Boninger, and D.J. Reinkensmeyer, *Personalized neuromusculoskeletal modeling to improve treatment of mobility impairments: a perspective from European research sites*. J Neuroeng Rehabil, 2012. **9**: p. 18.
331. Prilutsky, B.I. and V.M. Zatsiorsky, *Optimization-based models of muscle coordination*. Exerc Sport Sci Rev, 2002. **30**(1): p. 32-8.
332. Sauer, T., *Numerical Analysis*. 2nd ed. 2012, Boston, MA: Pearson Education.
333. Llewellyn, M., J.F. Yang, and A. Prochazka, *Human H-reflexes are smaller in difficult beam walking than in normal treadmill walking*. Exp Brain Res, 1990. **83**(1): p. 22-8.
334. Lloyd, D.G. and T.S. Buchanan, *Strategies of muscular support of varus and valgus isometric loads at the human knee*. J Biomech, 2001. **34**(10): p. 1257-67.
335. Hug, F., P.W. Hodges, and K. Tucker, *Muscle force cannot be directly inferred from muscle activation: illustrated by the proposed imbalance of force between the vastus medialis and vastus lateralis in people with patellofemoral pain*. J Orthop Sports Phys Ther, 2015. **45**(5): p. 360-5.
336. Cerulli, G., et al., *In vivo anterior cruciate ligament strain behaviour during a rapid deceleration movement: Case report*. Knee Surgery, Sports Traumatology, Arthroscopy, 2003. **11**(5): p. 307-311.
337. Englander, Z.A., et al., *In Vivo Anterior Cruciate Ligament Deformation During a Single-Legged Jump Measured by Magnetic Resonance Imaging and High-Speed Biplanar Radiography*. American Journal of Sports Medicine, 2019. **47**(13): p. 3166-3172.
338. Taylor, K.A., et al., *Measurement of in vivo anterior cruciate ligament strain during dynamic jump landing*. Journal of Biomechanics, 2011. **44**(3): p. 365-371.
339. Nasser, A., et al., *Modelling the loading mechanics of anterior cruciate ligament*. Comput Methods Programs Biomed, 2020. **184**: p. 105098.
340. Hashemi, J., et al., *Hip extension, knee flexion paradox: a new mechanism for non-contact ACL injury*. J Biomech, 2011. **44**(4): p. 577-85.
341. Boden, B.P., et al., *Video analysis of anterior cruciate ligament injury: abnormalities in hip and ankle kinematics*. Am J Sports Med, 2009. **37**(2): p. 252-9.
342. Schilaty, N.D., et al., *Sex-Based Differences in Knee Kinetics With Anterior Cruciate Ligament Strain on Cadaveric Impact Simulations*. Orthop J Sports Med, 2018. **6**(3): p. 2325967118761037.
343. Bates, N.A., et al., *Multiplanar Loading of the Knee and Its Influence on Anterior Cruciate Ligament and Medial Collateral Ligament Strain During Simulated Landings and Noncontact Tears*. Am J Sports Med, 2019. **47**(8): p. 1844-1853.

344. Bencke, J., P. Aagaard, and M.K. Zebis, *Muscle Activation During ACL Injury Risk Movements in Young Female Athletes: A Narrative Review*. Front Physiol, 2018. **9**(MAY): p. 445.
345. Maniar, N., et al., *Lower-limb muscle function during sidestep cutting*. J Biomech, 2019. **82**: p. 186-192.
346. Adouni, M., A. Shirazi-Adl, and H. Marouane, *Role of gastrocnemius activation in knee joint biomechanics: gastrocnemius acts as an ACL antagonist*. Comput Methods Biomech Biomed Engin, 2016. **19**(4): p. 376-85.
347. Shelburne, K.B. and M.G. Pandy, *Determinants of cruciate-ligament loading during rehabilitation exercise*. Clin Biomech (Bristol, Avon), 1998. **13**(6): p. 403-413.
348. Bakker, R., et al., *Effect of sagittal plane mechanics on ACL strain during jump landing*. J Orthop Res, 2016. **34**(9): p. 1636-44.
349. MacWilliams, B.A., et al., *Hamstrings cocontraction reduces internal rotation, anterior translation, and anterior cruciate ligament load in weight-bearing flexion*. J Orthop Res, 1999. **17**(6): p. 817-22.
350. Carolan, B. and E. Cafarelli, *Adaptations in coactivation after isometric resistance training*. J Appl Physiol (1985), 1992. **73**(3): p. 911-7.
351. Kean, C.O., D.G. Behm, and W.B. Young, *Fixed foot balance training increases rectus femoris activation during landing and jump height in recreationally active women*. J Sports Sci Med, 2006. **5**(1): p. 138-48.
352. Mausehund, L., A.E. Skard, and T. Krosshaug, *Muscle Activation in Unilateral Barbell Exercises: Implications for Strength Training and Rehabilitation*. J Strength Cond Res, 2019. **33 Suppl 1**: p. S85-S94.
353. Hewett, T.E., et al., *Utilization of ACL Injury Biomechanical and Neuromuscular Risk Profile Analysis to Determine the Effectiveness of Neuromuscular Training*. Am J Sports Med, 2016. **44**(12): p. 3146-3151.
354. Hewett, T.E., et al., *Effectiveness of Neuromuscular Training Based on the Neuromuscular Risk Profile*. Am J Sports Med, 2017. **45**(9): p. 2142-2147.
355. Hume, D.R., et al., *Comparison of Marker-Based and Stereo Radiography Knee Kinematics in Activities of Daily Living*. Ann Biomed Eng, 2018. **46**(11): p. 1806-1815.
356. Shultz, S.J., A.D. Nguyen, and R.J. Schmitz, *Differences in lower extremity anatomical and postural characteristics in males and females between maturation groups*. J Orthop Sports Phys Ther, 2008. **38**(3): p. 137-49.
357. Schilaty, N.D., et al., *Sex-Based Differences of Medial Collateral Ligament and Anterior Cruciate Ligament Strains With Cadaveric Impact Simulations*. Orthop J Sports Med, 2018. **6**(4): p. 2325967118765215.
358. Kim, K.W. and B.O. Lim, *Effects of menarcheal age on the anterior cruciate ligament injury risk factors during single-legged drop landing in female artistic elite gymnasts*. Arch Orthop Trauma Surg, 2014. **134**(11): p. 1565-71.
359. Huang, Y.J., S.H. Wong, and J. Salmon, *Reliability and validity of the modified Chinese version of the Children's Leisure Activities Study Survey (CLASS) questionnaire in assessing physical activity among Hong Kong children*. Pediatr Exerc Sci, 2009. **21**(3): p. 339-53.
360. Temfemo, A., et al., *Relationship between vertical jumping performance and anthropometric characteristics during growth in boys and girls*. Eur J Pediatr, 2009. **168**(4): p. 457-64.
361. Smith, S.W., *Digital signal processing: a practical guide for engineers and scientists*. 2003: Newnes.

362. Sartori, M., et al., *EMG-Driven Forward-Dynamic Estimation of Muscle Force and Joint Moment about Multiple Degrees of Freedom in the Human Lower Extremity*. PLoS ONE, 2012. **7**(12).
363. Saxby, D.J., et al., *Tibiofemoral Contact Forces in the Anterior Cruciate Ligament-Reconstructed Knee*. Med Sci Sports Exerc, 2016. **48**(11): p. 2195-2206.
364. Modenese, L., A.T. Phillips, and A.M. Bull, *An open source lower limb model: Hip joint validation*. Journal of Biomechanics, 2011. **44**(12): p. 2185-2193.
365. Hosseinzadeh, S. and A.M. Kiapour, *Age-related changes in ACL morphology during skeletal growth and maturation are different between females and males*. Journal of Orthopaedic Research. **n/a**(n/a).
366. Pataky, T.C., *One-dimensional statistical parametric mapping in Python*. Comput Methods Biomech Biomed Engin, 2012. **15**(3): p. 295-301.
367. Cohen, J., *Statistical Power Analysis for the Behavioral Sciences*. 2nd ed. 1988, New York.
368. Walter, J.P., et al., *Decreased knee adduction moment does not guarantee decreased medial contact force during gait*. J Orthop Res, 2010. **28**(10): p. 1348-54.
369. Trepczynski, A., et al., *Impact of antagonistic muscle co-contraction on in vivo knee contact forces*. J Neuroeng Rehabil, 2018. **15**(1): p. 101.
370. Tuca, M., et al., *Anterior cruciate ligament and intercondylar notch growth plateaus prior to cessation of longitudinal growth: an MRI observational study*. Knee Surg Sports Traumatol Arthrosc, 2016. **24**(3): p. 780-7.
371. Beck, N.A., et al., *ACL Tears in School-Aged Children and Adolescents Over 20 Years*. Pediatrics, 2017. **139**(3).
372. Finch, C.F., et al., *Preventing Australian football injuries with a targeted neuromuscular control exercise programme: comparative injury rates from a training intervention delivered in a clustered randomised controlled trial*. Inj Prev, 2016. **22**(2): p. 123-8.
373. Hewett, T.E., et al., *The effect of neuromuscular training on the incidence of knee injury in female athletes. A prospective study*. Am J Sports Med, 1999. **27**(6): p. 699-706.
374. Mandelbaum, B.R., et al., *Effectiveness of a neuromuscular and proprioceptive training program in preventing anterior cruciate ligament injuries in female athletes: 2-year follow-up*. Am J Sports Med, 2005. **33**(7): p. 1003-10.
375. Johnson, W.R., et al., *Predicting Athlete Ground Reaction Forces and Moments From Spatio-Temporal Driven CNN Models*. IEEE Trans Biomed Eng, 2019. **66**(3): p. 689-694.
376. Johnson, W.R., et al., *Predicting athlete ground reaction forces and moments from motion capture*. Med Biol Eng Comput, 2018. **56**(10): p. 1781-1792.
377. Johnson, W.R., et al., *On-field player workload exposure and knee injury risk monitoring via deep learning*. J Biomech, 2019. **93**: p. 185-193.
378. Sherbondy, P.S., et al., *Soleus and gastrocnemius muscle loading decreases anterior tibial translation in anterior cruciate ligament intact and deficient knees*. J Knee Surg, 2003. **16**(3): p. 152-158.
379. Anderst, W., et al., *Validation of three-dimensional model-based tibio-femoral tracking during running*. Med Eng Phys, 2009. **31**(1): p. 10-6.
380. Miranda, D.L., et al., *Static and dynamic error of a biplanar videoradiography system using marker-based and markerless tracking techniques*. J Biomech Eng, 2011. **133**(12): p. 121002.

381. Oberhofer, K., et al., *The influence of muscle-tendon forces on ACL loading during jump landing: a systematic review*. Muscles Ligaments Tendons J, 2017. **7**(1): p. 125-135.
382. Kutzner, I., et al., *Loading of the knee joint during activities of daily living measured in vivo in five subjects*. J Biomech, 2010. **43**(11): p. 2164-73.
383. Schellenberg, F., et al., *Review of Modelling Techniques for In Vivo Muscle Force Estimation in the Lower Extremities during Strength Training*. Comput Math Methods Med, 2015. **2015**: p. 483921.
384. Herzog, W. and P. Binding, *Cocontraction of pairs of antagonistic muscles: analytical solution for planar static nonlinear optimization approaches*. Math Biosci, 1993. **118**(1): p. 83-95.
385. Binding, P., A. Jinha, and W. Herzog, *Analytic analysis of the force sharing among synergistic muscles in one- and two-degree-of-freedom models*. J Biomech, 2000. **33**(11): p. 1423-32.
386. Menegaldo, L.L. and L.F. Oliveira, *An EMG-driven model to evaluate quadriceps strengthening after an isokinetic training*. Procedia IUTAM, 2011. **2**: p. 131-141.
387. Hopkins, J.T., et al., *Changes in soleus motoneuron pool excitability after artificial knee joint effusion*. Arch Phys Med Rehabil, 2000. **81**(9): p. 1199-203.
388. Brandon, S.C., et al., *Selective lateral muscle activation in moderate medial knee osteoarthritis subjects does not unload medial knee condyle*. J Biomech, 2014. **47**(6): p. 1409-15.
389. Zebis, M.K., et al., *Identification of athletes at future risk of anterior cruciate ligament ruptures by neuromuscular screening*. Am J Sports Med, 2009. **37**(10): p. 1967-73.
390. Hewett, T.E., et al., *A review of electromyographic activation levels, timing differences, and increased anterior cruciate ligament injury incidence in female athletes*. Br J Sports Med, 2005. **39**(6): p. 347-50.
391. Beynnon, B.D., et al., *The Effects of Level of Competition, Sport, and Sex on the Incidence of First-Time Noncontact Anterior Cruciate Ligament Injury*. Am J Sports Med, 2014. **42**(8): p. 1806-12.
392. Lind, M., F. Menhert, and A.B. Pedersen, *The first results from the Danish ACL reconstruction registry: epidemiologic and 2 year follow-up results from 5,818 knee ligament reconstructions*. Knee Surg Sports Traumatol Arthrosc, 2009. **17**(2): p. 117-24.
393. Renstrom, P., et al., *Non-contact ACL injuries in female athletes: an International Olympic Committee current concepts statement*. Br J Sports Med, 2008. **42**(6): p. 394-412.
394. Sanders, T.L., et al., *Incidence of Anterior Cruciate Ligament Tears and Reconstruction: A 21-Year Population-Based Study*. Am J Sports Med, 2016. **44**(6): p. 1502-7.
395. Chappell, J.D., et al., *Kinematics and electromyography of landing preparation in vertical stop-jump: risks for noncontact anterior cruciate ligament injury*. Am J Sports Med, 2007. **35**(2): p. 235-41.
396. Colby, S., et al., *Electromyographic and kinematic analysis of cutting maneuvers. Implications for anterior cruciate ligament injury*. Am J Sports Med, 2000. **28**(2): p. 234-40.
397. Landry, S.C., et al., *Neuromuscular and lower limb biomechanical differences exist between male and female elite adolescent soccer players during an unanticipated run and crosscut maneuver*. Am J Sports Med, 2007. **35**(11): p. 1901-11.

398. Malinzak, R.A., et al., *A comparison of knee joint motion patterns between men and women in selected athletic tasks*. Clinical Biomechanics, 2001. **16**(5): p. 438-445.
399. Sigward, S.M. and C.M. Powers, *The influence of gender on knee kinematics, kinetics and muscle activation patterns during side-step cutting*. Clin Biomech (Bristol, Avon), 2006. **21**(1): p. 41-8.
400. Konrath, J.M., et al., *Muscle contributions to medial tibiofemoral compartment contact loading following ACL reconstruction using semitendinosus and gracilis tendon grafts*. PLoS One, 2017. **12**(4): p. e0176016.
401. Ebben, W.P., et al., *Gender-based analysis of hamstring and quadriceps muscle activation during jump landings and cutting*. J Strength Cond Res, 2010. **24**(2): p. 408-15.
402. Zebis, M.K., et al., *Effects of evidence-based prevention training on neuromuscular and biomechanical risk factors for ACL injury in adolescent female athletes: a randomised controlled trial*. Br J Sports Med, 2016. **50**(9): p. 552-7.
403. Bencke, J. and M.K. Zebis, *The influence of gender on neuromuscular pre-activity during side-cutting*. J Electromyogr Kinesiol, 2011. **21**(2): p. 371-5.
404. Hanson, A.M., et al., *Muscle activation during side-step cutting maneuvers in male and female soccer athletes*. J Athl Train, 2008. **43**(2): p. 133-43.
405. Nagano, Y., et al., *Gender differences in knee kinematics and muscle activity during single limb drop landing*. Knee, 2007. **14**(3): p. 218-23.
406. McKay, M.J., et al., *Normative reference values for strength and flexibility of 1,000 children and adults*. Neurology, 2017. **88**(1): p. 36-43.
407. Ahmad, C.S., et al., *Effect of gender and maturity on quadriceps-to-hamstring strength ratio and anterior cruciate ligament laxity*. Am J Sports Med, 2006. **34**(3): p. 370-4.
408. Maniar, N., et al., *Muscle contributions to tibiofemoral shear forces and valgus and rotational joint moments during single leg drop landing*. Scand J Med Sci Sports, 2020. **n/a**(n/a).
409. Pizzolato, C., et al., *Real-time inverse kinematics and inverse dynamics for lower limb applications using OpenSim*. Comput Methods Biomech Biomed Engin, 2017. **20**(4): p. 436-445.
410. Bahr, R., *Why screening tests to predict injury do not work-and probably never will...: a critical review*. Br J Sports Med, 2016. **50**(13): p. 776-80.